University of Southampton
Faculty of Engineering and Applied Science
Department of Electronics and Computer Science

Adaptive Equalisation for Downlink UMTS Terrestrial Radio Access

by

Mahmoud Hadef

A doctoral thesis submitted in partial fulfilment of the requirement for the award of Doctor of Philosophy at the University of Southampton

March 2007

Supervised by:

Dr. Stephan Weiss

©Mahmoud Hadef 2007

This thesis is dedicated to my beloved mother, Rabiaa,
for her incredible support and tremendous patience and care.

UNIVERSITY OF SOUTHAMPTON

ABSTRACT

FACULTY OF ENGINEERING AND APPLIED SCIENCE

SCHOOL OF ELECTRONICS AND COMPUTER SCIENCE

Doctor of Philosophy

Adaptive Equalisation for Downlink UMTS Terrestrial Radio Access

by Mahmoud Hadef

The third generation mobile system Universal Mobile Telecommunications System (UMTS) Terrestrial Radio Access (UTRA) has been mainly specified to provide various multimedia capabilities and good service quality. However, since UMTS is based on direct sequence CDMA (DS-CDMA) techniques the performance and the capacity of such systems is significantly limited by multiuser access interference (MAI) and inter-symbol interference (ISI). Therefore, robust and reliable detectors are required to mitigate these effects. Specifically, the multi-user detector exhibits a significant improvement in capacity and spectrum efficiency compared with the conventional matched filter receiver and single-user detector. Nevertheless, its complexity and prior knowledge requirement render it unsuitable for application in the downlink due to handset constraints.

In this thesis, we propose a new robust and simple blind multiuser equaliser for downlink DS-CDMA systems, the so-called filtered-R multiple error CM algorithm (FIRMER-CMA) equaliser. The latter has a relatively low computational complexity, shows good convergence behaviour and a BER performance close to the MMSE solution. The FIRMER-CMA is further modified to be readily reconfigured to different modes such as partial loading schemes, multi-rate transmission, and semi-blind adaptation employing the aid of pilots. A considerable complexity reduction is achieved by adopting a novel adaptation strategy based on considering a new small virtual population of active users.

The robustness of the FIRMER-CMA to carrier frequency offset is addressed whereby a combined scheme based on FIRMER-CMA equaliser and a blind carrier frequency offset estimator is introduced. Furthermore, convergence speed of the proposed algorithm is increased by intro-

ducing an affine projection scheme, and steady state MSE is lowered by adopting a concurrent FIRMER-CMA and decision directed (DD) mode. A system relying on both latter principles is derived whereby substantial performance improvements can be gained over either technique on its own. Finally, a significant gain in data rate and spectrum efficiency is achieved by adopting a new homogeneous burst type and a semi-blind approach based on the proposed algorithm for the UMTS TDD component.

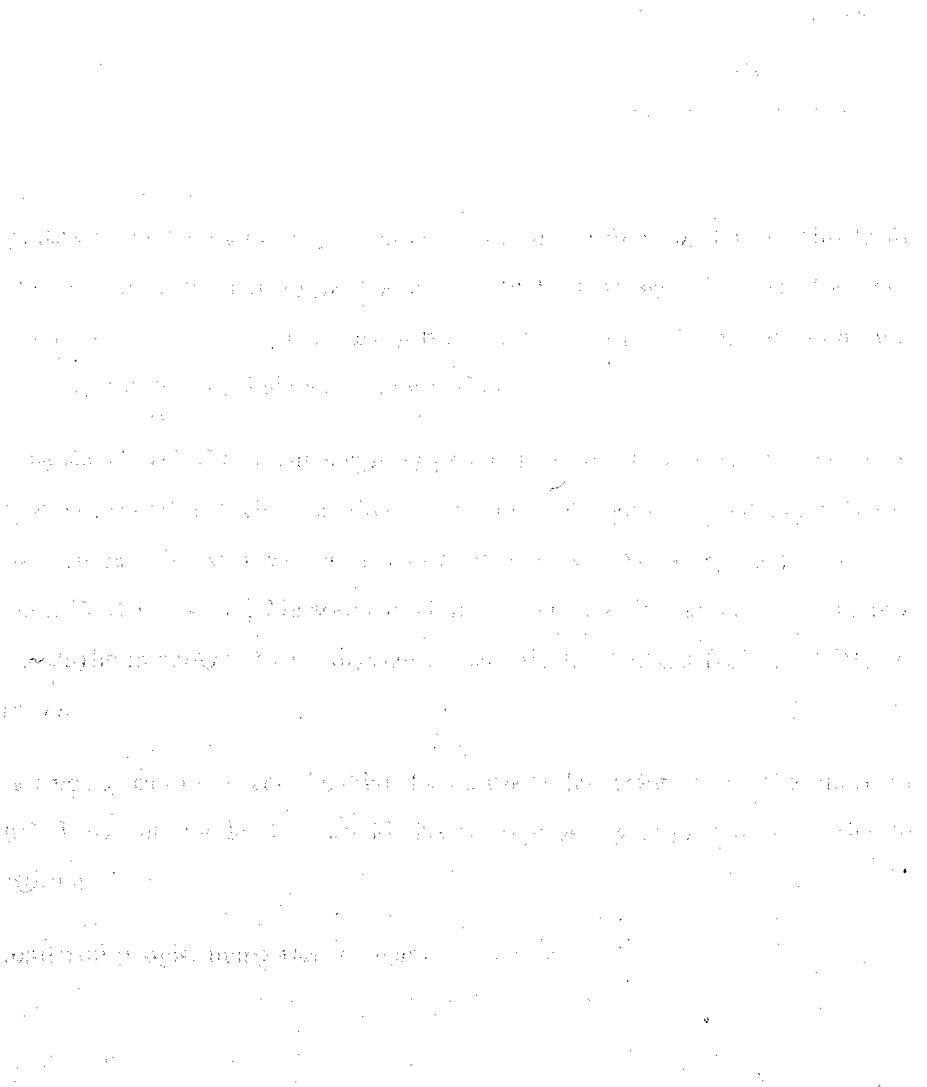

Acknowledgements

I am truly and deeply indebted to my supervisor Dr. Stephan Weiss for his insightful guidance, never ending kindness, and supreme friendship. His intuitive spontaneity, exceptional sense of humour, and shrewd wisdom make him a unique advisor. The greater part of work in this thesis would not exist without Stephans high expertise and willingness to help. I am also grateful to my internal examiner Prof. Sheng Chen, for the thoughtful comments and constructive suggestions he offered towards shaping and improving this dissertation, and to my external examiner Dr. Sangarapillai Lambotharan, for his judicious questions during my oral defense.

I am also sincerely thankful to Prof. Lajos Hanzo, Dr Soon Xin Ng, and Denise Harvey, Charles Tibenderana, Choo Leng Koh, Chunguang Liu, Chi Hieu Ta, Samir Bendoukha, and all the staff and colleagues in the communications research group of the University of Southampton, who enriched my academic and social experience and helped me in various ways.

My immense gratitude goes undoubtedly to my dear mother Rabia, my father Ahmed for their overwhelming tenderness, incredible support and persistent encouragements over the past thirty years. Special thanks are also devoted to my sisters Djohra, Radhia, Imen and Asma who have kindly cheered me up by their optimism and motivation.

I truly appreciate the efforts of brilliant inspiring people like Mr Chenouf Hocine who has served as my teacher and mentor and who has shaped my mindset towards achieving noble goals in my life. Thanks are also due to my friends who have always been by my side. Special thanks go to Abdessalam Bouferrouk and Merzouki Rochdi for their continuous encouragements. I am also thankful to all the members of the Algerian Society for Intellectual Liaison (ASIL) for their amazing inspiration.

My special gratitude goes out to the Algerian Government for granting me the opportunity to obtain the PhD. Last but not least, I would like to express my appreciation to the Algerian Consulate in Britain.

To all these wonderful people, many thanks again.

List of Publications

1. **Mahmoud Hadef, Stephan Weiss, Markus Rupp** "Adaptive Blind Multiuser DS-CDMA Downlink Equaliser" in *IEE Electronics Letters*,Vol.41, No.21, pp.1184–1186, October 2005.

2. **Mahmoud Hadef, Adel Daas, Stephan Weiss, Josh Reiss, Xiaodong Chen** "A Robust Pilot-Assisted Equaliser for the Partially Loaded Downlink UMTS TDD" submitted to *15th European Signal Processing Conference EUSIPCO 2007*, Poland, September 2007.

3. **Bendoukha Samir, Mahmoud Hadef, Stephan Weiss** "Adaptive Receivers for Space-Time Spreading over Dispersive Channels" in *40th Asilomar Conference on Signals, Systems, and Computers*, Pacific Grove.USA, November.2005, accepted for publication.

4. **Mahmoud Hadef, Bendoukha Samir, Stephan Weiss,** "A Fast and Robust Blind Detection Scheme for Downlink UMTS TDD Component" in *2nd International Symposium on Control, Communications, and Signal Processing*, Marrakech. Morocco, March.2006.

5. **Mahmoud Hadef, Bendoukha Samir, Stephan Weiss, Markus Rupp** "A New UMTS-TDD burst structure with a semi-blind Equalisation scheme" in *39th Asilomar Conference on Signals, Systems, and Computers*, Vol.1, pp.417–421, Pacific Grove.USA, November.2005.

6. **Mahmoud Hadef, Bendoukha Samir, Stephan Weiss, Markus Rupp** "Affine Projection Algorithm for Blind Multiuser Equalisation of Downlink DS-CDMA system" in *39th Asilomar Conference on Signals, Systems, and Computers*, Vol.1, pp.802–806, Pacific Grove.USA, November.2005.

7. **Mahmoud Hadef, Stephan Weiss,** "A Fast Converging Concurrent Affine Projection Algorithm for Blind Multiuser Equalisation." in *2nd IEE/EURASIP Conference on DSP Enabled Radio*, Vol.2005/11086, pp.23/1–23/4, Southampton.UK, September.2005.

8. **Liu Chunguang, Ta Chi H, Mahmoud Hadef, Stephan Weiss,** "A Coding and Equalisation Approach for Dispersive Channels with Structured Additive Noise." in *2nd IEE/EURASIP Conference on DSP Enabled Radio*, Vol.2005/11086, pp.33/1–33/4, Southampton.UK, September.2005.

9. **Mahmoud Hadef, Stephan Weiss,** "Concurrent Constant Modulus Algorithm and Decision Directed Scheme for Synchronous DS-CDMA Equalisation" in *IEEE Workshop on Statistical Signal Processing (SSP)*, Vol.1, pp.203–208, Bordeaux.France, July.2005.

10. **Mahmoud Hadef, Stephan Weiss,** "A Pilot-Assisted Equalisation Scheme for the UMTS-TDD Downlink with Partial Loading" in *IEEE 61st Semiannual Vehicular Technology Conference (VTC)*, Vol.1, pp.548–551, Stockholm.Sweden, June.2005.

11. **Mahmoud Hadef, Stephan Weiss,** "A Semi-Blind Channel Equalisation Strategy for the UMTS-TDD Downlink" in *Proceedings of the 3rd Workshop on the Internet, Telecommunications, and Signal Processing*, Vol.1, pp262–267, Adelaide.Australia, December.2004.

12. **Stephan Weiss, Mahmoud Hadef, and Markus Rupp,** "Blind Multi-User Equalisation for a Dispersive DS-CDMA Downlink under Carrier Frequency Offset Conditions," in *Proceedings of 12th European Signal Processing Conference* , Vienna.Austria, September.2004.

13. **Mahmoud Hadef, Stephan Weiss,** " Adaptive Blind Chip-Level Multiuser Detection in Multi-Rate Synchronous DS-CDMA System with Partial Loading" in *Proceedings of 2nd International Workshop on Signal Processing for Wireless Communications*,Vol.1, pp.115–118, Kings' College London.UK, June.2004.

14. **Mahmoud Hadef, Stephan Weiss,** "A Blind Synchronous Multi-User DS-CDMA Equaliser with Partial Loading" in *International Symposium on Control, Communications, and Signal Processing*, Vol.1, pp.803–806, Hammamet.Tunisia, March.2004.

15. **Stephan Weiss, Mahmoud Hadef, Markus Konrad, and Markus Rupp,** "Adaptive Chip-Rate Equalisation for TD-CDMA Downlink Receiver," in *37th Asilomar Conference on Signals, Systems, and Computers*, Vol.2, pp.1283–1287, Pacific Grove.USA, November.2003.

16. **Stephan Weiss and Mahmoud Hadef,** "Blind Chip-Rate Multiuser Equalisation," in *IEE colloquium on DSP enabled Radios*, Vol.1, pp.436–443, Livingston. Scotland, September. 2003.

17. **Stephan Weiss, Mohamad Hafizal, and Mahmoud Hadef,** "Switching between Two Different Sub-band Equalisation Structures," in *2nd IMA International Conference Mathematics in Communications*, Lancaster, UK, December 2002.

Contents

Chapter 1

Introduction

1.1 Research Motivation

For more than a decade, research has been ongoing to find enabling standards which ensure that wireless communications offer multimedia capabilities and service quality similar to the wire-line network. In January 1998, the European standardisation body for third generation mobile radio systems, the European Telecommunications Standards Institute-Special Mobile Group (ETSI-SMG), agreed on a radio scheme for third generation mobile radio system, called Universal Mobile Telecommunications System (UMTS) [1, 2]. UMTS typically provides low to high data rate services for multimedia applications such as voice, audio/video, graphics, data, inter-net access and e-mail with a significant maximum data rate of 2 Mb/s. The complex air interface between the mobile station (MS) and the base station (BS) adopted for UMTS system, the so-called UMTS Terrestrial Radio Access (UTRA) consists of two modes, a frequency division duplex (FDD) and a time division duplex (TDD) mode. Both modes have been specified and harmonised in the third generation partnership project (3GPP) [3, 4], and they are mainly based on the direct sequence code division multiplexing access (DS-CDMA) technology.

In DS-CDMA all users' signals are spread and multiplexed by distinct codes which overlap in time and frequency. In a synchronous system and over a non-dispersive channel, the desired user's signal could be simply detected by correlating the entire received signal with this user's

code waveform. However, both in an asynchronous system and a dispersive channel, the random time offsets between users' signals lead to multiple access interference (MAI) and inter-symbol interference (ISI) factors, which limit the capacity and the performance of such DS-CDMA systems.

There have been widespread investigations and extensive research efforts to introduce a reliable DS-CDMA detector, apt to alleviate the effect of MAI and ISI interferences and able to achieve optimum near far effect resistance. Extensive references and discussions can be found in a number of articles and books [5, 6, 7, 8, 9, 10]. Most of the proposed detectors can be classified into one of two main categories: multi-user techniques or single-user schemes. The multi-user detector, where information about multiple users are used jointly to better detect each individual user, exhibits a significant improvement in capacity and spectrum efficiency compared with the conventional matched filter receiver [8]. Nevertheless, its complexity and prior knowledge requirement render it unsuitable for downlink applications, noting that matters of cost, size, and weight are of more concern to the handset than for the base station.

However, nowadays increasing demand for high data rate services and multimedia applications in downlink (DL) transmission propels researches toward exploiting the high capacity gain provided by multiuser detection. In fact, by taking into consideration the following specifications for the DL: i) DL signals are perfectly synchronised at the transmitter, ii) spreading sequences are orthogonal, and iii) all DL signals experience the same dispersive channel, the use of a multiuser equaliser in front of the matched code filters would be a good choice to mitigate the effect of the multipath channel distortions. The commonly proposed linear multiuser equalisers [11, 12] are based on training adaptation. These algorithms necessitate the implementation of training sequences which can be considered as a waste of the available valuable bandwidth. A novel class of multiuser equalisers, equally referred to as blind detectors, do not require explicit knowledge of training sequences and channel parameters. Instead, these parameters are estimated blindly according to certain criteria. The most popular blind approach is the constant modulus algorithm (CMA) [13, 14]. CMA is a robust algorithm which has a low computational complexity and is widely used in practice [15]. Consequently, a few multiuser equalisation strategies based on the CM criterion have been proposed [16, 17, 18]. However, the proposed CMA-based algorithms for multi-user system either neglect the spreading [17] or the dispersiveness of the channel [16, 18]. In this work, we are concerned with developing a new robust and low-complexity blind multiuser equaliser

based on CM criterion for the DS-CDMA downlink which considers both spreading process and dispersiveness of the channel

1.2 Original Contributions

The main original contributions in this dissertation are:

- **A Blind Multiuser FIRMER-CMA Algorithm.** [19, 20, 21, 22, 23]

  Fully Loading [19, 20, 23]. A new blind equalisation approach, the so-called filtered-R multiple error CM algorithm (FIRMER-CMA), suitable for fully loaded DS-CDMA downlink systems has been derived. This algorithm aims to enforce CM conditions on the various user signals, whereby its stochastic gradient algorithm differs from previous CM algorithms by a code-prefiltering of its input. FIRMER-CMA is a flexible and a low complexity algorithm which can be readily reconfigured to perform in different modes and with various algorithms such as least mean square (LMS) and decision directed (DD) algorithms. Furthermore, FIRMER-CMA has been extensively tested and proven very stable and exhibits a performance close to the minimum mean square error (MMSE) solution.

  Partial Loading [21]. The above FIRMER-CMA is only suitable for a fully loaded system, in which all possible users are active. In a partially loading scenario, inactive codes in the system must be considered, for which we have proposed and compared three different methods: (i) a mean square error criterion for absent users, which is referred to as FIRMER-CMA/LMS, and a CM approach with (ii) zero modulus or (iii) the transmission of arbitrary signals with small code amplitude. For all three cases, stochastic gradient descent algorithms are derived and compared. It was shown that the first method, the FIRMER-CMA/LMS algorithm, is superior to both other strategies in convergence performance. Moreover, it has a lower implementational cost and does not increase the power of the transmitted signal.

  Multi-rate transmission [22]. For multi-rate transmission, we have proposed two modified FIRMER-CMA/LMS equalisation approaches using either variable spreading length (VSL) or multi-code (MCD) access modes for a multi-rate DS-CDMA downlink. The VSL algorithm shows faster convergence and outperforms the MCD equaliser in both fully and

partially loading scenarios.

- **Carrier Frequency Offset Compensation** [24]
  Unlike the standard CMA, the FIRMER-CMA has been identified to be sensitive to carrier frequency offset. The latter has been circumvented by modifications to the algorithm, necessitating the blind detection of the carrier frequency offset. A combined scheme based on the multiuser CM algorithm and a blind estimation of the carrier frequency offset has shown good results in terms of convergence speed and BER performance, and in some cases very closely approaches the MMSE solution.

- **Fast and Robust Multiuser Equalisers** [25, 26, 27] An affine projection algorithm for blind multiuser equalisation, suitable for DS-CDMA downlink scenario, has been derived. The proposed algorithm presents a faster convergence over the normalised FIRMER-CMA approach with additional computational complexity cost. A concurrent FIRMER-CMA+DD algorithm has been derived. The proposed algorithm is based on performing both CMA and DD adaptation concurrently and enables faster convergence and lower steady state mean square error compared to the standard FIRMER-CMA approach. Furthermore, the algorithm can limit phase ambiguity found in FIRMER-CMA case by locking the solution onto the prescribed constellation pattern. A hybrid structure AP-FIRMER-CMA+DD which combines advantages of both the AP-FIRMER-CMA and FIRMER-CMA+DD has been introduced. The proposed AP-FIRMER-CMA+DD provides a further increase in convergence speed over the FIRMER-CMA+DD and a lower BER than the AP-FIRMER-CMA.

- **Pilot-Assisted Detection for Downlink UMTS-TDD** [28, 29, 30]
  A pilot-assisted channel equalisation scheme for the downlink time-division duplex (TDD) component of the universal mobile telecommunication system (UMTS) has been derived. In addition to the basic MSE chip rate equalisation performed over the training field of each UMTS TDD time burst, a semi-blind adaptation, similar in structure to the FIRMER-CMA/LMS algorithm is adopted over data fields. A number of inactive users are exploited to load pilot signals in order to enhance the system tracking performance and eliminate the typical CMA phase ambiguity problem. Furthermore, a new UMTS TDD burst structure,

which provides better spectrum efficiency than the standard bursts, has been introduced.

1.3 Outline of Thesis

The following chapters are organised as outlined below:

Chapter 2 reviews the principles of DS-CDMA systems, its characteristics and problems. Starting from a simple presentation of the synchronous downlink scenario. A mathematical model of a DS-CDMA system is derived and used to determine the causes of MAI an ISI. The weak performance of the matched filter is identified and various alternative detection strategies are classified and briefly explained.

Chapter 3 is a brief survey of adaptive equalisation concepts in digital communications. The main characteristics of the fractionally spaced and baud-spaced equalisers are reviewed. Then, the need of blind equalisation in various communication systems is highlighted. Specifically, properties of the most popular blind algorithm, the constant modulus algorithm, are discussed and analysed.

Chapter 4 presents and evaluates the performance of the proposed blind multiuser adaptive equaliser based on the FIRMER-CMA algorithm under various modes and different conditions. First, a fully loaded and single rate system is assumed whereby the corresponding stochastic gradient is derived and its robustness is tested through various simulations. Second, inactive users are considered, whereby three models are proposed to deal with unused codes in order to ensure algorithm convergence. Third, two modified versions of the proposed algorithm which suit both VSL and MCD multi-rate access modes are proposed and compared. Finally, the flexibility and computational issues of the FIRMER-CMA are discussed.

Chapter 5 identifies the sensitivity of the FIRMER-CMA to the carrier frequency offset and proposes an offset compensation algorithm which blindly estimates this frequency offset. The performance of the combined FIRMER-CMA and the offset estimator algorithm is tested over various simulations. Furthermore fast and robust multiuser equalisers are derived and tested.

Chapter 6 introduces a pilot-assisted equalisation approach for the downlink UMTS TDD system. First, the physical channel for such systems is briefly presented, then a suitable cost function for a pilot assisted scheme and an associated stochastic gradient algorithm are derived. We illustrate that the proposed semi-blind approach outperforms the basic equalisation scheme in terms of MSE and BER. Finally, a new burst structure which is more suitable for the proposed pilot-assisted scheme is presented.

Chapter 7 summarises the main results of this report, and puts forward ideas and suggestions for future investigation.

Chapter 2

Synchronous DS-CDMA System Overview

This chapter reviews the basic concepts of a synchronous DS-CDMA system. Firstly, duplex procedures and multiple access techniques commonly used in mobile radio communications are explained and compared in Sec. 2.1 and Sec. 2.2 respectively. Secondly, the general technique of spreading a signal over a wide band of frequencies is presented in Sec. 2.3. In Sec. 2.4, the most commonly used spreading codes for such techniques are described. This is followed by a brief description of a synchronous DS-CDMA system in Sec. 2.5, whereby a baseband mathematical model of this system is derived in Sec. 2.6. In Sec. 2.7, the weak performance of the matched filter receiver in cancelling both multiple access and inter-symbol interferences is highlighted. Finally, Sec. 2.8 introduces the most common detection strategies for DS-CDMA systems.

2.1 Duplex Procedures

Duplex refers to a two way communication, here between a base station (BS) and a mobile station (MS). The connection from BS to MS is known as downlink (DL) and from MS to BS as uplink (UL). Hence the transmission medium needs to be shared between DL and UL. In order to accomplish this, UTRA provides two possible sharing modes, time division duplex (TDD) and frequency division duplex (FDD), as shown in Fig. 2.1.

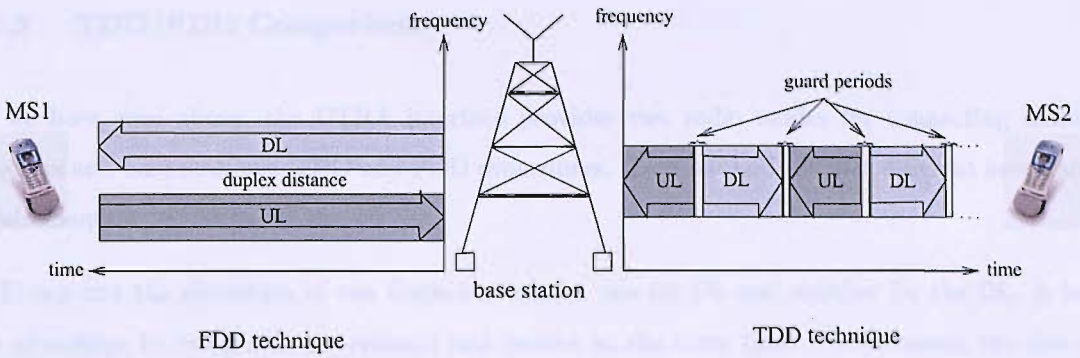

Figure 2.1: Duplex communication modes in UTRA

2.1.1 Frequency Division Duplex (FDD) Technique

FDD is a technique that is extensively used in the separation of UL and DL for which global system for mobile communications (GSM) is a classic representative. With FDD stations transmit and receive in different, usually paired, frequency bands. The width of the guard band between UL and DL bands is called the duplex distance, as shown in Fig. 2.1. It is mainly introduced to avoid interferences between UL and DL signals. In a cellular mobile radio the higher frequency band is usually dedicated for DL and the lower frequencies for UL [31]. The main reason for this selection is that higher frequency electro-magnetic waves experience a stronger attenuation in air as a propagation medium and the base station can provide a higher transmit power than a mobile station to bridge the same distance.

2.1.2 Time Division Duplex (TDD) Technique

In the TDD technique UL and DL signals are separated in time. It uses the same frequency band for both the UL and the DL by allocating distinct time slots to the two links. Time is divided in frames which are divided in slots of short duration. Each time slot can be allocated either to the UL or to the DL, as shown in Fig. 2.1. TDD can therefore allocate more time slots on the link that requires more throughput and adjusts itself continuously. Hence asymmetric data rates can easily be realised [31]. Due to the medium propagation delay a guard period must be included between TDD time slots to make sure only one link is active at the same time.

2.1.3 TDD/FDD Comparison

As we have seen above, the UTRA interface provides two radio modes for connecting mobile handsets and base stations: TDD and FDD procedures. Each method satisfies different needs and requirements.

FDD requires the allocation of two frequency bands: one for UL and another for the DL. It has the advantage to being able to transmit and receive at the same time. Furthermore, the size of the cell is not limited by a propagation delay like in TDD because of the absence of time slots and guard periods, which also makes the timing synchronisation between base and mobiles less critical than in TDD. Hence, FDD is more suitable for applications with large coverage areas such as public Macro and Micro cell environments with data rates of up to 384 Kb/s and high mobility [1]. However, FDD radio units need duplexer in order to separate the incoming and outgoing signals at the antenna. Another drawback is that FDD does not allocate efficiently the available bandwidth for all types of services. For example, Internet access requires more allocation on the DL than on the UL.

TDD uses the same frequency band for both the UL and the DL by allocating distinct time slots to the two links. Time is divided in frames which are divided in slots of short duration. Each time slot can be allocated either to the UL or to the DL. TDD can therefore allocate more time slots on the link that requires more throughput and adjusts itself continuously, which makes it more bandwidth efficient than FDD. Hence, it is particularly well suited for asymmetric, high traffic density and indoor coverage [1, 2], where the applications require high data rates and tend to create highly asymmetric traffic (e.g., Internet access). Incidentally, TDD terminals do not need a duplexer and hence offer lower hardware complexity than FDD terminals. Nevertheless, the crucial limiting factors are synchronisation complications and the associated interference problems [32, 33]. TDD requires better timing synchronisation between the users than FDD, because of its time division nature; the base station cannot be allowed to transmit at the same time as the mobile stations. Furthermore, for mobile stations far from the base station, the propagation time of the signal may become important. This limits the size of the cell. Therefore, TDD is more suitable for small cells, such as public Micro and Pico cell environments. The TDD mode also has the benefit of reciprocal nature of the channel, such that we can use a channel estimate of the UL channel for

the DL as well [34].

2.2 Multiple Access Procedure

In a multi-user communications system where many users share a common channel, interference from various users may distort the detection of a single user. Therefore in the receiver the respective signals require to be separated in a manner that such interference is reduced. Depending on how the various users are multiplexed, we can distinguish between frequency, time, space and code division multiple access, which will be briefly reviewed in the following.

2.2.1 Frequency Division Multiple Access (FDMA)

FDMA is one of the earliest multiple access techniques for analogue cellular systems. In this technique the available bandwidth is divided into bands allocated to different users for the whole time period of the communication. Whereby, a user is able to send or receive within a frequency channel. FDMA does not require synchronisation or timing control, which makes it algorithmically simple. However, the channels are assigned only when demanded by the users, hence unused channels are a wasted resource. Moreover, even though no two users use the same frequency band at the same time, guard bands are introduced between frequency bands to minimise adjacent channel interference. Guard bands are unused frequency slots and can be considered as an additional waste of bandwidth. Furthermore, since the bandwidth of a channel is narrower than the overall bandwidth of a system, the transmission speed achievable in a channel is correspondingly lower than the overall transmission speed. Therefore, only part of the overall capacity is available to a user.

2.2.2 Time Division Multiple Access(TDMA)

TDMA is another technique to multiplex user signals. Different users are assigned dissimilar time slots during which they transmit their information using the accessible bandwidth. With TDMA, users do not transmit concurrently in different frequency channels, as is the case with FDMA, but instead successively in the same frequency band. Unlike FDMA, in TDMA better

spectrum efficiency and higher transmission speed can be achieved since the whole bandwidth is exploited at each time slot. However, similar to TDD (see Sec. 2.1), channel delay spread and time synchronisation could be considered as the main limitations of this technique.

2.2.3 Space Division Multiple Access (SDMA)

SDMA technique takes advantage of spatial separation between user to increase the capacity of a cellular system. The base station does not transmit the signal to the entire cell area, as in conventional access techniques, but concentrates power in the direction of the mobile unit for which the signal is intended, while reducing it in the directions where other units are present. SDMA uses smart antenna techniques that employ antenna arrays to steer the antenna pattern in the direction of the desired user and places nulls in the direction of the interfering signals. Since these arrays can produce narrow spot beams, the frequency can be re-used within the cell as long as the spatial separation between the users is sufficient. Usually, SDMA is used in conjunction with other multiple access techniques such as FDMA, TDMA and code division multiple access (CDMA).

2.2.4 Code Division Multiple Access (CDMA)

CDMA strategy is widely used in commercial and military communication systems and it is adopted in both TDD and FDD modes in the UMTS standard. In CDMA different users share the same bandwidth at the same time and are separated by means of different spreading codes. It utilises a spread spectrum technique in which a spreading code which is uncorrelated to the signal and has a large bandwidth is used to spread the narrowband message signal. Direct sequence Spread Spectrum is most commonly used for CDMA. Unlike TDMA, CDMA does not require time synchronisation between the users. However, CDMA is interference limited system and suffers from MAI and self jamming effects. In the following we address CDMA systems in more detail, whereby a brief description of the spread spectrum technique is given first in the next section.

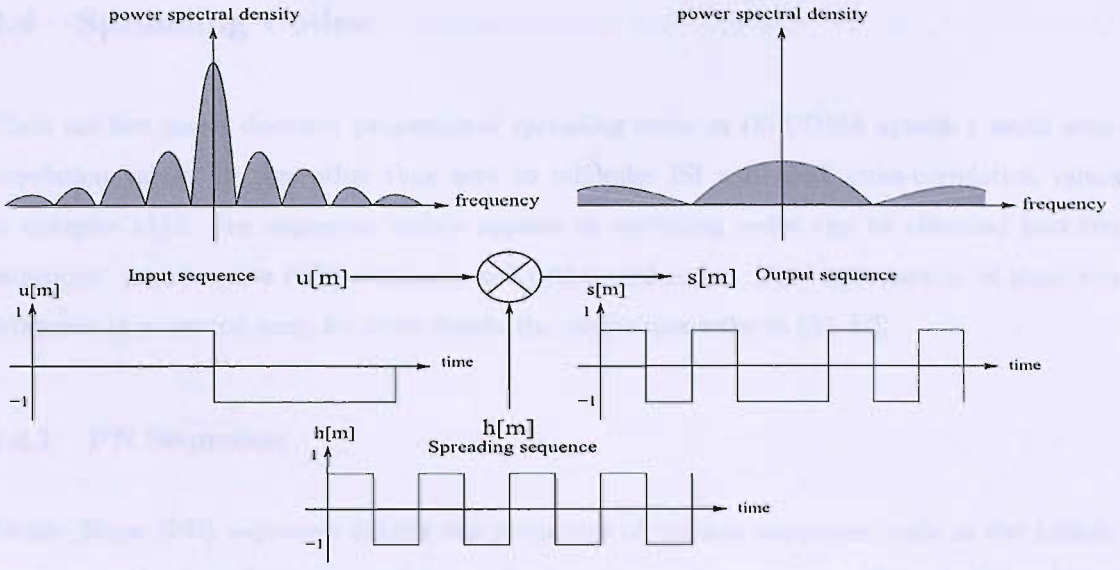

Figure 2.2: Effect of spread spectrum

2.3 Spread Spectrum

The term spread spectrum (SS) has been used in a wide variety of military and commercial communication systems. It is a technique whereby a transmitted signal is spread over a frequency band much wider than the minimum bandwidth required, as shown in Fig. 2.2. Spreading is accomplished by means of spreading sequences, often called signature or code sequences, for which more details are provided in Sec. 2.4. The waveform resulting from this modulation technique appears as a random signal and is difficult to detect and demodulate by other listeners.

SS development was motivated primarily by the desire to achieve high jamming resistance and secure communication [35, 36]. As a result of this development other attractive applications and potential advantages emerged such as interference rejection [37, 38], energy density reduction [36], lower cost of implementation [39], message privacy, and particularly the multiple access technique CDMA [35, 39]. SS is classified into two major categories, Direct Sequence (DS) and Frequency Hopping (FH), for which the interested reader is referred for more details to [37, 38, 36]. Basically, DS-CDMA, which is widely used in air interface standards such as UMTS [2, 31], and IS-95 [9], is one of the most important application of the DS SS category.

2.4 Spreading Codes

There are two major desirable properties of spreading codes in DS-CDMA system : small auto-correlation values for lags other than zero to minimise ISI and small cross-correlation values to mitigate MAI. The sequences widely applied as spreading codes can be classified into two categories: pseudo noise (PN) sequences and orthogonal codes. Brief introduction of these two categories is presented next; for more details the reader may refer to [40, 37].

2.4.1 PN Sequences

Pseudo Noise (PN) sequences exhibit the properties of random sequences, such as the balance property, as they have been produced from a fair "coin tossing" experiment. Basically PN codes are deterministic signals and they are generated by shift registers with linear feedbacks [6]. Maximum-length, Gold, and Kasami sequences are the most known PN sequences in DS-CDMA systems.

Maximum-length codes or m-sequences are, by definition, the largest codes that can be generated by a given shift register, they are periodic and have length $2^p - 1$ chips, where p is the number of register stages. An important characteristic of the m-sequences is their good autocorrelation properties, particularly the small delayed autocorrelation value [40]. This is one of the main reasons for the use of m-sequences in preamble design for bit timing and synchronisation [36]. However, it is shown that the cross-correlation function between any two pairs of m-sequences of the same period can have relatively large peaks [37]. Such high values for the cross-correlation are undesirable in DS-CDMA, because they enhance the MAI phenomenon.

PN sequences with better periodic cross-correlation properties are provided by Gold and Kasami. From a pair of preferred sequences, Gold constructs a set of sequences of the same length by taking the modulo-2 sum of one of these sequences with shifted version of the second sequence or vice versa [37]. As result gold sequences are generated with three different cross-correlation values [40]. The most significant advantages in Gold sequences is the large number of sequence sets offered with good cross-correlation properties [40]. A procedure similar to that used for generating Gold sequences will generate the small set of Kasami sequences. They are optimum and exhibit a very

low cross-correlation [40]. Gold and Kasami sequences are particularly used as scrambling codes [36].

2.4.2 Orthogonal Codes

The most significant attribute of orthogonal codes is their zero cross-correlation when there is no offset between codes. However, they show poor delayed cross-correlation (some codes are merely the shifted version of others). This drawback limits the implementation of the orthogonal codes to a synchronised scenario such as DL transmission, where all users are synchronised in time. As a further drawback, even in DL transmission the orthogonality will not be preserved due to the multi-path aspect of the channel [40].

One of the most well-known orthogonal codes is the Walsh -Hadamard sequences [40]. Walsh functions are generated by mapping codeword rows of special square matrices called Hadamard matrices. The Hadamard matrix can be generated by the following recursive procedure:

$$\mathbf{H}(1) = [1], \mathbf{H}(2) = \begin{bmatrix} 1 & 1 \\ 1 & -1 \end{bmatrix}, \mathbf{H}(4) = \begin{bmatrix} 1 & 1 & 1 & 1 \\ 1 & -1 & 1 & -1 \\ 1 & 1 & -1 & -1 \\ 1 & -1 & 1 & -1 \end{bmatrix}, ..\mathbf{H}(2N) = \begin{bmatrix} \mathbf{H}(N) & \mathbf{H}(N) \\ \mathbf{H}(N) & -\mathbf{H}(N) \end{bmatrix} \tag{2.1}$$

where each row or column presents a Walsh function. Hadamard matrix can also be obtained by using the Kronecker product [40].

DS-CDMA systems need to be designed to support a variety of data services from low to very high bit rates. These multi-rate systems require multiple spreading factors since the spread signal bandwidth is the same for all users. Therefore, the fixed-length orthogonal codes (Walsh functions), presented earlier, are not able to fulfil this task. Variable length orthogonal codes can be implemented in that case [41, 40], which can be derived by rearranging Walsh functions. The

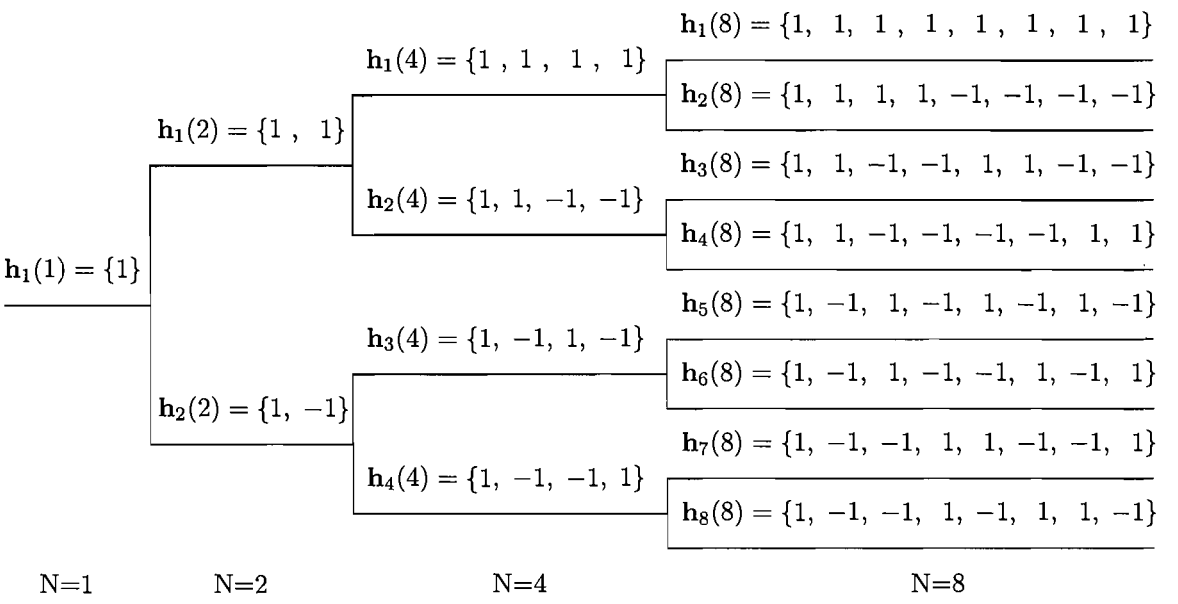

Figure 2.3: OVSF code tree

codes, known as Orthogonal Variable Spreading Factor (OVSF) codes can be generated recursively using the tree structure shown in Fig. 2.3. The significant result from this tree is that all codes from different branches are orthogonal except when one of the codes is a mother code [40].

2.5 DS-CDMA System Description

In a DS-CDMA system a number of user signals $u_l[n]$, $l = 0(1)K-1$ share a common channel bandwidth, and each user l is provided with an individual spreading sequence $\mathbf{h}_l$. In the transmission procedure, symbols will be spread by a certain factor called processing gain or spreading factor N [6]. The samples of the resulting signals are called chips, to differentiate them from the bits or symbols of the user data stream. Specifically, we consider a DS-CDMA downlink system in Fig. 2.4, whereby the users' spread sequences are synchronous and can be added together chip by chip. The resulting signal is further scrambled by multiplication with a scrambling sequence $c[m]$ prior to transmission over a dispersive channel $g[m]$ with additive noise $v[m]$.

In the receiver the conventional DS-CDMA detector correlates the received signal $r[m]$ with a

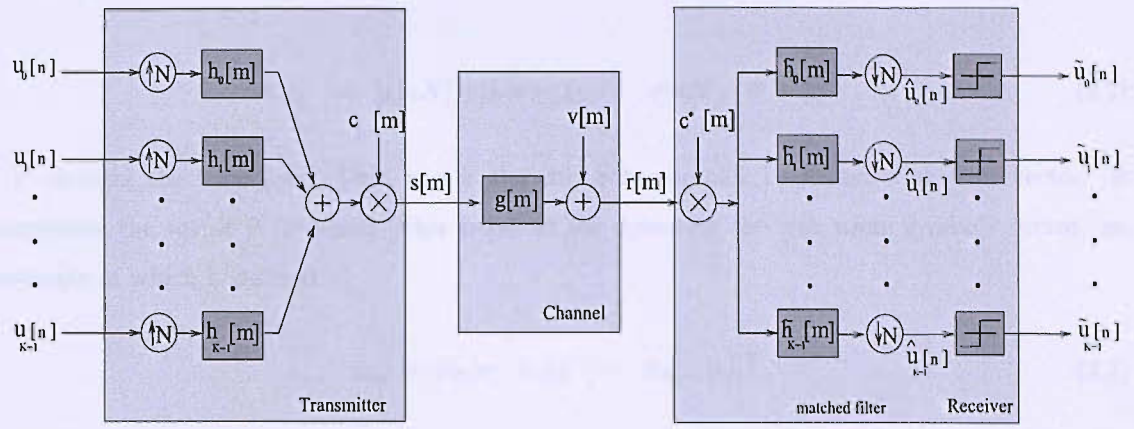

Figure 2.4: Equivalent baseband representation for synchronous DS-CDMA system with a conventional detector

replica of each user's code or spreading waveform to recover the particular transmitted symbols. The correlation detector can be equivalently implemented through what is known as matched filtering [37]. The output of the correlators or matched filters (MFs) are sampled at the symbol rate, which yields soft estimation of transmit symbols. The final hard symbol decisions are made by means of nonlinear decision devices, as illustrated in Fig. 2.4. However this kind of detector does not take into account the effect of interferences and distortions generated in channels and by other users' signals, see Sec. 2.7 . In fact complex detectors are required to mitigate such effects in DS-CDMA systems, which will be addressed as part of a more detailed description of detection techniques for DS-CDMA receivers presented in Sec. 2.8. First a mathematical framework for a synchronous baseband DS-CDMA system is presented in the next section.

2.6 Synchronous Baseband Model

In this section a discrete baseband model for the synchronous DS-CDMA system, described above in Sec. 2.5, is derived. This model is the prototype of downlink systems of concern in this thesis. The main goal in the following is to derive a vector $\mathbf{r}_{nN}$ which contains N consecutively received samples as a function of the transmitted users' symbols. The received signal vector $\mathbf{r}_{nN}$ is given by

$$\mathbf{r}_{nN} = [r[nN] \; r[nN-1] \; \cdots \; r[nN-N+1]]^{\mathrm{T}}. \tag{2.2}$$

$(.)^T$ denotes the transpose. Thus $\mathbf{r}_{nN}$ is the chip rate complex baseband equivalent vector. It comprises the set of N received chips required for detecting the nth users symbols vector, an estimate of which is defined by

$$\hat{\mathbf{u}}_n = [\hat{u}_0[n] \; \hat{u}_1[n] \; \cdots \; \hat{u}_{K-1}[n]]^{\mathrm{T}}. \tag{2.3}$$

where K is the number of active users and N is the spreading code factor. The spreading process is performed by means of Walsh sequences, contained in $\mathbf{h}_l$, $l = 0(1)K-1$, which can be taken from an $N \times N$ normalised Hadamard matrix. Correspondingly, we define the K codes matrix $\mathbf{H}$ such as

$$\mathbf{H} = [\mathbf{h}_0 \; \mathbf{h}_1 \; \cdots \; \mathbf{h}_{K-1}]. \tag{2.4}$$

with $\mathbf{H}^{\mathrm{T}}\mathbf{H} = \mathbf{I}_K$ ($\mathbf{I}_K$ is the $K \times K$ identity matrix). Note that the matrix $\mathbf{H} \in \mathbb{Z}^{N \times K}$ is not the complete $N \times N$ Hadamard matrix, described in Sec. 2.4, since it includes only the active users' spreading signatures. At the base station, the K synchronised signals $u_l[n]$, $l = 0(1)K-1$ are first multiplied by $\mathbf{H}$ and then multiplexed. The resulting signal is further scrambled by a complex scrambling code $c[m]$ before transmission, as shown in Fig. 2.4. Therefore, the transmitted N chips which correspond to the nth users symbols vector $\mathbf{u}_n = [u_0[n] \; u_1[n] \; \cdots \; u_{K-1}[n]]^{\mathrm{T}}$ can be expressed as

$$\begin{bmatrix} s[nN-N+1] \\ s[nN-N+2] \\ \vdots \\ s[nN] \end{bmatrix} = \begin{bmatrix} c[nN-N+1] & & \mathbf{0} \\ & c[nN-N+2] & \\ & & \ddots \\ \mathbf{0} & & c[nN] \end{bmatrix} \mathbf{H}\mathbf{u}_n \,. \tag{2.5}$$

Hence, by reversing (2.5), the nth chip rate regressive vector $\mathbf{s}_{nN} = [s[nN] \; s[nN-1] \; \cdots \; s[nN-N+1]]^{\mathrm{T}}$ of the signal to be sent can be conveniently written as

$$\begin{aligned}\mathbf{s}_{nN} &= \mathbf{J}_N \begin{bmatrix} s[nN-N+1] \\ s[nN-N+2] \\ \vdots \\ s[nN] \end{bmatrix} \\ &= \begin{bmatrix} c[nN] & & \mathbf{0} \\ & c[nN-1] & \\ & & \ddots \\ \mathbf{0} & & c[nN-N+1] \end{bmatrix} \tilde{\mathbf{H}}\mathbf{u}_n. \end{aligned} \tag{2.6}$$

where $\mathbf{J}_N$ is the $N \times N$ reverse identity matrix and $\tilde{\mathbf{H}}$ is the flipped spreading codes matrix which can be given by

$$\begin{aligned}\tilde{\mathbf{H}} &= \mathbf{J}_N\mathbf{H} \\ &= [\mathbf{J}_N\mathbf{h}_0 \ \mathbf{J}_N\mathbf{h}_1 \ \cdots \ \mathbf{J}_N\mathbf{h}_{K-1}] \\ &= \left[\tilde{\mathbf{h}}_0 \ \tilde{\mathbf{h}}_1 \ \cdots \ \tilde{\mathbf{h}}_{K-1}\right]. \end{aligned} \tag{2.7}$$

For presentational simplicity the scrambling code can be absorbed into the flipped spreading codes matrix $\tilde{\mathbf{H}}$, such that

$$\mathbf{s}_{nN} = \tilde{\mathbf{H}}_{nN}\,\mathbf{u}_n. \tag{2.8}$$

Here $\tilde{\mathbf{H}}_{nN} \in \mathbb{C}^{N\times K}$ is a time varying matrix because the scrambling code is usually much longer than the spreading sequence [40]. Furthermore $\tilde{\mathbf{H}}_{nN}$ is periodic with a period equal to the least common multiple of the spreading factor N and the length of the scrambling code. The propagation environment adopted here is a dispersive channel defined by its channel impulse response (CIR) $g[m]$ sampled at the chip rate, with an associate coefficient vector

$$\mathbf{g} = [g_0 \ g_1 \ \cdots \ g_{L_c-1}]^{\mathrm{T}}. \tag{2.9}$$

where L_c is the length of CIR. The channel is further corrupted with zero-mean additive white Gaussian noise (AWGN) $v[m]$. Thus, the received chip $r[m]$ can be expressed as

$$r[m] = [g_0 \; g_1 \; \cdots \; g_{L_c-1}] \begin{bmatrix} s[m] \\ s[m-1] \\ \vdots \\ s[m-L_c+1] \end{bmatrix} + v[m]. \tag{2.10}$$

By substituting (2.10) into each element of the received signal vector described in (2.2) we obtain

$$\begin{aligned} \mathbf{r}_{nN} &= \begin{bmatrix} g_0 & g_1 & \cdots & g_{L_c-1} & 0 & \cdots & 0 & 0 \\ 0 & g_0 & g_1 & \cdots & g_{L_c-1} & 0 & \cdots & 0 \\ \vdots & & \ddots & & & \ddots & & \vdots \\ 0 & 0 & \cdots & 0 & g_0 & g_1 & \cdots & g_{L_c-1} \end{bmatrix} \begin{bmatrix} s[nN] \\ s[nN-1] \\ \vdots \\ s[nN-N-L_c+2] \end{bmatrix} + \begin{bmatrix} v[nN] \\ v[nN-1] \\ \vdots \\ v[nN-N-1] \end{bmatrix} \\ &= \mathbf{G} \begin{bmatrix} s[nN] \\ s[nN-1] \\ \vdots \\ s[nN-N-L_c+2] \end{bmatrix} + \mathbf{v}_{nN}. \end{aligned} \tag{2.11}$$

with $\mathbf{G} \in \mathbb{C}^{N \times (N+L_c-1)}$ being the CIR Toplitz convolutional matrix, and $\mathbf{v}_{nN}$ is a vector containing channel noise samples at the chip rate. Since $N + L_c - 1$ transmitted chips $s[m]$ contribute to build $\mathbf{r}_{nN}$,with another d vectors $\mathbf{s}_{iN}, i = n-1(-1)n-d$, where d is given by

$$d = \left\lceil \frac{L_c - 1}{N} \right\rceil. \tag{2.12}$$

will contribute to (2.11). The operator $\lceil \cdot \rceil$ denotes the ceiling operator (round up). We define $f = N \times d - (L_c - 1)$ as the number of chips $s[m]$ required to construct an integer number of transmitted vectors $\mathbf{s}_{iN}$. Therefore, by concatenating the f chip sequence $[s[nN - N - L + 1], s[nN - N - L], \cdots s[(n-d)N]]$ to the vector $[s[nN, s[nN-1], \cdots s[nN-N-L+2]]$ and a zero

matrix $\mathbf{0}_{N\times f}$ to the CIR matrix $\mathbf{G}$, equation (2.11) can be expanded to

$$\mathbf{r}_{nN} = [\mathbf{G}|\mathbf{0}_{N\times f}] \begin{bmatrix} \mathbf{s}_{nN} \\ \mathbf{s}_{(n-1)N} \\ \vdots \\ \mathbf{s}_{(n-d)N} \end{bmatrix} + \mathbf{v}_{nN} \tag{2.13}$$

$$= \tilde{\mathbf{G}} \begin{bmatrix} \mathbf{s}_{nN} \\ \mathbf{s}_{(n-1)N} \\ \vdots \\ \mathbf{s}_{(n-d)N} \end{bmatrix} + \mathbf{v}_{nN}. \tag{2.14}$$

with $\tilde{\mathbf{G}} \in \mathbb{C}^{N\times((d+1)\times N)}$ being the expanded CIR matrix. As we can see that due to the delay introduced by the channel, a set of $d+1$ signal vectors $\mathbf{s}_{iN}$, $i = n(-1)n - d$ are involved in producing the received signal $\mathbf{r}_{nN}$. Now, by using (2.8) we can set

$$\begin{bmatrix} \mathbf{s}_{nN} \\ \mathbf{s}_{(n-1)N} \\ \vdots \\ \mathbf{s}_{(n-d)N} \end{bmatrix} = \begin{bmatrix} \tilde{\mathbf{H}}_{nN} & & & \mathbf{0} \\ & \tilde{\mathbf{H}}_{(n-1)N} & & \\ & & \ddots & \\ \mathbf{0} & & & \tilde{\mathbf{H}}_{(n-d)N} \end{bmatrix} \begin{bmatrix} \mathbf{u}_n \\ \mathbf{u}_{n-1} \\ \vdots \\ \mathbf{u}_{n-d} \end{bmatrix}. \tag{2.15}$$

By substituting equation (2.15) into (2.14) this yields

$$\mathbf{r}_{nN} = \tilde{\mathbf{G}} \begin{bmatrix} \tilde{\mathbf{H}}_{nN} & & & \mathbf{0} \\ & \tilde{\mathbf{H}}_{(n-1)N} & & \\ & & \ddots & \\ \mathbf{0} & & & \tilde{\mathbf{H}}_{(n-d)N} \end{bmatrix} \begin{bmatrix} \mathbf{u}_n \\ \mathbf{u}_{n-1} \\ \vdots \\ \mathbf{u}_{n-d} \end{bmatrix} + \mathbf{v}_{nN}. \tag{2.16}$$

Finally, the equation which represents $\mathbf{r}_{nN}$ as a function of transmitted users symbols is reached and could be simply written in the form

$$\mathbf{r}_{nN} = \mathbf{P}_{nN}\mathbf{u}_n^{(d)} + \mathbf{v}_{nN}. \tag{2.17}$$

with $\mathbf{P}_{nN} \in \mathbb{C}^{N\times((d+1)\times K)}$ being the system matrix which resumes the channel dispersion effect, spreading and scrambling procedures. Note that $\mathbf{u}_n^{(d)}$ includes the current and d previous transmitted symbols of all active users.

In this thesis, the scrambling procedure is not considered any more and the scrambling code is omitted in all future derivations and discussions. Therefore the matrix $\tilde{\mathbf{H}}_{nN}$ is no longer time varying and is equal to $\tilde{\mathbf{H}}$. Hence, the matrix system can simply be expressed as

$$\mathbf{P}_{nN} = \mathbf{P} = \tilde{\mathbf{G}} \begin{bmatrix} \tilde{\mathbf{H}} & & & \mathbf{0} \\ & \tilde{\mathbf{H}} & & \\ & & \ddots & \\ \mathbf{0} & & & \tilde{\mathbf{H}} \\ \cdot & & & \end{bmatrix} \tag{2.18}$$

In other terms, only spreading and the CIR effects are considered in our detection analysis. A phenomenon known as near far effect, where a stronger user signal shadows a weaker one, is not considered here, because in downlink the base station sends all signals through the same channel at the same time from the same place and with same amplitudes. So the mobile station receives all signals with same power. Furthermore, based on our previous assumption on the absence of intra-cell interference, there are no signals from other cells which could shadow our desired signal. Let us now consider the conventional receiver based on the matched filter, where its coefficients given by the spreading sequence of the desired user, as depicted in Fig. 2.4. The performance of this receiver over both AWGN channel and multipath propagation environment is presented next.

2.7 Matched Filter Receiver Performance

In an ideal AWGN channel the length of the CIR is $L_c = 1$. Hence from (2.12) we deduce that the delay is $d = 0$. Therefore the previous transmitted user symbols blocks do not contribute to the received signal vector $\mathbf{r}_{nN}$. Furthermore the matrix system will include only the spreading sequences $\mathbf{P} = \tilde{\mathbf{H}}$, since $\mathbf{G}$=$\mathbf{I}_N$, whereby the equation (2.17) for AWGN channels can be expressed as

$$\mathbf{r}_{nN} = \tilde{\mathbf{H}}\mathbf{u}_n + \mathbf{v}_{nN}. \tag{2.19}$$

In order to detect the nth symbols of all active users, $\mathbf{u}_n$, using the conventional receiver, the received signal is deccorelated by the transpose of the spreading code matrix $\tilde{\mathbf{H}}^{\mathbf{T}}$ as follows

$$\begin{aligned}\hat{\mathbf{u}}_n &= \tilde{\mathbf{H}}^{\mathrm{T}}\mathbf{r}_{nN} \\ &= \tilde{\mathbf{H}}^{\mathrm{T}}\tilde{\mathbf{H}}\mathbf{u}_n + \tilde{\mathbf{H}}^{\mathrm{T}}\mathbf{v}_{nN} \\ &= \mathbf{I}_K\mathbf{u}_n + \hat{\mathbf{v}}_n \\ &= \mathbf{u}_n + \hat{\mathbf{v}}_n. \end{aligned} \tag{2.20}$$

Note that since the spreading codes used here are the normalised Walsh codes, the flipped codes contained in $\tilde{\mathbf{H}}$ are orthogonal and normalised such that $\tilde{\mathbf{H}}^{\mathrm{T}}\tilde{\mathbf{H}} = \mathbf{I}_K$. This means neither MAI or ISI occurring in detection and the desired symbols are only corrupted by the coloured noise $\hat{\mathbf{v}}_n$. Therefore, the matched filter receiver is optimum in AWGN channels. Fig. 2.5 shows the bit error performance of the matched filter receiver of the $N = 16$ QPSK downlink DS-CDMA system over the AWGN channel for various loading conditions. As we can see, loading additional users in the AWGN case does not affect the BER performance of the system. But How the performance of the matched filter will be over a multipath channel?

We now consider the detection of the nth symbol of the lth user signal $u_l[n]$ transmitted over a multipath channel $g[m]$ with $L_c > 1$. For this we need to decorrelate the received signal (2.17) by the flipped spreading sequence of the desired user $\hat{\mathbf{h}}_l$ as follow

$$\begin{aligned}\hat{u}_l[n] &= \hat{\mathbf{h}}_l^{\mathrm{T}}\mathbf{r}_{nN} \\ &= \hat{\mathbf{h}}_l^{\mathrm{T}}\mathbf{P}\mathbf{u}_n^{(d)} + \mathbf{h}_l^{\mathrm{T}}\mathbf{v}_{nN} \\ &= \mathbf{q}_l^{\mathrm{T}}\mathbf{u}_n^{(d)} + \hat{v}_l[n]. \end{aligned} \tag{2.21}$$

with $\mathbf{q}_l$ being the lth user's correlator vector which comprises the ISI and MAI terms. In order to separate and emphasise these interferences the correlator vector $\mathbf{q}_l$ can be divided into $(d+1)$ sub-vectors $\mathbf{q}_{l,i}$ which correspond to the various symbols vectors $\mathbf{u}_{n-i}, i = 0(1)d+1$ such that

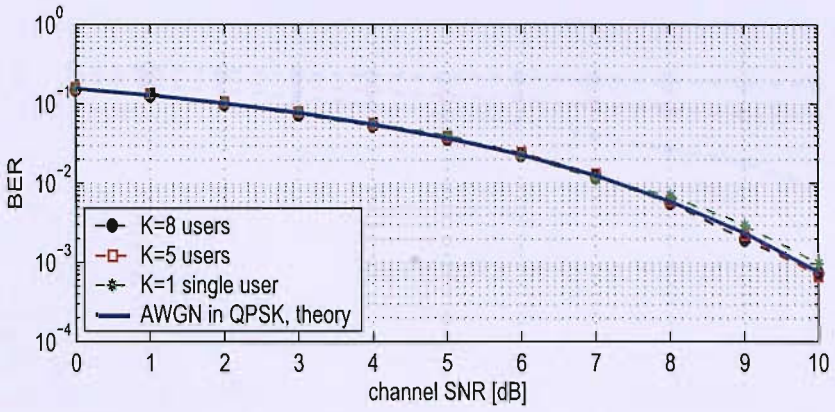

Figure 2.5: optimum performance of the matched filter receiver over AWGN channel

$$\hat{u}_l[n] = \begin{bmatrix} \mathbf{q}_{l,0} \\ \mathbf{q}_{l,1} \\ \vdots \\ \mathbf{q}_{l,d} \end{bmatrix}^{\mathrm{T}} \begin{bmatrix} \mathbf{u}_n \\ \mathbf{u}_{n-1} \\ \vdots \\ \mathbf{u}_{n-d} \end{bmatrix} + \tilde{v}_l[n] \tag{2.22}$$

$$= \sum_{i=0}^{d} \mathbf{q}_{l,i}^{\mathrm{T}} \mathbf{u}_{n-i} + \hat{v}_l[n] \tag{2.23}$$

$$= \sum_{i=0}^{d} \sum_{j=0}^{K-1} q_{l,i}[j] u_j[n-i] + \hat{v}_l[n]. \tag{2.24}$$

$$\tag{2.25}$$

where $q_{l,i}[j]$ represents the contribution of the symbol $u_j[n-i]$ in estimating the symbol $\hat{u}_l[n]$. Equation (2.25) can be rearranged and written in the following form

$$\hat{u}_l[n] = \underbrace{q_{l,0}[l]u_l[n]}_{desired} + \underbrace{\sum_{i=1}^{d} q_{l,i}[l]u_l[n-i]}_{ISI} + \underbrace{\sum_{i=0}^{d} \sum_{\substack{j=0 \\ j\neq l}}^{K-1} q_{l,i}[j]u_j[n-i]}_{MAI} + \underbrace{\hat{v}_l[n]}_{noise}. \tag{2.26}$$

It is obvious that the output signal is formed from 4 terms. The first term is the desired signal and constitutes the symbol of interest attenuated by $q_{l,0}$. The second term is the self-interference term due to ISI, and is highly dependent on the shifted auto-correlation of a spreading sequence. The

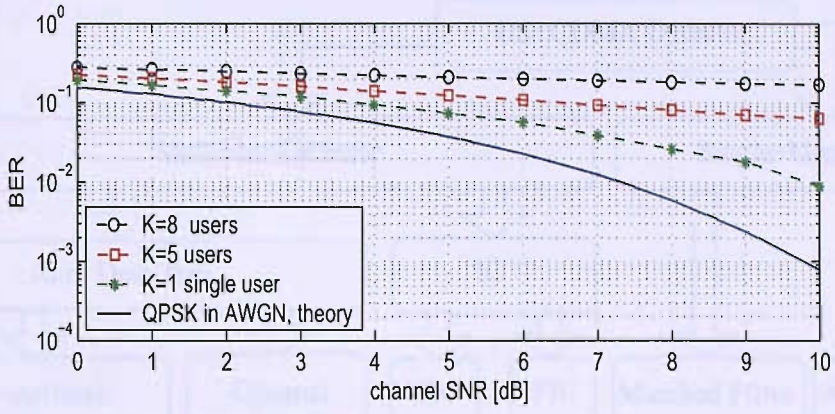

Figure 2.6: effect of MAI on BER performance of the matched filter receiver

third term, of (2.26), includes MAI components due to the shifted cross-correlation of different user's spreading sequences and to the CIR. The last term is the coloured noise. To show the effect of these interferences on the performance of the conventional receiver, we perform the following experiment. We consider a synchronous $N = 16$ DS-CDMA system with various loading of users. The propagation environment adopted is the chip-rate multipath channel represented by its CIR's transfer function

$$G(z) = 0.67 + (0.54 - 0.20j) \cdot z^{-4} + (0.40 + 0.14j) \cdot z^{-7} - 0.20j \cdot z^{-11} \tag{2.27}$$

As it is shown in Fig. 2.6 the BER performance of the matched filter is significantly degraded. The effect of the ISI can be specifically seen from the mismatch between the single user BER plot and the theoretical AWGN curve. Furthermore, as the number of active users increases in the system, additional reductions in the performance of the conventional receiver are occurred. This is mainly due to the increase on the contribution of the third term of equation (2.26) representing MAI. Therefore, the presence of MAI and ISI has a considerable impact on the performance of the traditional detector.

Many research efforts have been directed towards mitigating the effect of MAI and ISI through several areas such as: the design of more powerful forward error correction (FEC) codes to allow acceptable error rate performance [42], the use of adaptive antennas to focus the reception over a narrow desired angle range [9], the design of spreading codes with good correlation proprieties

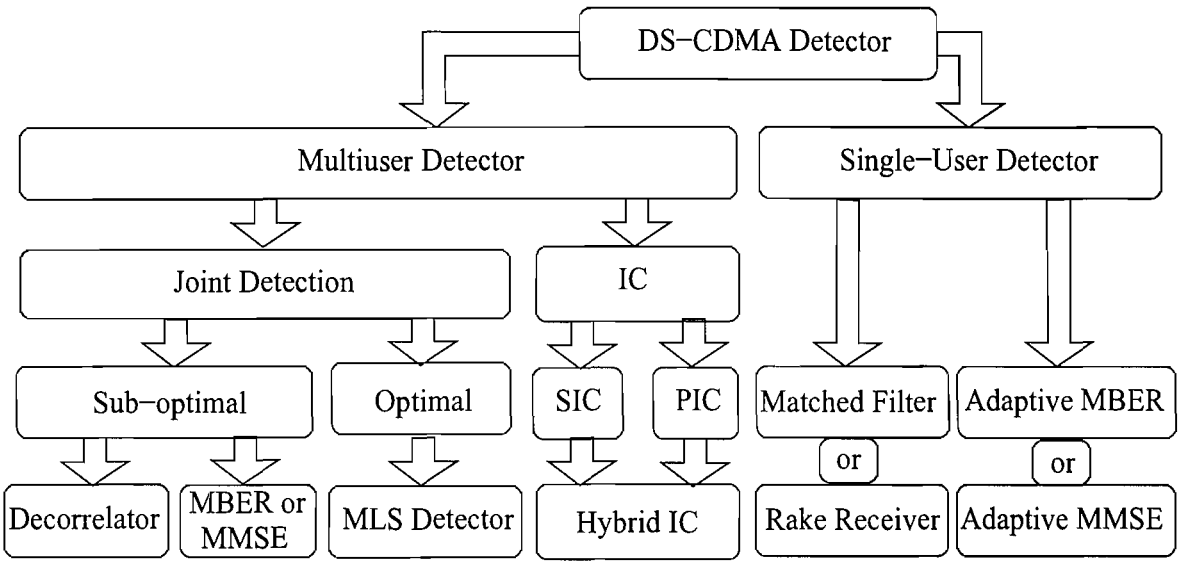

Figure 2.7: Classification of some DS-CDMA detectors

[40], and mainly developing other robust detection strategies.

2.8 Detection Strategies in DS-CDMA

As mentioned previously in this chapter, MAI and ISI limit the capacity of DS-CDMA systems. However, the weak performance of the conventional detector in mitigating those interferences, and the rising needs to increase data throughput in such systems, led to wide investigations and extensive research efforts to introduce a reliable detector, apt to mitigate the effect of MAI and ISI interferences.

In this section, numerous DS-CDMA detector structures are introduced. Most of the proposed detectors can be classified into one of two main categories: multi-user detectors, where information about multiple users is used jointly to better detect each individual user, and single-user detectors, where only information of the user in concern is required. An expanded detector's classification is presented in Fig. 2.7. The interested reader can find additional references and discussions in a number of survey articles and books [6, 43, 7, 8, 9].

2.8.1 Single-User Detection

In single-user strategy each desired user signal is detected separately without regard for other users' signals. In other terms, no prior knowledge or accurate estimations of the remaining users' parameters are required. Hence, the single-user technique is more suitable and practical for the DL situation due to its low complexity and privacy considerations. Several single-user detectors have been proposed in the literature, such as the Rake receiver, the adaptive minimum mean square error (MMSE) and the minimum bit error rate (MBER) detector, all of which we will briefly review below.

Rake Receiver

The Rake receiver is extensively used in detection and adopted by many standards such as WCDMA and IS-95. In the latter it has been even used in both MS and BS terminals. In the Rake receiver, the various channel multipath arrivals are considered as independent receptions of the signal and are exploited to give more beneficial multipath diversity [44]. It basically contains a number of correlators, so-called fingers, for each resolvable path of the channel. The output of these fingers are then either coherently or non-coherently combined in order to improve the signal to noise ratio at the receiver[5].

Adaptive MMSE Detector

Another popular single user detector is the adaptive MMSE receiver. It was initially proposed in [45] for a multi-user detector as MFs bank followed by a linear transformation which minimises the MSE criterion. As matched filtering is a linear operation it can be combined with the linear transformation, therefore the whole MMSE detector can be easily represented as a bank of FIR filters [41], where the MSE criterion can be minimised on a user by user basis. Thus, the MMSE receiver can be considered as a single-user detector where the only knowledge required is the training sequence for the user of interest and no knowledge of other users is required [7].

The adaptive MMSE usually provides good performance and can readily be implemented using standard adaptive filter techniques such us the least mean square (LMS) algorithm.

Adaptive MBER Detector

Since the BER, and not the MSE, is the capital criterion to be examined in order to assess the performance of a receiver in communication systems, a few adaptive detectors based on the MBER solution have been proposed in the literature [46, 47]. Based on the approach of Parzen window or kernel density estimation for approximating the probability density function of the received signal [48], an adaptive algorithm called the least bit error rate LBER is developed [48, 49]. The LBER exhibits promising performance in terms steady state error and convergence speed. In particularly the approximate LBER (ALBER) algorithm has a simple computational complexity similar to the LMS and can be extended to the nonlinear multiuser detection [46].

The single user detectors are inefficient because the interference from other users is treated as noise and there is no utilisation of the available knowledge about the mobile channel and other users. Another weakness due to a phenomena known as the near-far effect; for efficient operation the signals from all users have to arrive at the receiver with approximately the same power; if the signals are unbalanced, the user whose signal is weaker will be swamped by signals of higher power, and the performance of the signal user detector will be severely degraded. Alternatively, multiuser detection can often address these two drawbacks mentioned above.

2.8.2 Multiuser Detection

In multiuser detection, similarly to the conventional detector, a bank of matched filters are used in the front-end to produce a soft output. However, unlike the conventional detector, producing hard decision by means of of its decision device, based on the observations the multiuser receiver jointly estimates all users signals and thus tries to evaluate the interference they create for the user of interest. A significant number of parameters of all active users such as time and phase synchronisation, spreading sequence, power, and channel conditions should be known or estimated a priori.

Multiuser detectors offer potential benefits, such as significant improvement in capacity [9], more efficient spectrum utilisation [43, 9] and optimum near-far resistance [6, 9]. These performance gains result in lower power consumption (increased battery life) and processing gain requirement (lower bandwidth for the same information rates). Multiuser detection techniques can be classified in one of two main categories: Joint detection or interference cancellation

Interference Cancellation

Interference cancellation techniques involve the explicit detection and cancellation of each user's signal from the others. There are two main cancellation techniques: multistage receivers, sometimes called parallel interference cancellation (PIC) and successive interference cancellation (SIC). Such techniques require accurate knowledge of channel parameters and may incur excessive complexity [9].

The SIC is similar to the feedback equaliser [50] used to combat ISI. It detects the data of the strongest user with a conventional detector and then subtracts the signal component due to that user from the received waveform. The process can then be repeated with the resulting waveform which ideally contains no trace of the strongest user, extracting the second strongest user, and so forth. Accurate estimations of the received amplitudes are required.

The PIC technique is based on the same principle but unlike the SIC where only the strongest user at a time is subtracted from the received signal, all the users' interference is removed from the received signal in a parallel approach. Accurate amplitude estimates are critical to the performance of PIC and SIC schemes, with incorrect ordering of user powers, a SIC can lead to degraded performance [50]. For more details about interference cancellation detection refer to [50, 9].

Hybrid SIC and PIC schemes have been proposed in [51, 52], where SIC is first performed on the received signal, followed by a multistage PIC arrangement. This work has been extended to an adaptive hybrid scheme for flat Rayleigh fading channels [53]. In [54] a pilot symbol assisted multistage hybrid successive-parallel cancellation scheme has been proposed. At each stage data estimation is carried out successively for all the users, commencing with the user having the

strongest signal and ending with the weakest signal. For each user, interference from other users is regenerated using the estimates of the current stage for the stronger users and the estimates of the previous stage for the weaker users. Channel estimates are obtained for each user by employing pilot symbols and a recursive estimation algorithm.

Joint Detection

Unlike interference cancellation techniques, where the desired user's signal is extracted after successive or parallel cancellation of interference caused by other users, joint detection can achieve this aim implicitly, using soft estimation of user data. Joint detection can be classified into optimum detection and sub-optimum detection.

Optimum Detection

The optimum detector was initially proposed and analysed by Verdu in 1986 [6]. It compromises of a bank of MFs, one for each user, followed by a Viterbi algorithm [9] for maximum likelihood sequence estimation (MLSE). The optimum detector selects the most likely data based on the observation of the output of the front-end bank of matched filters. The adaptive search for the most likely sequence can be achieved by using a genetic algorithm [5]. In this technique the sequences are updated at each iteration according to certain probabilistic aptly termed genetic operations, known as reproduction, crossover or mutation operations [5].

Despite the near-far resistance property and the considerable capacity gains over conventional detection, the optimum detector is not practical. The Viterbi algorithm's complexity grows exponentially complex with the number of active users and the channel order [6], thus with large user populations or channels with more than a couple of coefficients the optimum detector becomes intractable. Numerous simplified algorithms have been proposed to replace the Viterbi algorithm in an attempt to make this approach less computationally demanding [7, 45, 55]. In the following section we look at suboptimal multi-user detectors that are simpler to implement.

	Signature of desired user	Signatures of interferer	Timing of desired user	Timing of interferer	Relative amplitude	Training sequence
Conventional detector	Yes	No	Yes	No	Yes	No
Optimum Multiuser	Yes	Yes	Yes	Yes	Yes	No
Decorrelator	Yes	Yes	Yes	Yes	No	No
SIC and PIC	Yes	Yes	Yes	Yes	Yes	No
Adaptive MMSE	No	No	Yes	No	No	Yes

Table 2.1: Required knowledge for different DS-CDMA detectors [7]

Suboptimal Detectors

An important class of suboptimal receivers is the linear multi-user detector [56]. This detector has a complexity that is linear on the number of users, by applying a linear transformation to the soft output of the matched filters to reduce the MAI seen by each user. In this section we briefly review the decorrelating detector.

In the decorrelating detector the Viterbi algorithm is replaced by the decorrelator block, in order to decouple the desired data. The decorrelator computes the inverse of the cross-correlation (CCL) matrix which has been constructed from the spreading codes of the users. It has been shown that this decorrelator exhibits the same degree of near-far resistance as the optimum multiuser detector. Thus, we see that the decorrelating detector completely eliminates MAI. However, in a manner analogous to zero forcing equalisation, noise enhancement may be a problem [56]. A large amount of information about all users is still required such as signature waveforms and timing. However, unlike the optimum detector the received amplitudes need not be known or estimated. Different required knowledge about the user of interest and the interfering users of some DS-CDMA detectors discussed so far are summarised in Tab. 2.1 [7].

The optimal near-far resistance property [6] coupled with the fact that it does not require knowledge of the received amplitudes make the decorrelating detector attractive from the standpoint of implementation. However, in addition to noise enhancement, the main disadvantage lies in

the requirement to compute the inverse of the CCL. Using simple inversion algorithms, such as Gaussian elimination, introduce potential problems [9, 56]. Alternative detectors which alleviate the problem of noise enhancement are the multiuser MMSE [57], the multiuser ALBER [46].

Other proposed multi-user detectors and their variations such as the neural network receiver, iterative detection, the maximum a posterior (MAP) have not been covered in this survey. However, the interested reader can find additional references and discussions in [43, 9, 6, 5]. Mainly, there are two drawbacks of multiuser detection for the cellular environment. The first disadvantage is the existence of inter-cell interference [7]. A base station may only have information about its own cell users, i.e. the intra-cell interference. However, information about inter-cell interference might be unavailable, or at best inaccurate and incomplete, which can lead to a severe reduction in the performance of the detector. The second drawback is the difficulty of implementation for the DL [9]. Because matters such as cost, size, and weight are more of a concern for handsets than for base stations, it is not presently practical to adopt multi-user detection techniques in the DL, and its use has therefore been restricted to the UL and operation in the base station.

However, nowadays increasing demand for high data rate services and multimedia applications such as Internet access, videos and graphics in DL transmission pushes research toward exploiting the high capacity gain provided by multiuser detection. In fact, by taking into consideration the following characteristics of the DL:

- DL signals are perfectly synchronised at the transmitter,
- spreading sequences are orthogonal,
- all DL signals face the same dispersive channel,
- the performance of the matched filter receiver over AWGN channels,

the use of a multiuser equaliser to cancel the effect of the multipath channel distortions prior to matched filtering could be a promising solution. The commonly proposed linear multiuser equalisers [11, 12] are based on training or pilot assisted adaptation, which lower the spectrum efficiency. A more advanced class of multiuser equalisers, referred to as blind detectors, does not require explicit knowledge of a training sequence or channel parameters. Instead the parameters are estimated blindly according to certain criteria. A popular blind approach is the minimum

output power (MOE) algorithm blindly cancelling MAI and ISI terms but passing the desired user by code-constraints [8, 58], which is essentially Frost's linearly constrained minimum variance beamformer [59]. Recovering several users at the same time exploits more knowledge of the system and has been performed blindly using a constant modulus (CM) criterion [16, 17, 18], whereby the derived algorithms either neglect spreading [17] or the dispersiveness of the channel [16, 18]. In this work, we are concerned with blind multiuser equalisation using CM criterion.

2.9 Concluding Remarks

This chapter has introduced synchronous DS-CDMA system. A discrete mathematical framework for a baseband model of this system has been derived. By analysing this model, it has been shown that MAI and ISI considerably limit the capacity of such a system. The weak performance of the matched filter receiver in mitigating these interferences has been identified. Therefore, powerful detectors are indispensable. Various alternative detectors proposed in literature have been presented. The multiuser detector exhibits a significant improvement in capacity and spectrum efficiency. However, its complexity and prior knowledge requirement make it unsuitable for application in the DL. Alternatively, promising adaptive blind multiuser equalisation strategies could render multiuser detection practical for such application. In the following chapter, the main adaptive equalisation strategies used to combat the channel distortions are reviewed and discussed.

Chapter 3

Adaptive Equalisation

This chapter discusses the general adaptive equalisation concept. Sec. 3.1 explains how an adaptive equaliser can mitigate ISI introduced by a dispersive channel. The MMSE solution is derived in Sec. 3.2. Next, in Sec. 3.3 the well known least mean square (LMS) adaptive algorithm is highlighted. Then, the need for adaptive blind equalisation in various scenarios is explained in Sec. 3.4. Specifically the blind algorithm so-called the decision-directed (DD) mode is briefly described in Sec. 3.5. Finally, Sec. 3.6 reviews the general concept of the constant modulus algorithm (CMA) and discusses its most important characteristics.

3.1 General Adaptive Equalisation Problem

In digital communication systems, equalisers are mainly designed to combat the multipath effect of the channel which generally causes ISI. A simple model for such systems is illustrated in Fig. 3.1. The equaliser is assumed to be a linear tapped delay line filter with finite impulse response (FIR) of length L, whose coefficients are organised in a vector $\mathbf{w}$,

$$\mathbf{w}^{\mathrm{H}} = [w_0 \; w_1 \; \cdots \; w_{L-1}]. \tag{3.1}$$

This structure is commonly used in practise [37, 60, 61], although other equaliser structures based on e.g. infinite impulse response (IIR) [62] exist. Such architectures can exhibit stability or robustness problems [37, 62] and are beyond the scope of this dissertation. Note that the simple

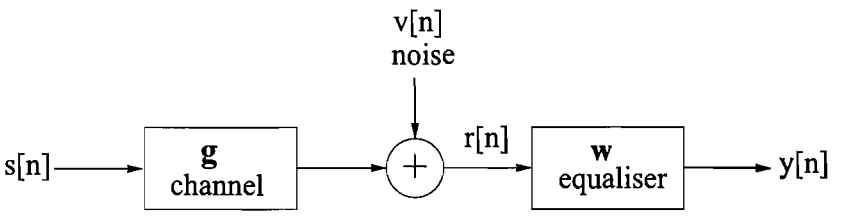

Figure 3.1: Channel equalisation

block diagram in Fig. 3.1 assumes that the channel $\mathbf{g}$ is also a linear tapped delay filter of length L_c with CIR coefficients

$$\mathbf{g} = [g_0 \; g_1 \; \cdots \; g_{L_c-1}]^{\mathrm{T}}. \tag{3.2}$$

This CIR contains the physical channel as well as any filtering at the transmitter and receiver, for example, pulse shaping.

3.2 Mean Square Error Criterion

The ultimate goal of the equaliser is usually to minimise the probability of occurrence of an incorrect decision, or bit error ratio (BER). The BER however is usually a highly non-linear function which limits its implementation in the modern high data rate and dense signalling systems [63]. Although promising efforts in implementing simple filtering structures based on the MBER criterion have recently shown outstanding performance at a moderate computational complexity [49], the MMSE receiver still widely popular due to its maturity and is usually considered as the benchmark to which the performance of other linear equalisers is compared. The MMSE or Wiener-Hopf solution for $\mathbf{w}$ minimises the MSE between the transmitted signal $s[n]$ and the equaliser output $y[n]$.

In the following we aim to derive the Wiener-Hopf or MMSE solution for the equaliser coefficients, by minimising the expected squared magnitude of the error

$$e[n] = y[n] - s[n-\alpha] \quad , \tag{3.3}$$

for a specific choice of delay α in the presence of independent identically distributed (i.i.d.) noise

whose samples are collected in a vector $\mathbf{v}_n$,

$$\mathbf{v}_n = [v[n] \; v[n-1] \; \cdots \; v[n-L+1]]^{\mathrm{T}} \quad . \tag{3.4}$$

First, we collect $s[n]$ and the previous $p = L_c + L - 2$ elements of the source sequence into the vector

$$\mathbf{s}_n = [s[n] \; s[n-1] \; \cdots \; s[n-p]]^{\mathrm{T}} \quad . \tag{3.5}$$

The source signal $s[n]$ is also assumed to be an i.i.d. sequence. With these quantities, the nth equaliser output can be written compactly as

$$y[n] = \mathbf{w}^{\mathrm{H}}\mathbf{G}\mathbf{s}_n + \mathbf{w}^{\mathrm{H}}\mathbf{v}_n \quad . \tag{3.6}$$

with $\mathbf{G} \in \mathbb{C}^{L \times p+1}$ being convolutional matrix[1]

$$\mathbf{G} = \begin{bmatrix} g_0 & g_1 & \cdots & g_{L_c-1} & 0 & \cdots & 0 & 0 \\ 0 & g_0 & g_1 & \cdots & g_{L_c-1} & 0 & \cdots & 0 \\ \vdots & & \ddots & & & \ddots & & \vdots \\ 0 & 0 & \cdots & 0 & g_0 & g_1 & \cdots & g_{L_c-1} \end{bmatrix} \quad . \tag{3.7}$$

By substituting (3.6) into (3.3) we obtain

$$\begin{aligned} e[n] &= \mathbf{w}^{\mathrm{H}}\mathbf{G}\mathbf{s}_n + \mathbf{w}^{\mathrm{H}}\mathbf{v}_n - s[n-\alpha] \\ &= \mathbf{w}^{\mathrm{H}}\mathbf{G}\mathbf{s}_n + \mathbf{w}^{\mathrm{H}}\mathbf{v}_n - \mathbf{f}_\alpha^{\mathrm{H}}\mathbf{s}_n \\ &= \left(\mathbf{w}^{\mathrm{H}}\mathbf{G} - \mathbf{f}_\alpha^{\mathrm{H}}\right)\mathbf{s}_n + \mathbf{w}^{\mathrm{H}}\mathbf{v}_n \quad . \end{aligned} \tag{3.8}$$

with $\mathbf{f}_\alpha \in \mathbb{Z}^{p+1}$ being a vector which represents a pure delay and is given by

$$\mathbf{f}_\alpha^{\mathrm{H}} = [0 \; \cdots \; 0 \; 1 \; 0 \; \cdots \; 0] \quad , \tag{3.9}$$

where the nonzero coefficient is in the αth position, and must satisfy $\alpha \in [0, p]$. Observe that in the absence of noise $\mathbf{v}_n$ a zero ISI can be obtained if the combined channel-equaliser impulse response $\mathbf{G}^{\mathrm{H}}\mathbf{w}$ is equal to the pure delay $\mathbf{f}_\alpha$. However such condition cannot be achieved in the baud-spaced case with finite length equalisers since the system is always over-determined with respect to $\mathbf{w}$.

[1]Note that $\mathbf{G}$ has a similar structure but different size compared to the matrix $\mathbf{G}$ defined in Sec. 2.6.

Under the assumption that the noise and source sequences are i.i.d. processes and mutually uncorrelated, with respective variances σ_v^2 and σ_s^2, the expected value of the magnitude-squared error becomes

$$\begin{aligned}
\mathcal{E}\{|e[n]|^2\} &= \left(\mathbf{w}^{\mathrm{H}}\mathbf{G} - \mathbf{f}_\alpha^{\mathrm{H}}\right)\sigma_s^2\left(\mathbf{G}^{\mathrm{H}}\mathbf{w} - \mathbf{f}_\alpha\right) + \mathbf{w}^{\mathrm{H}}\sigma_v^2\mathbf{w} \qquad (3.10)\\
&= \sigma_s^2\left[\left(\mathbf{w}^{\mathrm{H}}\mathbf{G} - \mathbf{f}_\alpha^{\mathrm{H}}\right)\left(\mathbf{G}^{\mathrm{H}}\mathbf{w} - \mathbf{f}_\alpha\right) + \frac{\sigma_v^2}{\sigma_s^2}\mathbf{w}^{\mathrm{H}}\mathbf{w}\right]\\
&= \sigma_s^2\left[\left(\mathbf{w}^{\mathrm{H}}\mathbf{G} - \mathbf{f}_\alpha^{\mathrm{H}}\right)\left(\mathbf{G}^{\mathrm{H}}\mathbf{w} - \mathbf{f}_\alpha\right) + \lambda\mathbf{w}^{\mathrm{H}}\mathbf{w}\right]\\
&= \sigma_s^2\left[\mathbf{w}^{\mathrm{H}}\mathbf{G}\mathbf{G}^{\mathrm{H}}\mathbf{w} - \mathbf{w}^{\mathrm{H}}\mathbf{G}\mathbf{f}_\alpha - \mathbf{f}_\alpha^{\mathrm{H}}\mathbf{G}^{\mathrm{H}}\mathbf{w} + \mathbf{f}_\alpha^{\mathrm{H}}\mathbf{f}_\alpha + \mathbf{w}^{\mathrm{H}}\lambda\mathbf{I}_L\mathbf{w}\right]\\
&= \sigma_s^2\left[\mathbf{w}^{\mathrm{H}}\left(\mathbf{G}\mathbf{G}^{\mathrm{H}} + \lambda\mathbf{I}_L\right)\mathbf{w} - \mathbf{w}^{\mathrm{H}}\mathbf{G}\mathbf{f}_\alpha - \mathbf{f}_\alpha^{\mathrm{H}}\mathbf{G}^{\mathrm{H}}\mathbf{w} + \mathbf{f}_\alpha^{\mathrm{H}}\mathbf{f}_\alpha\right] \qquad (3.11)
\end{aligned}$$

with $\lambda = \sigma_v^2/\sigma_s^2$ being the inverse of signal to noise ratio (SNR) and $\mathbf{I}_L$ the $L \times L$ identity matrix. Appendix A presents a more comprehensive derivation of the MMSE criterion. As can be seen from (3.10), the MSE contains two terms; the first term symbolises ISI and quantifies the mismatch between the desired pure delay system and the actual combined impulse response. Yet, the second term emphasises the dilemma of amplifying the noise by a factor of $\mathbf{w}^{\mathrm{H}}\mathbf{w}$ which is referred to as the noise gain.

Equation (3.11) reveals that the MSE cost function is a quadratic in the equaliser coefficients and should have a unique extremum. Indeed, Equation (3.11) can be further simplified in order to deduce the unique solution $\mathbf{w}_{opt}$ and its MMSE without performing any complex derivative such as Wirtinger calculus [64]. In fact, as discussed in Appendix A, by using the technique of "completing the square" the expected value of the magnitude-squared error can be written as[2]

$$\mathcal{E}\{|e[n]|^2\} = \sigma_s^2\left[\left(\mathbf{w} - \mathbf{A}^{-1}\mathbf{G}\mathbf{f}_\alpha\right)^{\mathrm{H}}\mathbf{A}\left(\mathbf{w} - \mathbf{A}^{-1}\mathbf{G}\mathbf{f}_\alpha\right) + \mathbf{f}_\alpha^{\mathrm{H}}\left(\mathbf{I}_{p+1} - \mathbf{G}^{\mathrm{H}}\mathbf{A}^{-1}\mathbf{G}\right)\mathbf{f}_\alpha\right], \qquad (3.12)$$

where $\mathbf{A} = \mathbf{G}^{\mathrm{H}}\mathbf{G} + \lambda\mathbf{I}_L$ and $\mathbf{I}_{p+1}$ is the $(p+1)\times(p+1)$ identity matrix. The final expression (3.12) of the MSE criterion remains a function of the system delay α, where the Wiener-Hopf solution $\mathbf{w}_{\mathrm{opt},\alpha}$ for a fixed value α can be readily given as

$$\mathbf{w}_{\mathrm{opt},\alpha} = \left(\mathbf{G}\mathbf{G}^{\mathrm{H}} + \lambda\mathbf{I}_L\right)^{-1}\mathbf{G}\mathbf{f}_\alpha \quad . \qquad (3.13)$$

Therefore, the corresponding MMSE value can be determined as

[2]The derivation here emulates that in [15].

$$\min_{\mathbf{w}} \mathcal{E}\{|e[n]|^2\} = \sigma_s^2 \left[\mathbf{f}_\alpha^{\mathrm{H}} \left(\mathbf{I}_{L_{p+1}} - \mathbf{G}\left(\mathbf{G}^{\mathrm{H}}\mathbf{G} + \lambda \mathbf{I}_L\right)^{-1} \mathbf{G}^{\mathrm{H}}\right) \mathbf{f}_\alpha\right] \quad , \tag{3.14}$$

which is the α^{th} diagonal element of $\sigma_s^2 \left(\mathbf{I}_{p+1} - \mathbf{G}^{\mathrm{H}}\left(\mathbf{G}\mathbf{G}^{\mathrm{H}} + \lambda \mathbf{I}_L\right)^{-1} \mathbf{G}\right)$. Therefore the MMSE solution is admittedly sensitive to the choice of delay α. To illustrate this sensitivity we consider the following experiment.

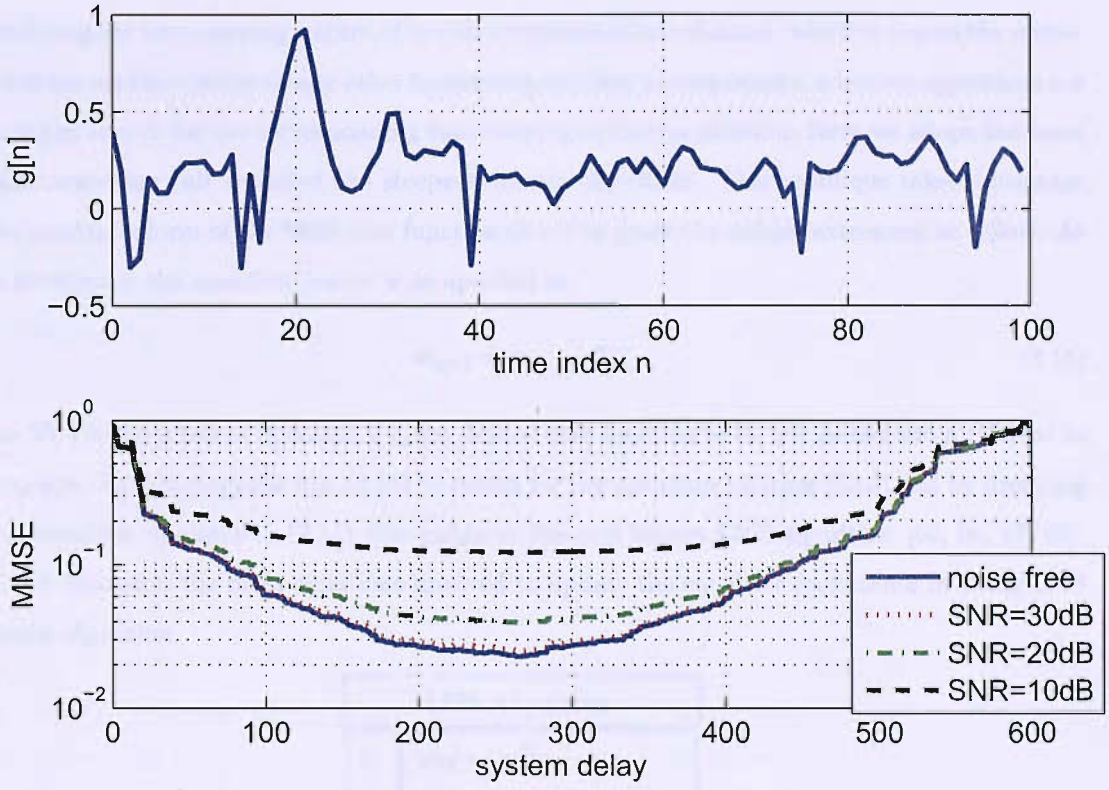

Figure 3.2: (top) The impulse response of the channel $g[n]$, (bottom) the MMSE sensitivity to the system delay α over $g[n]$. .

We assume a $L_c = 100$ taps dispersive channel, represented by its CIR depicted in the top plot of Fig. 3.2, and a baud-spaced equaliser with $L = 500$ coefficients. The bottom plot in Fig. 3.2 shows the four MMSE curves versus the possible system delay α, calculated according to (3.14), which correspond to the noise-free case and noisy corruption with an SNR of 10dB, 20dB, and 30dB. As can be seen, different delays produce a wide range of MMSE values with an optimum solution

which minimises the MMSE function in terms of α. Furthermore as channel noise is introduced, the MMSE curves are flattened and increased in value. Hence, we conclude that proper selection of α is crucial for determing the desired optimum equaliser.

3.3 Adaptive Least Mean Square Algorithm

Considering the time-varying nature of mobile communications channel, which is due to the mobility of either mobile station or any other interacting medium's components, adaptive algorithms are required to search for the corresponding time-varying optimum solution. Here we adopt the most popular searching rule so-called the steepest descent algorithm. This technique takes advantage of the quadratic form of the MSE cost function (3.11) to track the unique extremum as follow. At each iteration n the equaliser vector $\mathbf{w}$ is updated as

$$\mathbf{w}_{n+1} = \mathbf{w}_n - \mu\nabla\xi \tag{3.15}$$

where $\nabla(\cdot)$ is the gradient operator, ξ is the desired cost function to be minimised and μ referred to as step size. By adopting the rule (3.15) to search for the optimum solution (3.13) and by dropping the expectation operator in (3.11) this yields to the well known LMS algorithm [65, 66, 67, 68]. Tab. 3.1 illustrates the main equations involved to update the equaliser coefficients by using LMS adaptive algorithm.

LMS Algorithm	
1:	$y[n] = \mathbf{w}_n^{\mathrm{H}}\mathbf{r}_n$
2:	$e[n] = s[n-\alpha] - y[n]$
3:	$\mathbf{w}_{n+1} = \mathbf{w}_n + \mu\mathbf{r}_n e^*[n]$

Table 3.1: Equations for channel equalisation by LMS adaptive algorithm [65]

Note that $\mathbf{r}_n = [r[n], r[n-1]\cdots r[n-L+1]]$ where L is the equaliser length. LMS has the ability to adapt to the MMSE optimum equaliser coefficients (3.13) on average to the MMSE solution (3.14) from any equaliser initialisation [65]. This global convergence property and LMS's simplicity account for its analytic and empirical maturity, despite its need for a training signal and its relative slow convergence. Many other faster algorithms have been proposed in literature,

such as the recursive least squares (RLS) algorithm, and are beyond the scope of this dissertation due to complexity and stability issues. Excellent studies and references about general adaptive filtering issues can be found in [65, 66].

3.4 Training versus Blind Equalisation

A classical approach in an adaptive receiver is the transmission of the pre-arranged sequence, so-called training sequence. Training sequence is typically a fixed portion of the source sequence which is known a priori at the transmitter and receiver. Certain applications where a training sequence is too costly in terms of bandwidth require a receiver design which operates on the received signal and possibly some statistics of the source. Such an approach is termed blind. Many blind algorithms have been proposed such as second order statistics (SOS) [69, 70], minimum output energy (MOE) [8, 58] and constant modulus algorithm (CMA) which is discussed in more detail in Sec. 3.6. Next, the blind decision-directed algorithm is presented.

3.5 Decision Directed Mode

In the decision-directed (DD) mode the equaliser output $y[n]$ is passed through a non-linear decision device $q(.)$ which estimates the transmitted source symbol $s[n]$. The DD mode is usually used after trained adaptation, by e.g. the LMS algorithm, or after a successful convergence of another blind equalisation algorithm. Lucky [71] recognised that if decisions are correct, the reference sequence $s[n]$ in the LMS's error can be replaced with the estimate $q(y[n])$. This blind algorithm is thus termed Adaptive Decision Directed Algorithm. Tab. 3.2 illustrates the main equations involved to update the equaliser coefficients by using DD algorithm.

DD Algorithm	
1:	$y[n] = \mathbf{w}^{\mathrm{H}}\mathbf{r}_n$
2:	$e[n] = q(y[n]) - y[n]$
3:	$\mathbf{w}_{n+1} = \mathbf{w}_n + \mu \mathbf{r}_n e^*[n]$

Table 3.2: Equations for channel equalisation by DD adaptive algorithm

The DD mode has the ability to track slowly varying changes in the channel without explicit need for a training sequence and converges to the MMSE equaliser (3.13) when initialised at an open-eye setting [72]. However, the reliability of the DD basically depends on the reliability of the source estimate $q(y[n])$. Typically in a blind equalisation scenario another blind technique, which operates from a cold start settings such as the CMA, is used to reduce the error probability sufficiently in order to permit a successful switch to the DD mode.

3.6 Constant Modulus Algorithm

The constant modulus (CM) criterion was first proposed by Godard in [13] and developed independently by Treichler and Agee in [14]. The stochastic gradient descent implementation, or constant modulus algorithm (CMA), is widely used in practise. CMA is arguably the most popular blind algorithm for cold start-up of tapped-delay-line equaliser structures [37]. Godard's original intention was to develop an algorithm for phase and amplitude-modulated signals, for example QAM, which decoupled equalisation and carrier recovery so that carrier phase tracking could be accomplished at the equaliser output in DD mode [13]. Treichler and Agee's original intention was to develop a criterion which sensed multipath induced amplitude modulation (AM) on an otherwise constant envelope frequency modulation (FM) signal [14].

The CM criterion attempts to fit a power of the modulus of the equaliser output to a constant. This constant is chosen to essentially project all constellation points onto a circle. Mathematically from [13] this criterion is expressed as

$$\mathcal{E}\Big\{\left(|y[n]|^p - \gamma_p\right)^2\Big\} \quad , \tag{3.16}$$

with

$$\gamma_p = \frac{\mathcal{E}\{|s[n]|^{2p}\}}{\mathcal{E}\{|s[n]|^p\}} \quad , \tag{3.17}$$

whereby γ_p is often called the dispersion constant of the constellation. The case $p = 1$ is usually attributed to Sato [73]. We study solely the case $p = 2$ in the sequel and henceforth the term CMA refers to the $p = 2$ case. Tab. 3.3 illustrates the main equations involved to update the equaliser coefficients $w[n]$ by using the CMA algorithm. These equations are obtained by adopting the rule (3.15) and by dropping the expectation operator in (3.16).

CMA Algorithm	
1:	$y[n] = \mathbf{w}^{\mathrm{H}}\mathbf{r}_n$
2:	$e[n] = (\gamma_2^2 - \lvert y[n]\rvert^2)y[n]$
3:	$\mathbf{w}_{n+1} = \mathbf{w}_n + \mu \mathbf{r}_n e^*[n]$

Table 3.3: CMA equations at symbol rate iteration n

Since CMA uses the absolute value of $y[n]$, the algorithm is insensitive to the phase error, which can be caused by carrier frequency offset and or/and unknown channel phase [13]. Hence, carrier frequency offset estimation can be established separately after CMA equalisation.

3.6.1 Convergence Speed of CMA

The basic CMA discussed above as well as many other blind algorithms based on non-convex cost functions, exhibits local minima and slow convergence speed to the global solutions [74, 15]. There have been numerous attempts to improve the typical CMA slow convergence [75, 76, 77]. One can implement a CMA cost function for example with lattice filter equalisers [75], or with affine projection algorithm (APA) [76] or simply use the recursive least squares (RLS) [77]. It is known that for trained equalisers, these approaches show faster convergence speed than LMS type algorithms [65, 66, 78], however they require higher precision than the LMS as well as a higher computational complexity [74]. In order to obtain faster converging algorithms with CMA by using these algorithms, some modifications are needed. The Lattice CMA (LCMA), first proposed in [75] has shown faster convergence than the basic CMA. Similar modification has been adopted for RLS CMA where a simple version of this algorithm is presented in [66]. The APA CMA described in [76] has simpler structure than the lattice CMA and RLS CMA and it is known for its ability to escape from local minima as discussed in [76]. Note that there are other approaches which aim to speed up the convergence rate of CMA and not covered here such as the conjugate gradient search CMA [79] and normalised CMA [80]. Basically, the above approaches try to apply already known fast converging algorithms to CMA. The resulting convergence speeds are faster than that of a standard CMA. However, the increase of convergence speed is not as great as what may be expected from the RLS or Lattice algorithms with training sequences [74]. This is because the CM cost function being minimised differs significantly from the MSE, for which these algorithms

have originally been designed.

3.6.2 Ill-Convergence and Initialisation

Unlike the MSE, the CM cost function is a non-convex multi-modality function [15, 81]. Yet, in addition to the global minima other stationary points which includes saddles, local minima and maximum have been distinguished on the error surface of the CM cost function [81]. LeBlanc has counted these stationary points under non-correlated source assumption [81]. For example, since the CM criterion operates purely on the magnitude, not on the phase, of the equaliser output, all phase shifted versions of the MSE optimum solution also minimise the CM cost function. Other local minima of the CM error surface can correspond to other reasons such as the possible choices of system delay, additive noise and insufficient equaliser length [63]. Note, also the existence of the local maximum at the origin. It is shown that the origin is the only maximum of the CMA surface . Treichler and Agee recognise the local maximum and suggest it can be avoided by proper equaliser initialisation, whereby the traditional all zero initial vector should not be used [63].

A proper equaliser initialisation remains an open research issue, with various ideas in the literature [74]. The well-known strategy is the centre tap initialisation, proposed by Godard in [13]. On this technique the equaliser's centre tap is set to a non-zero constant greater than a threshold value and the remaining taps to zero.

3.7 Concluding Remarks

This chapter has reviewed the general concept of adaptive equalisation in digital communications. The Wiener receiver which is based on minimising the MSE has been highlighted. The LMS adaptive algorithm has been briefly presented. Then, the need for adaptive blind equalisation such as the DD mode is stressed. Finally, the concept of the CMA and its ill-Convergence issues have been discussed.

Chapter 4

Blind Multiuser FIRMER CMA Equaliser

In this chapter, we propose a new blind multiuser equalisation strategy for downlink DS-CDMA systems, the so-called filtered-R multiple error CM algorithm (FIRMER-CMA). We start by introducing the algorithm's cost function, discussing its local solutions, and deriving the corresponding stochastic gradient search in Sec. 4.1. The following Sec. 4.2 is dedicated to assess the convergence behaviour and the BER performance of the proposed algorithm. In fact, FIRMER-CMA presented in Sec. 4.1 is only suitable for fully loaded scenarios and single rate transmissions. In Sec. 4.3, partially loaded systems are considered, whereby three different methods which exploit inactive users' codes are proposed and compared. For multi-rate transmissions, two modified versions of FIRMER-CMA, using either variable spreading length (VSL) or multi-code (MCD) schemes, are derived and analysed in Sec. 4.4. Furthermore, an improved version of FIRMER-CMA is proposed where its implementation flexibility is discussed in Sec. 4.5. Finally, Sec. 4.6 introduces a new strategy based on the concept of virtual users which further reduces the FIRMER-CMA's computational complexity.

4.1 Standard FIRMER-CMA Receiver

As discussed in Chap. 2, transmissions over a dispersive channel destroy the mutual orthogonality of the codes which are used to multiplex the various users in downlink DS-CDMA systems. As a result, the code-demultiplexed users' signals are subject not only to ISI due to channel dispersion but also to MAI due to the loss of code orthogonality. In order to re-establish orthogonality of the codes, a chip level equaliser can be utilised [82, 83]. In fact, by introducing an equaliser in front of the matched filter, an optimum detection can be obtained if a perfect equalisation (zero ISI and MAI) is achieved. Furthermore, unlike in UL where different users are subject to different dispersive channels, in the DL users' signals are synchronous and go through the same medium rendering equalisation a simpler task.

Various blind equalisation techniques, which can simultaneously mitigate MAI and ISI and improve bandwidth efficiency, have been proposed [8, 84, 17]. The CM based multiuser equaliser is by far the most popular scheme. It has very low computational requirements and readily meets the real-time computational constraint, as mentioned in Chap. 3. In [84, 17], blind schemes based on the CM criterion have been performed which require either additional orthogonality constraints or mutual decorrelation of the recovered users' sequences. In this work, we propose a robust blind multiuser strategy, which exploits the CM criterion of all active users and is simpler than [84, 17] because neither orthogonality constraint nor mutual deccorelation are required. In the following, the derivation of the proposed algorithm is motivated and presented.

4.1.1 Demultiplexed User Signals

We consider the DS-CDMA downlink system in Fig. 4.1. This model is a simplified replica of the baseband model represented in Fig. 2.4, where a chip level equaliser $w[m]$ is introduced. The blocks p/s and s/p represent parallel to serial and serial to parallel converters, respectively. The analysis of this model using the conventional receiver has been presented in detail in Secs. 2.5, 2.6 and 2.7 . Here, we are concerned with blindly adapting the equaliser coefficients, where the system is fully loaded with $K = N$ multiple synchronous users, which for simplicity are assumed to have the same rate. First we derive the detected signal $\hat{u}_l[n]$ as a function of the chip rate equaliser w.

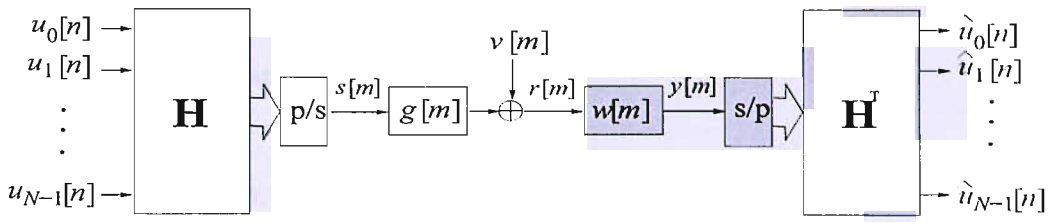

Figure 4.1: DS-CDMA downlink signal model with a chip rate equaliser.

Then, we state a suitable cost function based on which the equaliser can be adapted.

The code sequence for decoding the lth user by matched filtering, contained in a vector $\mathbf{h}_l$, can be taken from an $N \times N$ Hadamard matrix $\mathbf{H}$. Therefore, the lth user is thus decoded as

$$\begin{aligned}\hat{u}_l[n] &= \tilde{\mathbf{h}}_l^{\mathrm{T}} \cdot \begin{bmatrix} y[nN] \\ y[nN-1] \\ \vdots \\ y[nN-N+1] \end{bmatrix} \\ &= \tilde{\mathbf{h}}_l^{\mathrm{T}} \cdot \begin{bmatrix} \mathbf{w}^{\mathrm{H}} & & \mathbf{0} \\ & \mathbf{w}^{\mathrm{H}} & \\ & & \ddots \\ \mathbf{0} & & \mathbf{w}^{\mathrm{H}} \end{bmatrix} \cdot \begin{bmatrix} r[nN] \\ r[nN-1] \\ \vdots \\ r[nN-L-N+2] \end{bmatrix}\end{aligned}$$

where $\tilde{\mathbf{h}}_l$ is the flipped version of the lth user's spreading vector $\mathbf{h}_l$. The vector $\mathbf{w} \in \mathbb{C}^L$ contains the equaliser's L chip-spaced complex conjugate weights. Rearranging $\mathbf{w}$ and $\tilde{\mathbf{h}}_l$ yields

$$\begin{aligned}\hat{u}_l[n] &= \mathbf{w}^{\mathrm{H}} \cdot \begin{bmatrix} \tilde{\mathbf{h}}_l^{\mathrm{T}} & & \mathbf{0} \\ & \tilde{\mathbf{h}}_l^{\mathrm{T}} & \\ & & \ddots \\ \mathbf{0} & & \tilde{\mathbf{h}}_l^{\mathrm{T}} \end{bmatrix} \cdot \begin{bmatrix} r[nN] \\ r[nN-1] \\ \vdots \\ r[nN-L-N+2] \end{bmatrix} \\ &= \mathbf{w}^{\mathrm{H}} \, \mathbf{H}_l \, \mathbf{r}_{nN}, \end{aligned} \tag{4.1}$$

with $\mathbf{H}_l \in \mathbb{Z}^{L \times (N+L-1)}$ being a convolutional matrix comprising the lth user's flipped code vector $\tilde{\mathbf{h}}_l^{\mathrm{T}}$ and $\mathbf{r}_{nN} \in \mathbb{C}^{N+L-1}$. Note that $\mathbf{H}_l$ contains the decoding process of only the l th user's signal

and differs from $\mathbf{H}_{nN}$ presented in Sec. 2.6, which comprises the whole process of spreading and scrambling at the base station transmitter.

4.1.2 Cost Function

We assume that the users's signals $u_l[n]$ consist of symbols with a constant modulus γ, such as QPSK, or PAM. Therefore, we would like to blindly adapt the equaliser by forcing all the decoded symbols $\hat{u}_l[n]$ onto a constant modulus. This can be formulated, similarly to [17, 85], by a suitable cost function ξ_{CM},

$$\xi_{\mathrm{CM}} = \mathcal{E}\left\{\sum_{l=0}^{N-1}(\gamma^2 - |\hat{u}_l[n]|^2)^2\right\}, \tag{4.2}$$

which measures deviation of each of the N users' decoded symbols from the desired modulus[1]. The optimum equaliser coefficients $\mathbf{w}$ are given by

$$\mathbf{w}_{\mathrm{opt,CM}} = \arg\min_{\mathbf{w}} \xi_{\mathrm{CM}}. \tag{4.3}$$

There is no unique solution to (4.3), since minimising (4.2) is ambiguous with a manifold of solutions due to an indeterminism in phase rotation. However, any member of this manifold is a suitable solution for the equaliser $\mathbf{w}$, and can be used in combination with differential modulation schemes to recover $u_l[n]$.

Examples. Two examples for ξ_{CM} with $N = 4$ users employing QPSK with $\gamma = 1$ over a distortion-less and delay-less noise-free channel are given in Figs. 4.2 and 4.3. Fig. 4.2 shows ξ_{CM} in dependency of an equaliser $\mathbf{w}$ with a single complex coefficient w_0. The cost function shows that there is a manifold of solutions satisfying $|w_0| = \gamma$.

Fig. 4.3 presents a case, where the equaliser contains two coefficients which are constrained to be real, and therefore the cost function ξ_{CM} possesses two symmetric solutions $\mathbf{w}_{\mathrm{opt,CMA}} = [\pm 1 \;\; 0]^{\mathrm{T}}$ only. Note that the solutions $\mathbf{w} = [0 \;\; \pm 1]^{\mathrm{T}}$ would not synchronise the codes correctly and therefore have large cost function values associated.

[1] Other cost functions, such as $\mathcal{E}\{(\gamma^2 - |\hat{u}_l[n]|^2)^2\}$ with i arbitrary, have been suggested. While there is reason to believe that such a reduced cost function might be viable, our simulations have found that convergence cannot be achieved unless contributions from all users are taken into account. Our investigation into this is ongoing but beyond the scope of this thesis

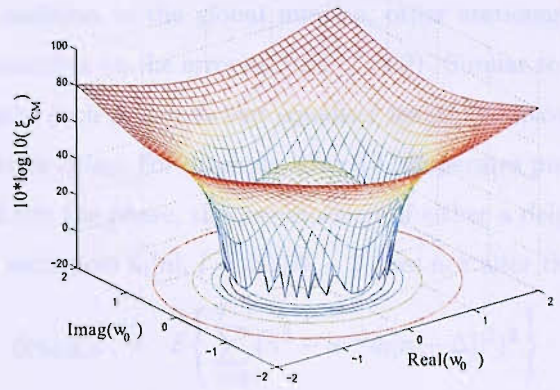

Figure 4.2: Cost function ξ_{CM} in dependency of a single complex valued coefficient w_0.

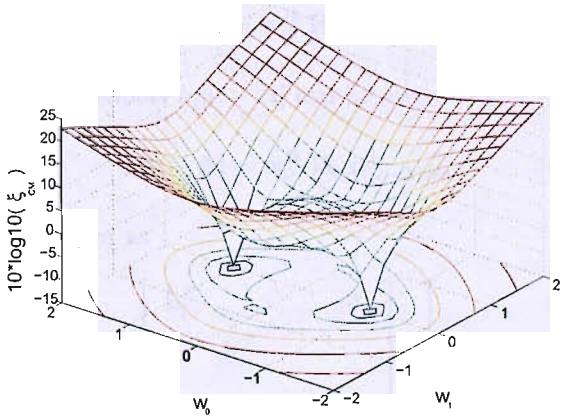

Figure 4.3: Cost function ξ_{CM} in dependency of a two coefficient equaliser $\mathbf{w} = [w_0 \;\; w_1]^{\mathrm{T}}$, which is constrained to be real.

4.1.3 Discussion of Local Solutions

The proposed cost function (4.2) is a non-convex multi-modal function since it is based on CM criterion. Therefore, in addition to the global minima, other stationary points including local minima are expected to manifest on the error surface of (4.2). Similar to CM, these local minima appear due to many reasons such as insufficient equaliser length, additive noise, phase ambiguity and various choices of system delay. For example, since (4.2) operates purely on the magnitude of the decoded symbols and not the phase, the introduction of either a delay Δ or a phase rotation ϕ to the infinite received sequences $\hat{u}_l[n]$, $l = 0(1)N-1$ does not alter the cost function value,

$$\begin{aligned} \xi_{\mathrm{CM},\Delta,\phi} &= \mathcal{E}\left\{\sum_{l=0}^{N-1}(\gamma^2 - |e^{j\phi}\hat{u}_l[n-\Delta]|^2)^2\right\} \\ &= \mathcal{E}\left\{\sum_{l=0}^{N-1}(\gamma^2 - |\hat{u}_l[n]|^2)^2\right\} \quad . \end{aligned} \tag{4.4}$$

Since the phase ambiguity can be resolved by differential encoding, only the effect of the delay Δ is considered next.

We assume an equaliser $\mathbf{w}_0$ which produces $\{\hat{u}_l[n], l = 0(1)N-1\}$ and optimises the MSE solution on the error surface (4.2). Therefore, by using (4.1) we obtain

$$\hat{u}_l[n] = \mathbf{w}_0^{\mathrm{H}}\, \mathbf{H}_l\, \mathbf{r}_{nN}, \tag{4.5}$$

Similarly to (4.5), the delayed symbols $\hat{u}_l[n-\Delta]$ can be given by

$$\hat{u}_l[n-\Delta] = \mathbf{w}_0^{\mathrm{H}}\, \mathbf{H}_l\, \mathbf{r}_{(n-\Delta)N}, \tag{4.6}$$

Alternatively, (4.6) can be written as

$$\begin{aligned} \hat{u}_l[n-\Delta] &= [\mathbf{0}_{N\Delta}^{\mathrm{H}} \quad \mathbf{w}_0^{\mathrm{H}}] \cdot \begin{bmatrix} \tilde{\mathbf{h}}_l^{\mathrm{T}} & & \mathbf{0} \\ & \tilde{\mathbf{h}}_l^{\mathrm{T}} & \\ & & \ddots \\ \mathbf{0} & & \tilde{\mathbf{h}}_l^{\mathrm{T}} \end{bmatrix} \cdot \begin{bmatrix} r[nN] \\ r[nN-1] \\ \vdots \\ r[(n-\Delta)N-L-N+2] \end{bmatrix} \\ &= \hat{\mathbf{w}}^{\mathrm{H}}\, \hat{\mathbf{H}}_l\, \hat{\mathbf{r}}_{nN}, \end{aligned} \tag{4.7}$$

with $\hat{\mathbf{H}}_l \in \mathbb{Z}^{(N\Delta+L)\times(N(\Delta+1)+L-1)}$ being the expanded convolutional matrix, $\hat{\mathbf{r}}_{nN} \in \mathbb{C}^{N(\Delta+1)+L-1}$ is the expanded received vector and $\hat{\mathbf{w}} \in \mathbb{C}^{N\Delta+L}$ is the expanded equaliser vector. Note that $\mathbf{0}_{N\Delta} \in \mathbb{Z}^{N\Delta}$ refers to a vector with $N\Delta$ zero elements.

Therefore, by considering $\hat{\mathbf{w}}$ as the new equaliser to be determined, it can be seen from (4.7) that the equaliser with coefficients shifted by $\alpha = N\Delta$ chips, is also an optimum solution to (4.2). Observe that the allowed shift values have to be be multiples of N in order to synchronise the system. Bearing in mind that the range of permitted shifts α is limited by the finite lengths of both the channel and the equaliser, as discussed in Sec. 3.2, the number of local minima in (4.2), generated from the system delay ambiguity, is decreased by a factor of N compared to the standard single user CM error surface.

Note that further reduction on the number of possible local solutions, which are due to the delay ambiguity, can be achieved by introducing the scrambling code. In the latter case, only shifts α which are multiple of the least common multiple of the spreading factor N and the period of the scrambling code, which is usually greater than N, lead to a synchronised scenario.

Example. In this example, we consider ξ_{CM} with either $N = 1$ (the standard CM cost function) or $N = 4$ users (multiuser case) employing BPSK with $\gamma = 1$ over a noisy channel which is described by its chip rate transfer function $G(z) = \frac{1}{1-0.125z^{-1}}$ under SNR = 25 dB. The adopted equaliser has two coefficients w_0 and w_1, wich are constrained to be real valued.

Fig. 4.4 shows the cost function ξ_{CM} and the corresponding contour for $N = 1$ (top) and for $N = 4$ (bottom) in dependency of the two equaliser's real taps w_0 and w_1. As can be seen, the standard CM cost function exhibits four minima. In addition to two global minima at $[\pm 1 \quad \mp 0.125]^{\mathrm{T}}$, two local minima exist at $[0 \quad \pm 1]^{\mathrm{T}}$, which show higher cost due the insufficient equaliser length. In fact, the latter minima correspond to the delay $\alpha = 1$. On the other hand, the bottom plots in Fig. 4.4 for the multiuser case $N = 4$ show two global minima at $[\pm 1 \quad \mp 0.125]^{\mathrm{T}}$ only, which correspond to the delay $\alpha = 0$. The two vectors $[0 \quad \pm 1]^{\mathrm{T}}$ do not synchronise this system and therefore are not associated with local minima but have large cost function values.

4.1.4 Blind Adaptation

A simple stochastic gradient descent update rule for $w[m]$ can be found by calculating the gradient of an instantaneous cost function, i.e. omitting the expectation operator in (4.2),

$$\hat{\xi}_{\mathrm{CM}} = \sum_{l=0}^{N-1} (\gamma^2 - |\hat{u}_l[n]|^2)^2 \quad . \tag{4.8}$$

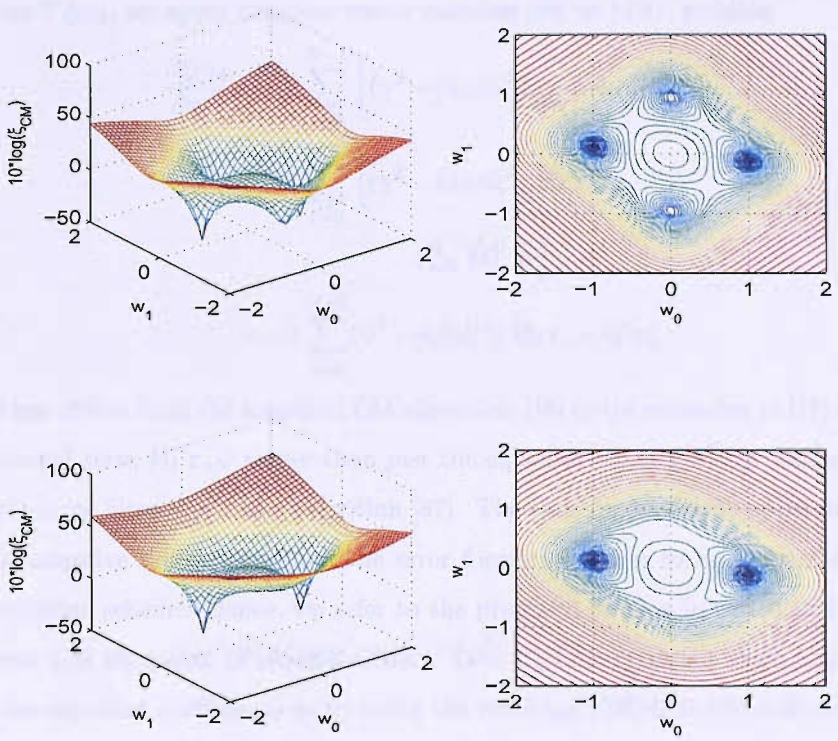

Figure 4.4: Cost function ξ_{CM} and the corresponding contour for $N = 1$ (top) and for $N = 4$ (bottom).

The resulting terms are then minimised w.r.t. $\mathbf{w}$ to obtain instantaneous estimates of the cost function gradient $\nabla\hat{\xi}(\mathbf{w}_n)$, leading to the stochastic gradient update

$$\mathbf{w}_{n+1} = \mathbf{w}_n - \mu\nabla\hat{\xi}_{\mathrm{CM}}(\mathbf{w}_n) \tag{4.9}$$

where μ is the step size. The intrinsic inaccurate estimates of the true underlying statistics in the update routine introduces gradient noise. This can assist the adaptation process in avoiding slow convergence in the vicinity of saddle points of the cost function.

To determine $\nabla\hat{\xi}_{\mathrm{CM}}$, we apply complex vector calculus [86] to (4.8), yielding

$$\begin{aligned}
\frac{\partial\hat{\xi}_{\mathrm{CM}}}{\partial\mathbf{w}^*} &= -2\sum_{l=0}^{N-1}\left[(\gamma^2 - |\hat{u}_l[n]|^2)\frac{\partial}{\partial\mathbf{w}^*}\,\hat{u}_l[n]\hat{u}_l^{\mathrm{H}}[n]\right] \\
&= -2\sum_{l=0}^{N-1}\Big[(\gamma^2 - |\hat{u}_l[n]|^2)\,\mathbf{H}_l\,\mathbf{r}_{nN}\cdot \\
&\qquad\qquad \cdot\,\mathbf{r}_{nN}^{\mathrm{H}}\,\mathbf{H}_l^{\mathrm{H}}\,\mathbf{w}\Big] \\
&= -2\sum_{l=0}^{N-1}(\gamma^2 - |\hat{u}_l[n]|^2)\,\mathbf{H}_l\,\mathbf{r}_{nN}\,\hat{u}_l^*[n]
\end{aligned} \tag{4.10}$$

This algorithm differs from the standard CM algorithm [15] or its extension in [17] in the inclusion of a code filtered term $\mathbf{H}_l\,\mathbf{r}_{nN}$ rather than just the equaliser input $r[n]$. It is structurally similar to a multiple-error filtered-X LMS algorithm [87]. The transfer functions appearing in the paths between the adaptive filter output and the error formations have to be accounted by modifying the LMS updating scheme. Hence, we refer to the proposed scheme in (4.10) as filtered-Receiver multiple-error CM algorithm (FIRMER-CMA). Tab. 4.1 illustrates the main equations involved to update the equaliser coefficients $\mathbf{w}$ by using the resulting FIRMER-CMA algorithm.

4.1.5 Computational Complexity

The computational complexity discussed in this section is based on counting the total number of complex operations (multiplications, additions and divisions) involved at each iteration. In fact, the number of real operations involved can be easily deduced from the number of complex operations. Effectively, a complex multiplication contains four real multiplications and two real additions and a complex addition includes two real additions[2]. Therefore, by following the

[2]While it is possible to exert only three real valued multiplications for a complex one, this comes at the cost of an increased number of additions [88], and is therefore not considered here.

FIRMER-CMA Algorithm	
1:	$\mathbf{x}_l[nN] = \mathbf{H}_l\, \mathbf{r}_{nN}$, for $l = 0(1)N-1$
2:	$\hat{u}_l[n] = \mathbf{w}_n^{\mathrm{H}} \mathbf{x}_l[nN]$, for $l = 0(1)N-1$
3:	$e_l[n] = (\gamma^2 - \lvert\hat{u}_l[n]\rvert^2)\hat{u}_l[n]$, for $l = 0(1)N-1$
4:	$\mathbf{w}_{n+1} = \mathbf{w}_n + \mu \sum_{l=0}^{N-1} \mathbf{x}_l[nN] e_l^*[n]$

Table 4.1: Equations for multiuser channel equalisation by FIRMER-CMA adaptive algorithm at symbol rate iteration n.

Algorithm steps	complex multiplications	complex addition
1:	N^2L	NL(N-1)
2:	NL	N(L-1)
3:	2N	N
4:	NL+L	NL
FIRMER-CMA	N^2L+2NL+2N+L	$N^2L + NL$

Table 4.2: Computational complexity of individual steps of FIRMER-CMA refer to the operations listed in Tab. 4.1.

FIRMER-CMA's steps, described in Tab. 4.1, the computational complexity of each step and of the whole algorithm is calculated and summarised in Tab. 4.2. Note that L is the equaliser length and N is the spreading factor or the number of users. Observe that the complexity presented in Tab. 4.2 is only for fully loaded and single rate systems. In case of other modes like partially loaded or multi-rate scenarios, the complexity can be easily obtained by considering the small modifications to be described in Sec. 4.3 and Sec. 4.4.

As can be seen from Tab. 4.2, the FIRMER-CMA exhibits a moderate complexity of the order of $\mathcal{O}(N^2L)$. Note that the latter complexity is calculated in order to retrieve the N users' symbols $\hat{u}_l[n]$, $l = 0(1)N-1$. In fact, either(i) cost per user symbol or (ii) cost per chip can be simply computed by dividing the total cost by N. In both cases, the algorithm is of the order of $\mathcal{O}(NL)$. Hence, the two factors to be considered in lowering the computational complexity of FIRMER-CMA are the equaliser length L and the number of users N. The former could be considerably

minimised by adopting fractionally spaced equalisers [15]. For example, for T/2-spaced equaliser it is sufficient to choose L to be equal to the length of the channel L_c rather than three or five times L_c as is generally the case for baud-spaced equalisers [63]. Furthermore, channel shortening techniques could be deployed to minimise the length of the channel itself to an effective and manageable length [89]. For minimising N, we propose a new multiuser equalisation approach in Sec. 4.6. It will be demonstrated that this approach can dramatically reduce the computational complexity and provides a faster adaptation speed by adopting the concept of virtual users.

4.2 Standard FIRMER-CMA Performance

For the simulations below, we consider a fully loaded synchronous DS-CDMA system, where the modulation scheme adopted is QPSK. We apply the FIRMER-CMA to two different channel impulse responses, a short $g_1[m]$ and a more dispersive $g_2[m]$, as characterised by the following chip rate transfer functions

$$G_1(z) = 0.89 + (0.36 - 0.27j)\, z^{-1} + 0.09\, z^{-3} \tag{4.11}$$

$$G_2(z) = 0.67 + (0.54 - 0.27j)z^{-4} + (0.41 - 0.07j)z^{-7} - 0.20jz^{-11} \tag{4.12}$$

The corresponding modulus and phase of these impulse responses and their pole-zero maps are shown in Fig. 4.5. Observe that the channel $g_2[m]$ has zeros near the unit circle which render the equalisation of this channel a difficult task due to the enhancement of noise at certain frequencies where nulls are located. In the following, we first demonstrate the convergence behaviour in Sec. 4.2.1 and then the bit error performance in Sec. 4.2.2.

4.2.1 Convergence

In order to demonstrate the convergence behaviour of the proposed algorithm, we transmit $N = 16$ QPSK user signals over $g_1[m]$ in the absence of channel noise, and utilise the FIRMER-CMA to update an equaliser with 10 coefficients. The adaptation is initialised with the second coefficient in the weight vector set to unity, while the optimal response will need to place the maximum

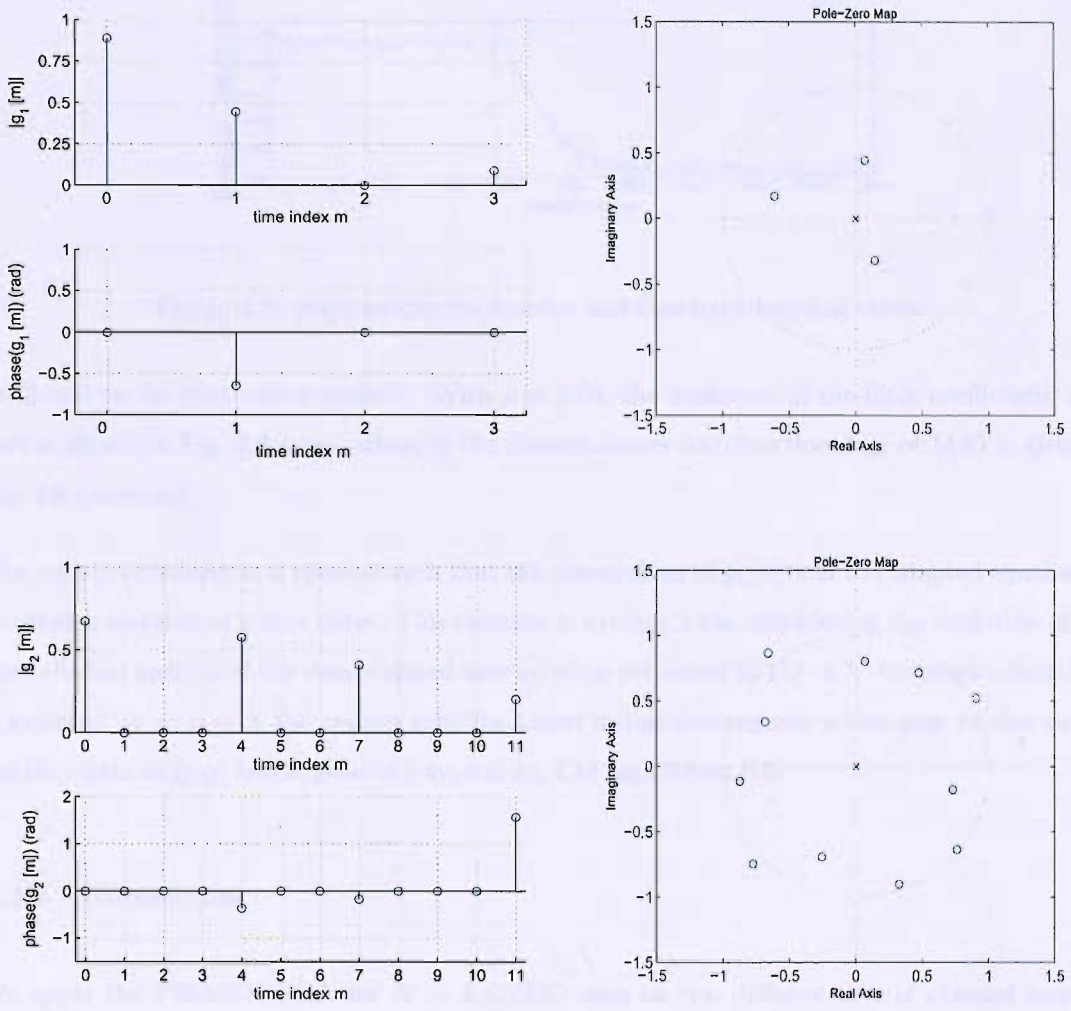

Figure 4.5: Modulus and phase of complex valued channel impulse responses $g_1[m]$ (top) and $g_2[m]$ (bottom) and their pole-zero maps.

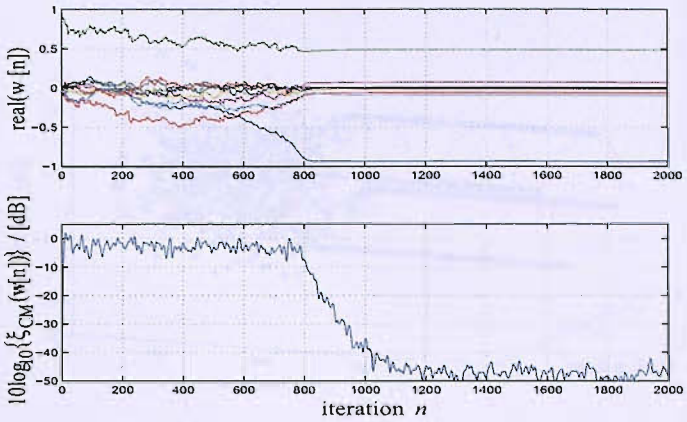

Figure 4.6: (top) weight trajectories and (bottom) learning curve.

coefficient in the first vector element. With $\mu = 0.05$, the evolution of the filter coefficients' real part is shown in Fig. 4.6 (top), whereby the instantaneous cost function $\hat{\xi}_{\mathrm{CM}}$ of (4.8) is given in Fig. 4.6 (bottom).

The system converges to a solution such that the convolution of $g_1[m]$ and the adapted equaliser is a complex rotation of a zero delay. This rotation is evident when considering the evolution of the constellation pattern of the demodulated user $u_0[n]$ as presented in Fig. 4.7. Although adaptation is switched on at $n = 0$, the system exhibits a slow initial convergence which may be due to the saddle points in ξ_{CM}, but is generally typical for CM algorithms [15].

4.2.2 Robustness

We apply the FIRMER-CMA for $N = 4$ QPSK users to two different sets of channel impulse responses. Both sets include 200 independent fixed channels and have the delay power spectral densities $|g_1[m]|$ and $|g_2[m]|$ depicted in Fig. 4.5. The multipath coefficients of both channel sets are drawn from Rayleigh distributions. The FIRMER-CMA is allowed sufficient time to reach its steady-state for each fixed channel realisation. The various BER curves for delay-corrected and rotation-corrected systems are compared to their analytic MMSE equaliser performances and to the theoretical performance of QPSK over a non-dispersive AWGN channel. The equaliser lengths adopted are $L = 20$ and $L = 64$ for the two channel sets represented by $|g_1[m]|$ and $|g_2[m]|$ respec-

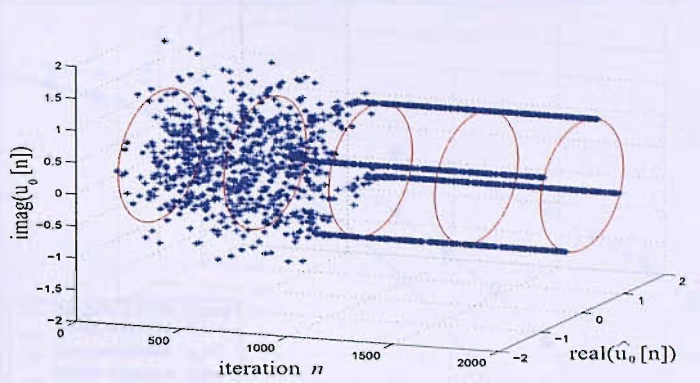

Figure 4.7: Evolution of the received constellation pattern of user $l = 0$.

tively. With the middle tap set to unity the algorithm has always been given 10^3 symbol periods to converge prior to correction of the phase rotation and bit error rate (BER) measurement. The BER results are given in Fig. 4.8 in comparison to the optimal QPSK performance in AWGN and the analytical minimum MSE (MMSE) solution. Note that the FIRMER-CMA closely approaches the MMSE performance.

In order to explore the steady-state performance of the system, the magnitude profile $|g_2[m]|$ in Fig. 4.5(right) has been used to produce an ensemble of random channel responses with Rayleigh distributed coefficients. We use this system to explore the influence of the step size parameter μ on the convergence. The various BER curves for rotation-corrected systems are compared to their analytic MMSE equaliser performances. The latter are chosen to realise a delay of $L/2 = 32$ chips for every channel, while the FIRMER-CMA is initialised with the centre coefficient set to unity. The results for step sizes of $\mu = 0.001$, $\mu = 0.0003$, and $\mu = 0.0001$ are given in Fig. 4.9, and compared to the theoretical performance of QPSK over a non-dispersive AWGN channel, as well the MMSE BER curve. It can be seen that for small values of μ, the steady-state performance of FIRMER-CMA approaches the MMSE performance closely. However, for larger μ the performance is seriously degraded, particularly when operating in higher SNR regions.

Therefore, better BER performance can be obtained by decreasing the step size μ. Nevertheless, small values of μ result in a slow convergence of the algorithm. A possible solution is to use FIRMER-CMA as a start-up algorithm whose sole job is to open the initially closed eye sufficiently

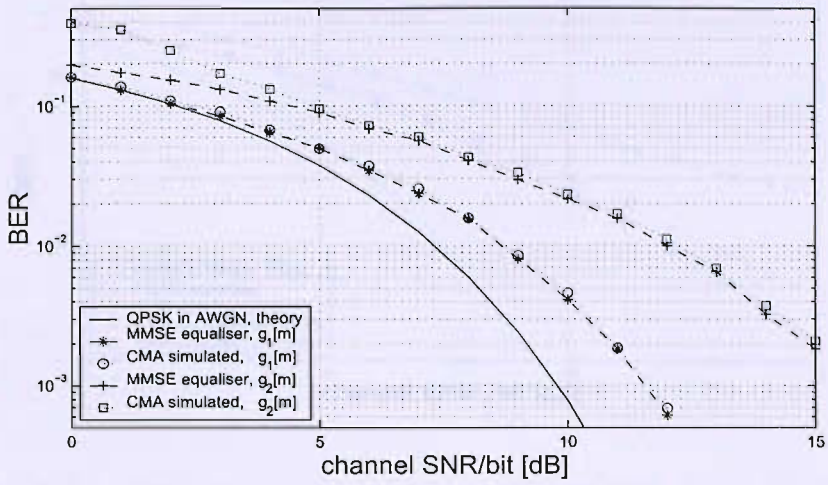

Figure 4.8: BER performance of the proposed FIRMER-CMA over two channels in dependency of the channel SNR compared to an analytical MMSE channel equaliser and the BER in an AWGN channel.

so that e.g. a decision directed (DD) mode could be implemented successfully [72]. However, the start-up algorithm is not always able to achieve the required switching level of MSE. Alternatively, another solution has been proposed in [90] for single user systems, whereby the DD mode operates concurrently with CMA rather than switching to DD after CMA convergence. Recently, a new promising low-complexity algorithm based on switching from the CMA to a soft decision directed mode (SDD) has been derived in [91]. The latter exhibits faster convergence rate, lower steady-state error and lower computational cost than the concurrent CMA-DD algorithm [91].

4.3 Partially Loading Scenario

As yet, the FIRMER-CMA equaliser has only been adapted over fully loaded channels where all available spreading codes, for a specific N, have been exploited. In fact, it has been observed, based on extensive simulations, that such equaliser has failed to converge once at least one of the available codes has not been considered during adaptation. Therefore, for partially loaded system inactive users should be considered during adaptation in order to ensure convergence. In this section, we address how the FIRMER-CMA equaliser can be updated even if not all possible

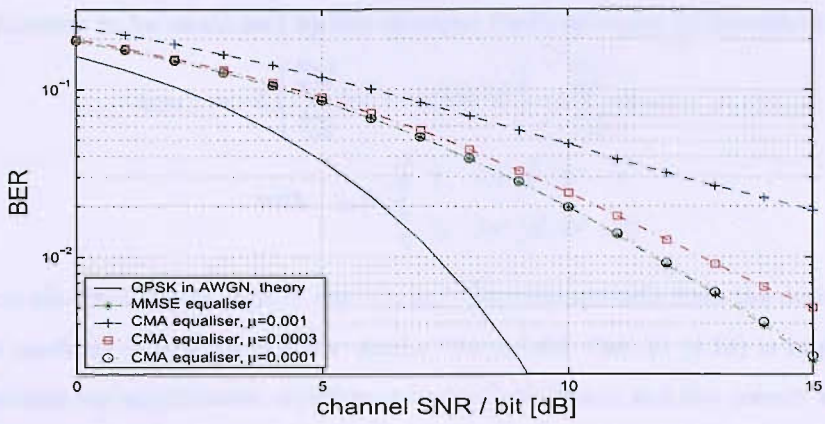

Figure 4.9: Steady-state BER performance of the proposed FIRMER-CMA with various step sizes μ over an ensemble of channels with average magnitude profile $|g_2[m]|$ as shown in Fig. 4.5(b), in comparison an analytical MMSE channel equaliser and the BER in a distortion-less AWGN channel.

users are active, i.e. the system is partially loaded. We propose and compare three different methods: (i) a mean square error criterion for absent users, and a CM approach with (ii) zero modulus or (iii) the transmission of arbitrary signals with small code amplitude. For all three cases, stochastic gradient descent algorithms are derived. The proposed algorithms are analysed and compared through various simulations, which demonstrate the algorithms' convergence and BER performances.

4.3.1 Modified Cost Functions

We consider the DS-CDMA downlink model in Fig. 4.1 with a maximum of N symbol-synchronous active users, which for simplicity are assumed to have the same rate. In the case of a partially loaded system with $K \leq N$, we assume the first K users with signals $u_l[n]$, $l = 0(1)K-1$, to be active, while for the remaining $K-N$ user signals $u_l[n] = 0$, $l = K(1)N-1$ and $\forall n$. Yet, the algorithm presented above in Sec. 4.1.4 is only suitable for fully loaded scenarios, whereby inactive users are not considered. In the following, we discuss three possible modified cost functions which may be suitably minimised for partially loaded systems.

CM Algorithm. By allowing different modulo γ_l for the various decoded signals $\hat{u}_l[n]$, we can set $\gamma_l = 0$ for the remaining $N-K$ inactive users signals $u_l[n] = 0$ for $l = K(1)N-1$. Thus, a

suitable cost function to be minimised by the equaliser coefficients can be formulated as ξ_{CM},

$$\xi_{\mathrm{CM}} = \mathcal{E}\left\{\sum_{l=0}^{N-1}(\gamma_l^2 - |\hat{u}_l[n]|^2)^2\right\} = \sum_{l=0}^{N-1}\xi_{\mathrm{CM},l} \tag{4.13}$$

$$\text{with} \quad \gamma_l = \begin{cases} \gamma, & l \in [0;\ K-1] \\ \tilde{\gamma}, & l \in [K; N-1] \end{cases}$$

which measures the deviation of each of the N users' decoded symbols from the desired modulus. Note that the modulus $\tilde{\gamma}_l = 0$ for inactive users. The second term in (4.13) is important to be included, otherwise the equalisation criterion is under-determined and the correct signals would not necessarily be extracted in the despreading operation. The decoded signals $\hat{u}_l[n]$ of inactive users contain channel noise and an MAI term. The minimisation of (4.13) mitigates the MAI effect on the inactive users and hence ensures that the overall system is fully determined.

CM Algorithm with Signal Injection. Alternative to setting $\tilde{\gamma}_l = 0$ for inactive users, arbitrary constant modulus user signals with a finite $\tilde{\gamma}_l \ll \gamma$ may be injected at the transmitter. This permits to persistently excite the system during adaptation, particularly if the DS-CDMA downlink is sparsely loaded. Yet, this has the disadvantage of somewhat increasing the transmitted signal power. A similar problem is however encountered in pilot-based adaptation schemes [92, 83].

CM/MSE Algorithm. Different from (4.13), driving the decoded inactive user signals to zero can also be accomplished in the mean squared error (MSE) sense, such that a combined CM/MSE cost function arises:

$$\xi_{\mathrm{CM/MSE}} = \sum_{l=0}^{K-1}\xi_{\mathrm{CM},l} + \sum_{l=K}^{N-1}\xi_{\mathrm{MSE},l} \tag{4.14}$$

$$\text{with} \quad \xi_{\mathrm{MSE},l} = \mathcal{E}\left\{|\hat{u}_l[n]|^2\right\} \quad .$$

The equaliser coefficients $\mathbf{w}$ can be determined such that the above cost functions are minimised. However, a manifold of solutions

$$\mathbf{w}_{\mathrm{opt}} = \arg\min_{\mathbf{w}} \xi_{\mathrm{CM}} \qquad \text{or} \quad \mathbf{w}_{\mathrm{opt}} = \arg\min_{\mathbf{w}} \xi_{\mathrm{CM/MSE}} \tag{4.15}$$

exists due to an ambiguity with respect to a complex rotation $e^{j\varphi}$, $\varphi \in [0; 2\pi]$, which cannot be resolved by any of the above criteria.

4.3.2 Stochastic Gradient Descent Algorithms

Simple adaption rules for the equaliser can be obtained by considering stochastic gradient descent techniques, whereby iterative update rules are utilised for the equaliser coefficients $\mathbf{w}_n$ at time n,

$$\begin{aligned} \mathbf{w}_{n+1} &= \mathbf{w}_n - \mu \nabla \hat{\xi} \\ &\text{with} \quad \hat{\xi} \in \left\{ \hat{\xi}_{\mathrm{CM}}, \hat{\xi}_{\mathrm{CM/MSE}} \right\} \end{aligned} \tag{4.16}$$

where μ is the algorithm step size and ∇ is the gradient operator applied to instantaneous cost functions $\hat{\xi}_{\mathrm{CM}}$ and $\hat{\xi}_{\mathrm{CM/MSE}}$. These instantaneous estimates are obtained from (4.13) and (4.14) by dropping expectation operations, resulting in

$$\hat{\xi}_{\mathrm{CM}} = \sum_{l=0}^{N-1} \hat{\xi}_{\mathrm{CM},l} = \sum_{l=0}^{N-1} (\gamma_l^2 - |\hat{u}_l[n]|^2)^2 \tag{4.17}$$

and

$$\hat{\xi}_{\mathrm{CM/MSE}} = \sum_{l=0}^{K-1} (\gamma_l^2 - |\hat{u}_l[n]|^2)^2 + \sum_{l=K}^{N-1} |\hat{u}_l[n]|^2, \tag{4.18}$$

where the instantaneous MSE related expression is referred to as LMS term. Similarly to the derivation of (4.10), the gradient terms can be obtained for the CM components of the instantaneous cost functions as

$$\frac{\partial \hat{\xi}_{\mathrm{CM},l}}{\partial \mathbf{w}^*} = -2(\gamma_l^2 - |\hat{u}_l[n]|^2)\, \mathbf{H}_l\, \mathbf{r}_{nN}\, \hat{u}_l^*[n], \tag{4.19}$$

and the gradient components of the MSE part of the instantaneous cost function can be derived as

$$\begin{aligned} \frac{\partial \hat{\xi}_{\mathrm{LMS},l}}{\partial \mathbf{w}^*} &= \frac{\partial}{\partial \mathbf{w}^*} (\mathbf{w}^{\mathrm{H}}\, \mathbf{H}_l\, \mathbf{r}_{nN}\, \mathbf{r}_{nN}^{\mathrm{H}}\, \mathbf{H}_l^{\mathrm{H}}\, \mathbf{w}) \\ &= \mathbf{H}_l\, \mathbf{r}_{nN}\, \hat{u}_l^*[n]. \end{aligned} \tag{4.20}$$

This permits to assemble stochastic gradient descent algorithms according to (4.16) for the various cost functions derived in Sec. 4.3.1. In the following, we refer to the third proposed updating rule based on (5.3) and (4.20) as FIRMER-CM/LMS algorithm.

4.3.3 Performance Comparison

The three stochastic gradient algorithms derived in Sec. 4.3.2 will be compared below for the two previous channel impulse responses given in Sec. 4.2. We first demonstrate and compare the convergence behaviour and then the bit error performance.

Convergence. In order to demonstrate and compare the convergence behaviour of the proposed algorithms, we utilise an $N = 16$ DS-CDMA downlink system to transmit $K = 12$ active QPSK users' signals over $g_1[m]$ in the absence of channel noise. The three proposed algorithms update the chip-level equaliser with $L = 10$ coefficients. The adaptation is initialised with the second coefficient in the weight vector set to unity. With the step size selected such as to obtain maximum convergence speed without incurring divergence, the evolution of the filter coefficients' real part for the three algorithms is shown in Fig. 4.10 compared to a $K = N = 16$ fully loaded system. The learning curves in Fig. 4.10 are the instantaneous cost functions $\hat{\xi}_{\text{CM}}$ in (4.17) and $\hat{\xi}_{\text{CM/MSE}}$ in (4.18) given in Fig. 4.11.

It can be noted from Figs. 4.10 and 4.11 that the algorithms succeed to minimise their cost functions, whereby a remaining error floor is due to model truncation. The injection of 4 QPSK signals with a small modulus for the inactive users can be seen to improve the convergence of the system somewhat compared to setting $\tilde{\gamma} = 0$. In contrast, the fully loaded system, which can be interpreted as a partially loaded system with $\tilde{\gamma} = \gamma$, can attain a faster rate, i.e. the convergence rate increases with increasing the modulus of the injected signals. Yet, the partially loaded FIRMER-CM/LMS outperforms the fully loaded system and has the additional advantage of a lower implementational cost and no increase of the power of the transmitted signals.

Bit Error Rate. For a spreading factor of $N = 8$ with $K = 6$ active users, we have adopted the previous three algorithms under various SNR conditions. An ensemble of random channel implementations with Rayleigh distributed coefficients fulfilling the magnitude profile of $|g_2[m]|$ has been employed, whereby the equaliser has a length of with $L = 64$ coefficients. With the centre tap set to unity and an appropriately adjusted μ, the algorithms have been given 10^3 symbol periods in all cases to converge prior to the correction of the phase rotation and the bit error ratio (BER) measurement. The BER results are given in Fig. 4.12 in comparison to the optimal QPSK performance in a dispersion-free AWGN channel and the analytical MMSE solution. Note that the three proposed algorithms show similar bit error performance and closely approach the MMSE performance, except for the FIRMER-CM cases at high SNR due to insufficient convergence, and at low SNR for all cases.

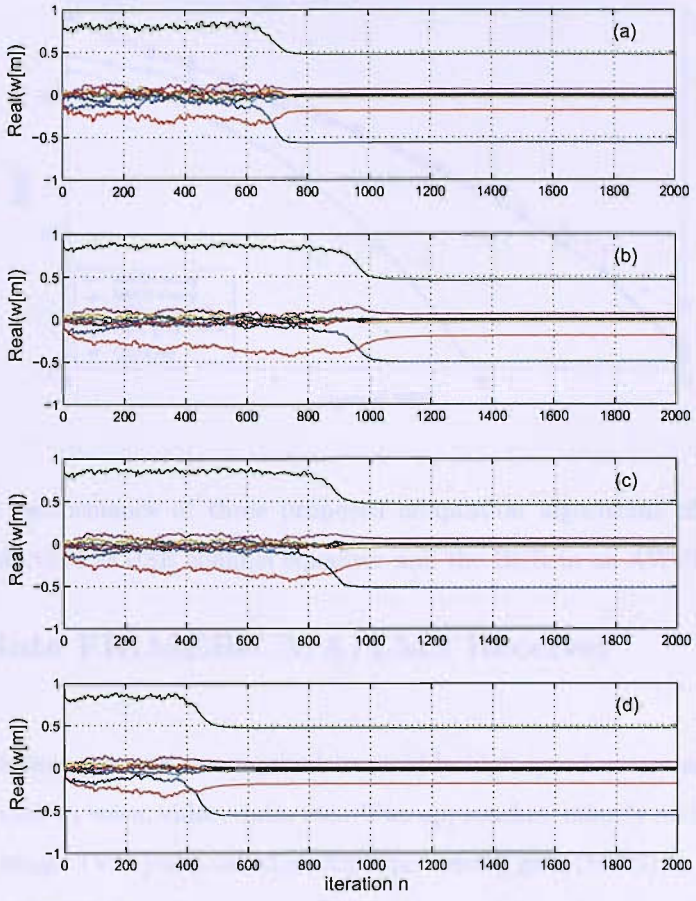

Figure 4.10: Weight trajectories of the (a) fully loaded system ($N = K = 16$) updated by FIRMER-CMA, and partially loaded systems ($N = 16$ and $K = 12$) updated by (b) FIRMER-CMA with $\tilde{\gamma} = 0$, (c) FIRMER-CMA with $\tilde{\gamma} = 0.1$, and (d) the combined FIRMER-CM/LMS algorithm.

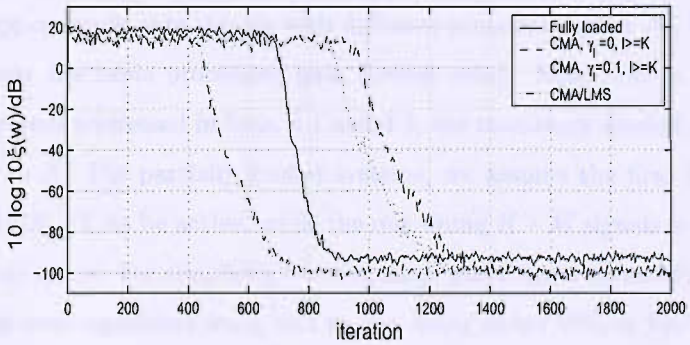

Figure 4.11: Learning curves corresponding to the cases in Fig. 4.10.

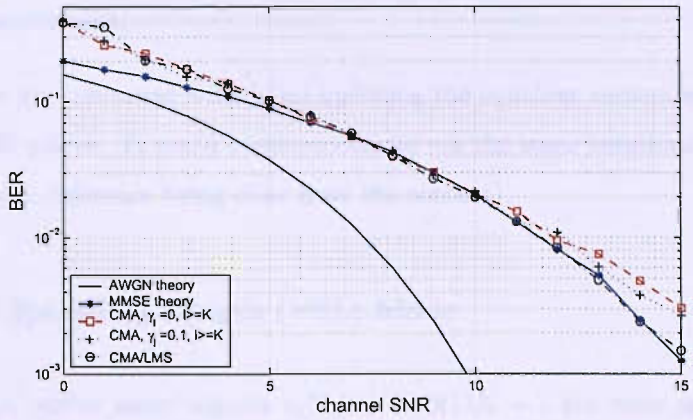

Figure 4.12: BER performance of three proposed adaptation algorithms of the channel SNR compared to an analytical MMSE channel equaliser and the BER in an AWGN channel.

4.4 Multi-Rate FIRMER-CMA/LMS Receiver

Next generation wireless systems are required to provide high-speed access and support various multi-rate services such as voice, video, data, etc.. Two approaches, namely multi-code (MCD) and variable spreading length (VSL) also called multiple processing gain (MPG) or variable processing gain (VPG) access schemes, have been proposed to support such multi-rate services [93, 94]. This section addresses the required modifications to FIRMER-CMA/LMS algorithm, proposed above in Sec. 4.3 to suit both VSL and MCD multi-rate modes.

We consider a DS-CDMA downlink model with a maximum of M symbol-synchronous active users, which can support multi-rate signals with different processing gains N_l, $l = 0(1)M-1$. Let $N = \max(N_l)$ denote the basic processing gain (lowest rate). Note that in case of single rate systems, such as the ones addressed in Secs. 4.1 and 4.3, the maximum symbol-synchronous active users will be equal to N. For partially loaded systems, we assume the first $K \leq M$ users with signals $u_l[n_l]$, $l = 0(1)K-1$, to be active, while the remaining $K-M$ signals are zeros, where n_l is the lth user's symbols index. For simplicity, we rearrange users' order to satisfy $N_0 \leq N_1 \cdots \leq N$. Specifically, two chip-level equalisers $\mathbf{w}_{\mathrm{VSL}}$ and $\mathbf{w}_{\mathrm{MCD}}$, using either VSL or MCD multi-rate access modes respectively, are proposed and tested. Both equalisers can be updated by minimising two hybrid CM/MSE cost functions based on the CM criterion for the active users and an MSE

criterion for the inactive ones.

In the following, we are concerned with blind updating the equaliser vectors $\mathbf{w}_{\mathrm{VSL}}$ and $\mathbf{w}_{\mathrm{MCD}}$ of both VSL and MCD modes. To avoid cumbersome, we use the same notations for both VSL and MCD derivations (the difference being clear from the context).

4.4.1 Variable Spreading Length (VSL) Mode

In the VSL scheme, active users' signals $u_l[n_l]$, $l = 0(1)K-1$ are code multiplexed using a fixed chip duration and Walsh sequences with different lengths N_l in order to ensure a multi-rate transmission. Hence, the sequence for decoding the lth user is contained in a vector $\mathbf{h}_l^{N_l}$, which can be taken from an $N_l \times N_l$ Hadamard matrix. By following similar derivation steps as presented in Sec. 4.1, the demultiplexed users' signals, cost function and the stochastic gradient adaptation rule can be reformulated to suit the VSL mode.

Demultiplexed User Signals. The lth user is thus decoded as

$$\begin{aligned}\hat{u}_l[n_l] = \mathbf{w}_{\mathrm{VSL}}^{\mathrm{H}} \cdot & \begin{bmatrix} (\tilde{\mathbf{h}}_l^{\mathrm{N_l}})^{\mathrm{T}} & & & \mathbf{0} \\ & (\tilde{\mathbf{h}}_l^{\mathrm{N_l}})^{\mathrm{T}} & & \\ & & \ddots & \\ \mathbf{0} & & & (\tilde{\mathbf{h}}_l^{\mathrm{N_l}})^{\mathrm{T}} \end{bmatrix} \cdot \begin{bmatrix} r[n_l N_l] \\ r[n_l N_l - 1] \\ \vdots \\ r[n_l N_l - L - N_l + 2] \end{bmatrix} \\ = \; & \mathbf{w}_{\mathrm{VSL}}^{\mathrm{H}} \, \mathbf{H}_l^{\mathrm{N_l}} \, \mathbf{r}_{n_l N_l}, \end{aligned} \tag{4.21}$$

with $\mathbf{H}_l^{\mathrm{N_l}} \in \mathbb{C}^{L \times (N_l + L - 1)}$ being a convolutional matrix comprising of the lth user's flipped code vector $\tilde{\mathbf{h}}^{\mathrm{N_l}}$ and $\mathbf{r}_{n_l N_l} \in \mathbb{C}^{N_l + L - 1}$. Where $\mathbf{w}_{\mathrm{VSL}} \in \mathbb{C}^{L}$ contains the equaliser's L chip-spaced complex conjugate weights of VSL system.

Cost Function. We adopt the structure of the cost function proposed for FIRMER-CMA/LMS in Sec. 4.3.1 for single user system. Hence, for the VSL scheme we define

$$\xi_{\mathrm{VSL}} = \sum_{l=0}^{K-1} \mathcal{E}\left\{(\gamma^2 - |\hat{u}_l[n_l]|^2)^2)\right\} + \sum_{l=K}^{M-1} \mathcal{E}\left\{(|u_l[n_l]|)^2\right\}) \quad . \tag{4.22}$$

Stochastic Gradient Adaptation. Since the VSL mode uses different spreading factors N_l, the equaliser vector $\mathbf{w}_{\mathrm{VSL}}$ can be updated at different rates. Here, we adopt the highest rate corresponding to the lowest spreading factor N_0 as our iteration unit, in order to obtain faster convergence. However, we should note that at each iteration not all users' symbols can contribute to updating the equaliser vector due to the difference in the lengths of spreading sequences. Therefore the adaptation rule can be written as

$$\begin{aligned} \mathbf{w}_{\mathrm{VSL},n_0+1} &= \mathbf{w}_{\mathrm{VSL},n_0} + \mu \sum_{l=0}^{K-1} \left\{ (\gamma^2 - |\hat{u}_l[n_l]|^2) \mathbf{H}_l^{\mathrm{N_l}} \mathbf{r}_{n_l N_l} \, \hat{u}_l^*[n_l] \right\} + \\ &\quad + \sum_{l=K}^{M-1} \left\{ \mathbf{H}_l^{\mathrm{N_l}} \mathbf{r}_{n_l N_l} \, \hat{u}_l^*[n_l] \right\} \qquad (4.23) \\ \text{with} \qquad n_l &= \left\lfloor \frac{n_0 N_0}{N_l} \right\rfloor, \quad l = 0(1)M-1 \end{aligned}$$

where μ is the algorithm step size and $\lfloor \cdot \rfloor$ is the floor operator (round off).

4.4.2 Multi-Code (MCD) Scheme

In MCD systems, the signals' streams $u_l[n_l]$ are split into d_l sub-streams. These sub-streams can be considered as virtual user signals with the same processing gain N at the same basic rate, which are code multiplexed using Walsh sequences extracted from an $N \times N$ Hadamard matrix. In MCD systems, the signals' streams $u_l[n_l]$ are split into d_l sub-streams $u_{l,p}[n]$, $p = 0(1)d_l - 1$, where p denotes the sub-stream number. The pth sub-stream of the lth user signal $u_{l,p}[n]$ can be derived, as shown in Fig. 4.13, from the original signal stream as

$$u_{l,p}[n] = u_l[nd_l + p], \qquad (4.24)$$

i.e. a polyphase decomposition of the lth user into d_l polyphase components. By following similar derivation steps as presented in Sec. 4.4.1, the demultiplexed users' signals, cost function and the stochastic gradient adaptation rule can be reformulated to suit the MCD mode.

Demultiplexed User Signals. The sub-streams can be considered as virtual users' signals, which are code multiplexed using Walsh sequences $\mathbf{h}_{l,p}$ extracted from an $N \times N$ Hadamard

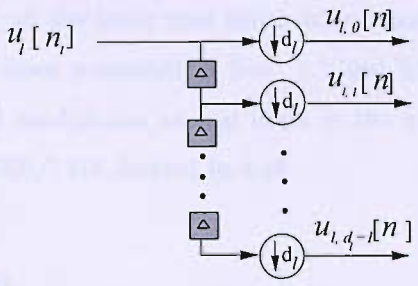

Figure 4.13: Multi-code (MCD) transmission scheme, whereby a high rate user is demultiplexed into d_l low rate signals or polyphase components.

matrix. Hence, the pth virtual user of the lth user signal is decoded as

$$\begin{aligned}\hat{u}_{l,p}[n] &= \mathbf{w}_{\mathrm{MCD}}^{\mathrm{H}} \cdot \begin{bmatrix} \tilde{\mathbf{h}}_{l,p}^{\mathrm{T}} & & 0 \\ & \tilde{\mathbf{h}}_{l,p}^{\mathrm{T}} & \\ & \ddots & \\ 0 & & \tilde{\mathbf{h}}_{l,p}^{\mathrm{T}} \end{bmatrix} \cdot \begin{bmatrix} r[nN] \\ r[nN-1] \\ \vdots \\ r[nN-L-N+2] \end{bmatrix} \\ &= \mathbf{w}_{\mathrm{MCD}}^{\mathrm{H}}\, \mathbf{H}_{l,p}\, \mathbf{r}_{nN} \quad , \end{aligned} \tag{4.25}$$

with $\mathbf{H}_{l,p} \in \mathbb{C}^{L\times(N+L-1)}$ being a convolutional matrix comprising of the pth virtual user's modified code vector $\tilde{\mathbf{h}}_{l,p}$.

Cost Function. Accordingly, by taking into consideration all virtual users resulting from MCD modulation, a hybrid cost function for MCD mode can be written as

$$\xi_{\mathrm{MCD}} = \mathcal{E}\left\{\sum_{l=0}^{K-1}\sum_{p=0}^{d_l-1}(\gamma^2 - |\hat{u}_{l,p}[n]|^2)^2\right\} + \mathcal{E}\left\{\sum_{l=K}^{M-1}\sum_{p=0}^{d_l-1}(\hat{u}_{l,p}[n])^2\right\}, \; . \tag{4.26}$$

Stochastic Gradient Adaptation. The adaptation rule for the MCD can simply be written as

$$\begin{aligned}\mathbf{w}_{\mathrm{MCD,n+1}} = \mathbf{w}_{\mathrm{MCD,n}} + \mu \sum_{l=0}^{K-1}\sum_{p=0}^{d_l-1}\{(\gamma^2 - |\hat{u}_{l,p}[n]|^2)\mathbf{H}_{l,p}\mathbf{r}_{nN}\, \hat{u}_{l,p}^*[n]\} + \\ + \sum_{l=K}^{M-1}\sum_{p=0}^{d_l-1}\{\mathbf{H}_{l,p}\mathbf{r}_{nN}\, \hat{u}_{l,p}^*[n]\} \quad . \end{aligned} \tag{4.27}$$

Note that this rule is updated at the basic rate which corresponds to the spreading factor N, analogously to the single rate cases presented in Secs. 4.1 and 4.3. In fact, if we consider the virtual users resulting in MCD modulation as real users in the system, the algorithm (4.27) is simply equivalent to the FIRMER/LMS derived in 4.18.

4.4.3 Simulation Results

We analyse and compare the performance of the two MCD and VSL equalisers in a multi-rate DS-CDMA downlink system with a basic processing gain of $N = 256$ for mainly two different transmissions over either a single channel $|g_1[m]|$ or an ensemble of 50 dispersive channels characterised by the magnitude profile $|g_1[m]|$. In the first case, we assume a fully loaded system with 9 users, of which two low rate users have a spreading factor of 256, and the seven remaining users employ spreading factors of $\{2, 4, 8, 16, 32, 64, 128\}$. In the second scenario, we assume a partially loaded system, whereby one of the lower rate users is removed. We first demonstrate and compare the convergence behaviour and then the bit error ratio performance.

Convergence. We utilise the two proposed algorithms to update two chip-level equalisers with $L = 10$ coefficients over the dispersive channel $g_1[m]$. The adaptation is initialised with the second coefficient in the weight vector set to unity, and the step size selected to be half the size of the value that would achieve maximum convergence speed in both algorithms. The evolution of the filter coefficients' real part of the two algorithms in a fully loaded scenario is shown in Fig. 4.14. Fig. 4.15 demonstrates the learning curves of both VSL and MDC algorithms for the two partially loaded schemes, whereby users with either spreading gains $N_8 = 256$ or $N_7 = 128$ have been removed. Obviously, the VSL-CDMA system exhibits faster convergence than the MCD-CDMA system for both fully and partially loaded scenarios due to its higher adaptation rate.

It can be noted from Figs. 4.14 and 4.15 that the algorithms succeed to minimise their cost functions, whereby a remaining error floor is due to model truncation. Moreover, inactivating a user (here with $N_7 = 128$) can be seen to improve the convergence of both systems considerably compared to systems with stronger load.

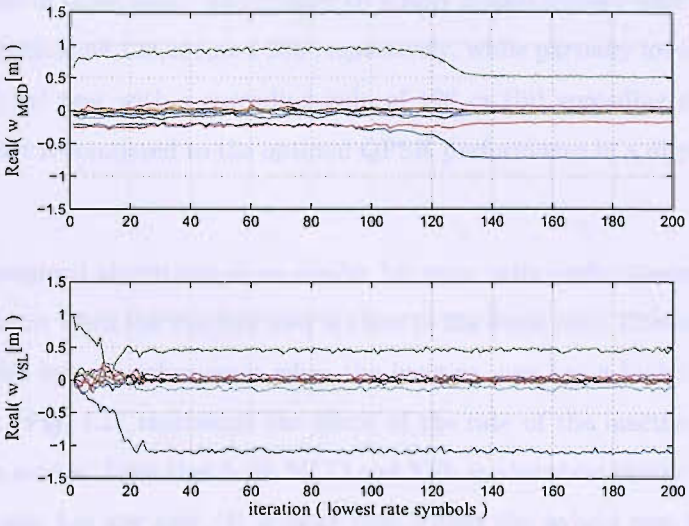

Figure 4.14: Convergence behaviour of the fully loaded system with $N = 256$ over a dispersive channel with SNR = 20dB based on (top) MCD-CDMA and (bottom) VSL-CDMA modes.

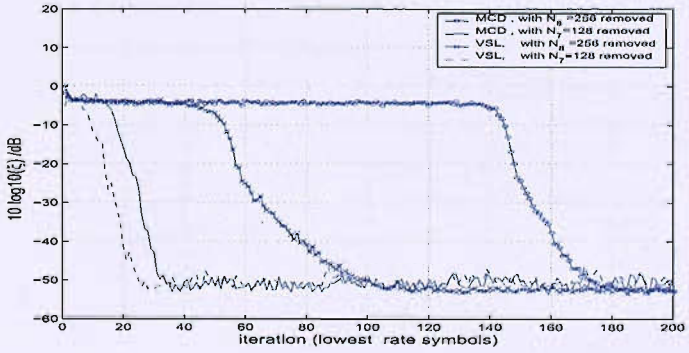

Figure 4.15: Learning curves of the partially loaded system for both MCD-CDMA and VSL-CDMA modes, based on the inactivation of two different users of different rates.

Bit Error Rate. In order to assess the BER performance, the algorithms have been implemented over the ensemble of 50 channels described above for various SNRs whereby both CMA's phase and delay ambiguities have been recovered prior BER calculations. Fig. 4.16 shows the BER of both MCD and VSL modes in three cases: we consider (i) a fully loaded system with 9 active users with spreading gains 2,4,8,16,32,64,128,256,and 256 respectively, while partially loaded systems include the cases where (ii) the user with a spreading gain of 128 or (iii) spreading gain 4 are inactive. The BER performance is compared to the optimal QPSK performance in a dispersion-free AWGN channel.

Note that the two proposed algorithms show similar bit error ratio performances in both fully and partially loaded systems when the inactive user is close to the basic rate. However the BER curves of both modes exhibit better performance when the inactive user has a higher rate $N_2 = 4$ than the two other cases. Fig. 4.17 represents the effect of the rate of the inactive user on the BER performance of both modes. Note that both MCD and VSL modes show similar BER performance when the removed user has low rate. It is clear that within the hybrid cost function, the MSE term for inactive users generally can, if present, enhance the system performance significantly.

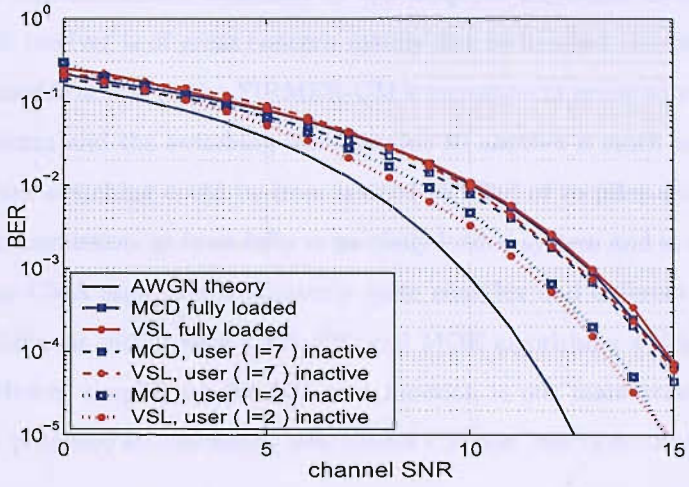

Figure 4.16: BER performance of both VSL and MCD modes in the three cases of (i) a fully loaded system and partially loaded scenarios with (ii) an inactive user with $N_7 = 128$, or (iii) $N_2 = 4$, benchmarked against the BER in an AWGN channel.

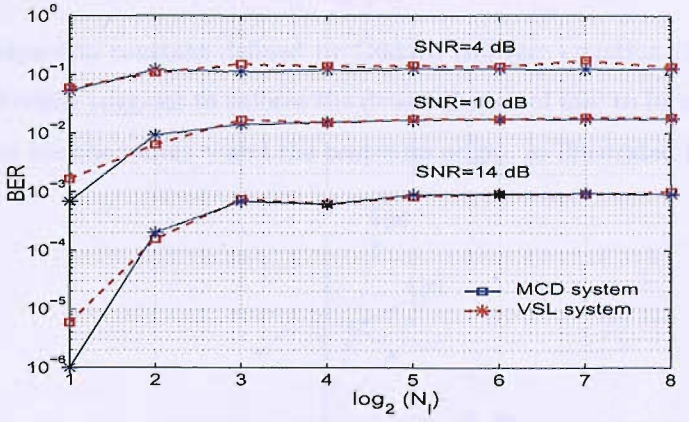

Figure 4.17: BER performance of both modes in dependence of the spreading gain of the removed user for different channel SNR values.

4.5 Modified FIRMER-CMA

In our context, the implementation flexibility of the adaptive algorithm to be employed in the downlink DS-CDMA receiver is of great concern mainly due to handset constraints. This section addresses possible modifications to the FIRMER-CMA structure in order to render the reconfiguration of the algorithm and the switching from a mode to another a much easier and smoother task. For example, the switching could be from trained to blind or to pilot-assisted scheme, from single to multirate transmission, or from fully to partially loaded system and so on. To achieve this aim, we noticed that CMA structure is relatively quite complex and different from other simple structures used in different modes such LMS, DD and MOE algorithms which enjoy similar and simple structure. Hence, simplifying the CM cost function is our main concern next. In fact, Papadias in [76] has proposed an interesting new simple CM cost function structure for single user mode as follows

$$\mathcal{E}\{|d[n] - \hat{u}[n]|^2\} \quad , \tag{4.28}$$

where $\hat{u}[n]$ is the user's detected signal and $d[n]$ is the CM reference signal given by [76]

$$d[n] = \gamma \frac{\hat{u}[n]}{|\hat{u}[n]|} \quad , \tag{4.29}$$

with γ being the dispersion constant defined by Godard [13] (see equation (3.17)). Hence, this alternative CM philosophy suggests to enforce the detected symbol $\hat{u}[n]$ to its nearest symbol $d[n]$ from the circle which has the radius γ and the centre its origin, as illustrated in Fig. 4.18.

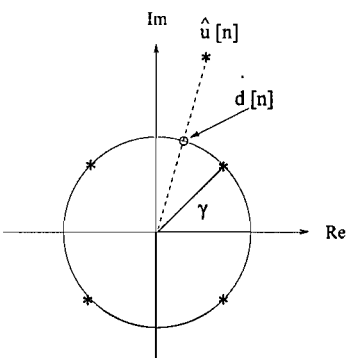

Figure 4.18: Definition of the desired response $d[n]$ for the CM criterion, assuming a QPSK constellation

The new CMA analogy presented above has a structure similar to the LMS, the DD and the minimum output energy [8, 58](MOE[3]) algorithms, where the only difference lies in the value of the desired symbol $d[n]$. Thus, the detected symbol is forced either to the known transmitted symbol $u[n]$ in case of the LMS, or to the closest alphabet symbol given by $q(\hat{u[n]})$ in the DD or to zero in the MOE scheme. Tab. 4.3 shows the different appropriate values of $d[n]$ for each of these algorithms.

	MSE	DD	CM	MOE
$d[n]$	$u[n]$	$q(\hat{u}[n])$	$\gamma\frac{\hat{u}[n]}{\lvert\hat{u}[n]\rvert}$	0

Table 4.3: $d[n]$ for different criteria

Similarly, FIRMER-CMA can be modified in order to gain the flexibility and the simplicity of the CM structure proposed in [76]. The resulting FIRMER-CMA algorithm is summarised in Tab. 4.4. In fact, this algorithm can be readily switched to different modes by only changing the parameter $d_l[n]$. In the following, three examples are presented to emphasise the gained flexibility of the modified FIRMER-CMA.

In the first example we assume a fully loaded downlink DS-CDMA system where a dispersive channel is being adaptively equalised by using the standard FIRMER-CMA. If we disactivate certain users, at some point during the equalisation process, the FIRMER-CMA should be replaced by a suitable algorithm such as the FIRMER-CMA/LMS, as discussed in Sec. 4.3. It can be seen that by implementing the modified FIRMER-CMA structure presented in Tab. 4.4, the switch from fully loaded to a partially loaded scenario can be easily achieved by only replacing the corresponding desired symbols $\gamma\frac{\hat{u}[n]}{|\hat{u}[n]|}$ of each disactivated user with zeros. The second example concerns switching FIRMER-CMA after a satisfactory MSE to a decision directed algorithm in order to increase convergence and tracking speed. The latter swap could be simply constructed by adopting the modified concept where only basic replacements of all decisions $d_l[n]$ from $\gamma\frac{\hat{u}[n]}{|\hat{u}[n]|}$ to $q(\hat{u}_l[n])$ would be sufficient to ensure a successful switch. The third example considers a semi-blind or pilot-assisted equalisation. In fact, some of the inactive users can be exploited to load a number of pilots in order to enhance the system performance. Let us assume one pilot $l = 0$ with signal

[3]no constraints are considered

$u_0[n]$ which is known at the receiver. Therefore, for the received symbols $\hat{u}[n]$ the LMS can be implemented rather than CMA. This can be achieved softly by substituting the parameter $d_0[n]$ by the transmitted symbol $u_0[n-\alpha]$ with a suitably chosen delay α. Further investigation on such semi-blind detection is addressed in Chap. 6.

Modified FIRMER-CMA Algorithm	
1:	$\mathbf{x}_l[nN] = \mathbf{H}_l \mathbf{r}_{nN}$, for $l = 0(1)N-1$
2:	$\hat{u}_l[n] = \mathbf{w}^{\mathrm{H}_n} \mathbf{x}_l[nN]$, for $l = 0(1)N-1$
3:	$d_l[n] = \gamma \frac{\hat{u}_l[n]}{\lvert\hat{u}_l[n]\rvert}$, for $l = 0(1)N-1$
4:	$e_l[n] = d_l[n] - \hat{u}_l[n]$, for $l = 0(1)N-1$
5:	$\mathbf{w}_{n+1} = \mathbf{w}_n + \mu \sum_{l=0}^{N-1} \mathbf{x}_l[nN] e_l^*[n]$

Table 4.4: Equations for channel multiuser equalisation by modified FIRMER-CMA at symbol rate iteration n.

The computational complexity of each step of the modified FIRMER-CMA algorithm is calculated and presented in Tab. 4.5.

algorithm step	complex multiplications	complex addition	complex division
1:	N^2L	NL(N-1)	-
2:	NL	N(L-1)	-
3:	N	-	N
4:	-	N	-
5:	NL+L	NL	-
total	$N^2L + 2NL + N + L$	$N^2L + NL$	N

Table 4.5: Computational complexity of the modified FIRMER-CMA receiver

As can be seen from Tab. 4.5, the modified FIRMER-CMA exhibits a moderate complexity of the same order like the order of the standard FIRMER-CMA's complexity. The only difference between the two algorithms' complexities is that the modified FIRMER-CMA saves N complex multiplications which have been replaced by N complex divisions.

4.6 Virtual Users Approach

In the following a new blind equalisation strategy is proposed which is based on gathering active users into various sets. Each set includes $N_q \leq N$ users which have the same mother spreading code of length $\frac{N}{N_q}$, where $q = 0(1)log_2(N)$. For example, let us consider the case of $N = 8$ active users with different spreading sequences extracted from the OVSF code tree represented in Fig. 2.3. Therefore, the possible divisions are four sets of two users with common mother code of length 4 or two sets of four users with common mother code of length 2 or even one set of all active users. The idea is to consider the multiplexed signals of each set as one new virtual user which has the common mother code as its new spreading code. Since mother codes are mutually orthogonal and have shorter length $\frac{N}{N_q}$ than the original spreading factor N, the computational complexity of FIRMER-CMA will be significantly reduced by adopting the above analogy.

For more clarifications, let us consider the extreme case where we choose a set of all active users $N_q = N$. Hence, the system will be considered as a single user system rather than a multiuser one and the new computational complexity can be calculated from Tab. 4.5 by replacing N by $\frac{N}{N_q} = 1$. Therefore, a very simple computational algorithm is obtained, which is similar to the single detection case and depends only on the length of equaliser L. However, we should notice that the new virtual users will have new higher order alphabet than the original one (for example QPSK) with different characteristics. Fig. 4.19 represents the new resulting constellation map of virtual users obtained from an original set of either 2 or 16 active users where the original constellation is QPSK.

As can be seen in Fig. 4.19, the new constellation maps have higher order than the original constellation QPSK and include N_q^2 symbols. Similarly to QAM mapping, they exhibit the nice symmetry property $\mathcal{E}\{s^2[m]\} = 0$ which is one of the main assumptions adopted by Godard [13] in his CMA's derivations. Furthermore, it has been shown that CMA is a robust to high order constellation, especially the concurrent CMA with either DD [90] or SDD [91]. Therefore, implementing these algorithms in the proposed strategy may lead to a promising performance. Finally, the above proposed strategy is in its first step and more investigations are required.

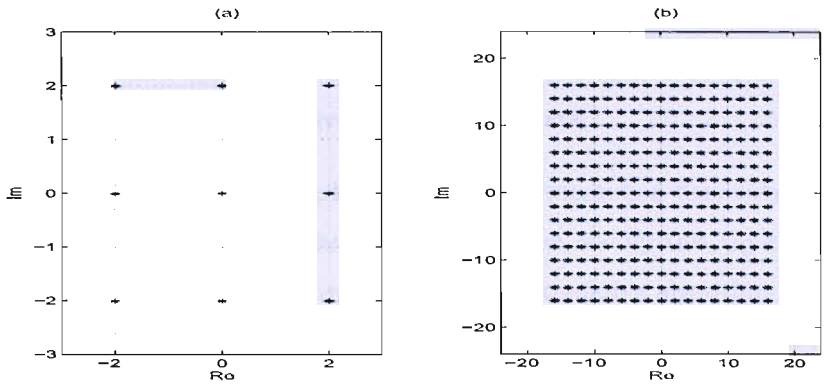

Figure 4.19: Constructed constellation maps from an original QPSK constellation for (a) 2 synchronous users (b) 16 synchronous users

4.7 Concluding Remarks

FIRMER-CMA. A blind equalisation approach for a DS-CDMA downlink scenario has been presented, which aims to enforce CM conditions on the various users' signals. A stochastic gradient algorithm has been derived, which differs from previous CM algorithms by a code-prefiltering of its input. This algorithm has been extensively tested and proven very stable. Representative simulations have been presented, highlighting the convergence behaviour as well as its BER performance, which is close to the performance of an MMSE equaliser.

Partial loading. For inactive users part of the system, it has been shown that a CM criterion, even if additional signals are injected into the system, is inferior to the introduction of an MSE cost function. The latter, the so-called FIRMER-CMA/LMS, has the additional advantage of a lower implementational cost and does not increase the power of the transmitted signal. For multi-rate transmissions, two modified FIRMER-CMA/LMS equalisation approaches using either VSL or MCD access modes have been presented. It has been shown that the VSL algorithm shows faster convergence and outperforms the MCD equaliser in both fully and partially loaded systems.

Multi-rate transmission. For multi-rate transmissions, two modified FIRMER-CMA/LMS equalisation approaches using either VSL or MCD access modes have been presented. Correspondingly, two hybrid CM/MSE blind equalisation algorithms are derived to be minimised. These algorithms are based on enforcing CM conditions on various active users' signals and MSE criteria

on the remaining inactive users. The VSL algorithm shows faster convergence and outperforms the MCD equaliser in both fully and partially loaded systems. Similar BER performance in both systems has been noticed when the inactive users have low rate.

Flexibility and Computational complexity. The implementation flexibility of the modified FIRMER-CMA has been identified. It has been shown how readily this algorithm can be implemented in different modes and operating with various alternative algorithm rather than only CMA. Furthermore, a new strategy based on a small population of virtual users has been proposed which further reduces the computational complexity of FIRMER-CMA.

Chapter 5

Fast and Robust Blind Multiuser Equalisation Schemes

The previously proposed blind multiuser FIRMER-CMA equaliser improves the bandwidth efficiency by avoiding the use of a training sequence and can, based on its computational complexity, be readily implemented on a real-time device. However, this algorithm has the drawbacks of slow convergence and only moderate levels of steady-state MSE which may limit its deployment in future wireless communication systems. Therefore, this chapter investigates remedies and proposes a number of novel fast and robust blind multiuser equalisation alternatives for the DS-CDMA downlink. We start by discussing the FIRMER-CMA's robustness and its sensitivity to carrier frequency offset, whereby an estimator for such an offset is derived in Sec. 5.1. In order to increase the convergence speed of the standard FIRMER-CMA, an affine projection (AP) scheme is introduced in Sec. 5.2. The following Sec. 5.3 is dedicated to derive a concurrent FIRMER-CMA with a decision directed (DD) algorithm, which is able to achieve a low steady-state MSE. For the purpose of gaining the benefits of both fast convergence and low steady-state MSE, a combined AP-FIRMER-CMA+DD structure is proposed in Sec. 5.4.

5.1 Robustness to Carrier Frequency Offset

Carrier frequency offsets may arise for various reasons, but are mostly caused by a clock mismatch between transmitter and receiver e.g. due to tolerances in the manufacturing of quartz crystals. Clock mismatches almost always exist, and can lead to substantial frequency offsets of an order of 0.01% of the carrier frequency [95]. In general, such carrier frequency offsets increase the difficulty in detecting symbols in the receiver and will in most cases require sophisticated offset detection and correction algorithms [96, 97, 98]

This section discusses the FIRMER-CMA's robustness to carrier frequency offset. In Sec. 5.1.1, we analyse the algorithm's sensitivity to such an offset, where we show that the filtered-error filtered-regressor algorithm requires modifications in order to cope with a carrier frequency offset. In Sec. 5.1.2, we introduce a carrier offset estimation strategy that can be combined with the FIRMER-CMA algorithm. Finally, the proposed scheme is evaluated in Sec. 5.1.3 by simulations in terms of convergence behaviour and BER performance.

5.1.1 Carrier Frequency Offset Influence

We consider the DS-CDMA downlink system in Fig. 5.1 with multiple symbol-synchronous users, which for the sake of simplicity are assumed to have the same rate and create a fully loaded system, although multiple rate users and partial loading can be taken into account Secs. 4.3 and 4.4. In the following, we are concerned with the influence of a carrier frequency offset $\Delta\Omega$ on the FIRMER-CMA algorithm with its update equation as defined in (4.10). Without loss of generality, we assume that the mismatch is localised in the demodulation process of the receiver, and can therefore be represented by a multiplicative complex exponential $e^{j\Delta\Omega m}$ in Fig. 5.1. A carrier offset compensation with a complex exponential $e^{-j\Xi m}$ is given in the same figure, and may be used to mitigate the offset by ideally setting $\Xi = \Delta\Omega$.

For the CMA algorithm, moving the factor $e^{-j\Xi m}$ from its input to the receiver's output has no impact on the algorithm. In contrast, below we will show that for the FIRMER-CMA, transferring the correction by $e^{-j\Xi m}$ to the user output $\hat{u}_l[n]$ with $l = 0, 1, \ldots (N-1)$ does change the algorithm.

Let us first assume that $\Xi = \Delta\Omega$, i.e. the received signal $\tilde{r}[m] = r[m] \cdot e^{-j\Xi m}$ as shown in Fig. 5.1

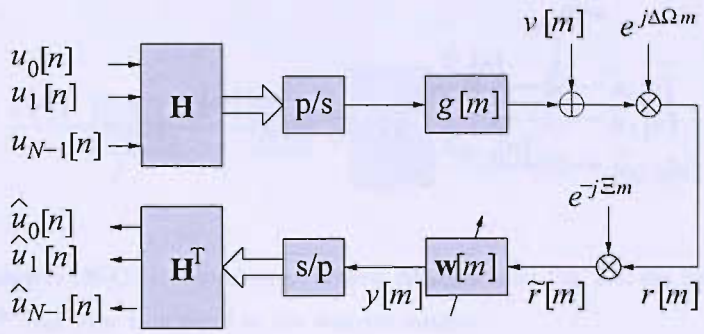

Figure 5.1: Flow graph for DS-CDMA downlink scenario including a carrier offset $\Delta\Omega$ and a carrier offset compensation in the receiver by Ξ.

is free of any carrier offset. Rather than applying the FIRMER-CMA directly to the offset-correct quantity $\tilde{r}[m]$, we want to feed the algorithm with the carrier-offset corrupted signal $r[m]$. Note that the tap delay line vector

$$\begin{aligned} \tilde{\mathbf{r}}_{nN} &= e^{-jN\Xi n}\,\mathrm{diag}\Big\{1,\ e^{j\Xi},\ \ldots\ e^{j(L+N-2)\Xi}\Big\}\,\mathbf{r}_{nN} \\ &= e^{-jN\Xi n}\mathbf{\Lambda}(\Xi)\,\mathbf{r}_{nN} \end{aligned} \tag{5.1}$$

can be substituted into (4.1) yielding

$$\hat{u}_l[n] = e^{-jN\Xi n}\,\mathbf{w}^{\mathrm{H}}\,\underbrace{\mathbf{H}_l\,\mathbf{\Lambda}(\Xi)}_{\tilde{\mathbf{H}}_l[\Xi]}\,\mathbf{r}_{nN}, \tag{5.2}$$

Here, the remaining carrier offset of the received user signals $\hat{u}_l[n]$ is compensated by the term $e^{-jN\Xi n}$ at the output of the multiuser detector. Analogous to (4.10), the gradient estimate can be derived as

$$\nabla\hat{\xi}_{\mathrm{CM}}(\mathbf{w}_n) = -2\sum_{l=0}^{N-1}(\gamma^2 - |\tilde{u}_l[n]|^2)\,\tilde{\mathbf{H}}_l[\Xi]\,\mathbf{r}_{nN}\,\tilde{u}_l^*[n] \quad . \tag{5.3}$$

i.e. the carrier offset needs to be incorporated into the update equation of the FIRMER-CMA in form of an offset-dependent code matrix $\tilde{\mathbf{H}}[\Xi]$ as shown in Fig. 5.2. Since the carrier frequency offset affects the error path in the FIRMER-CMA, it is known from other filtered-error filtered-regressor schemes that the code matrix $\mathbf{H}_l$ in (4.1) and (4.10) needs to be replaced by $\tilde{\mathbf{H}}_l[\Xi]$ in (5.2) and (5.3). Therefore, the proposed blind synchronous multiuser equaliser is — unlike standard CMA algorithm [13] — sensitive to carrier frequency offset, and hence must be supplied with an accurate estimate $\Xi \approx \Delta\Omega$.

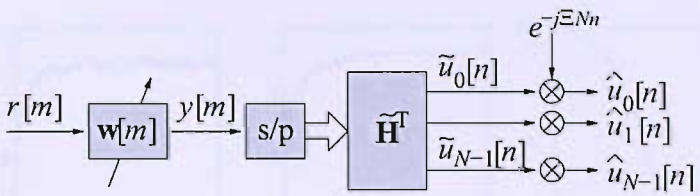

Figure 5.2: Flow graph of DS-CDMA receiver structure; different from Fig. 5.1, the carrier frequency offset compensation $e^{-jN\Xi n}$ has been transfered to the receiver output.

5.1.2 Carrier Frequency Offset Compensation

The aim is to estimate the carrier offset $\Delta\Omega$ from the decoded user data $\tilde{u}_l[n]$ in Fig. 5.2, in order to (i) supply the multiuser CM algorithm with an accurate carrier offset and (ii) compensate for the phase rotation to yield the carrier offset compensated user signals $\hat{u}_l[n]$. Assuming the transmission of QPSK user data, we investigate a carrier offset detection method raising the decoded samples to the fourth power similar to [99].

The carrier frequency offset is obtained by

$$\Xi = \frac{1}{4\alpha N^2} \sum_{l=0}^{N-1} \mathcal{E}\left\{ \angle \left(\hat{u}_l[n] \hat{u}_l^*[n-\alpha] \right)^4 \right\} \tag{5.4}$$

with a region of convergence if $|\Delta\Omega| < \pi/(2N\alpha)$ for a chosen delay α. The resulting Ξ is an estimate of $\Delta\Omega$, which however is biased if the noise $\tilde{v}[n]$ is correlated. If $v[m]$ in Fig. 5.1 is AWGN, then $\tilde{v}[n]$ is likely to be correlated due to the equaliser response $\mathbf{w}[n]$. Therefore, the bias term in Ξ in (5.4) can be reduced by selecting $\alpha > L/N$. However, this reduces the capability to estimate larger offset values due to the reduced region of convergence. This above carrier offset detection approach has been reported to operate reliably for channel SNRs above approximately 10dB [99].

5.1.3 Simulation Results

For the simulations below, we apply the proposed blind multiuser equaliser combined with a carrier frequency offset correction to the two types of channels $g_1[m]$ and $g_2[m]$, as characterised in Sec. 4.2.

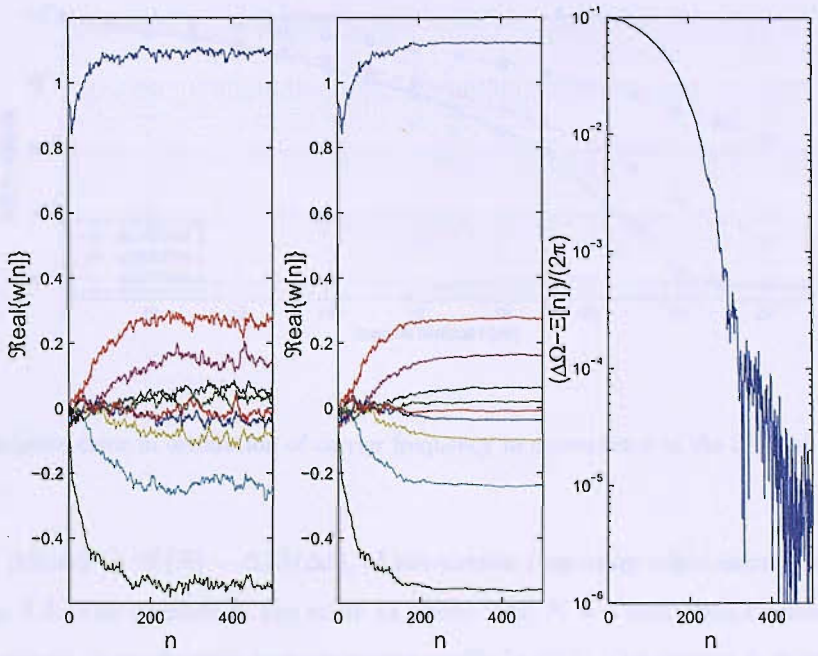

Figure 5.3: Real part of the equaliser coefficients trajectories during adaptation: (left) without adjusting Ξ, and (middle) with adjusting Ξ; (right) the learning curve of Ξ during adaptation.

In order to demonstrate the convergence behaviour of the proposed algorithm, we transmit $N = 4$ users with QPSK signals over $g_1[m]$ in the absence of channel noise, but with a carrier offset of $\Delta\Omega = 0.02\pi$. The equaliser comprises of 10 coefficients, with the second coefficient in $\mathbf{w}$ set to unity. With a step size $\mu = 0.05$, an initial value $\Xi = 0$ and a delay $\alpha = 6$, the evolution of the filter coefficients' real part is shown in Fig. 5.3. For the experiment in Fig. 5.3(left), the carrier frequency offset estimate was set to zero during adaptation, while the trajectories in Fig. 5.3(middle) are the ones of a blind multiuser CMA with the carrier frequency offset estimate incorporated. The estimate Ξ is calculated using a window of 200 symbol periods to evaluate (5.4) at each point in time. The learning curve for Ξ is given in Fig. 5.3(right), exhibiting a good convergence to the adjusted carrier frequency offset $\Delta\Omega$.

In the following, $g_1[m]$ and $g_2[m]$ have been replaced by randomised channels with Rayleigh distributed coefficients yielding average power profiles $|g_1[m]|$ and $|g_2[m]|$. Results have been average over 50 channel realisations each.

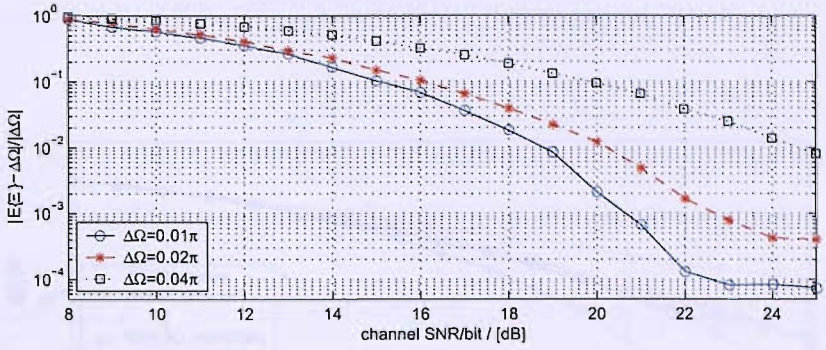

Figure 5.4: Relative error in estimation of carrier frequency in dependence of the SNR at the receiver.

The accuracy, defined by $[\mathcal{E}\{\Xi\} - \Delta\Omega]/\Delta\Omega$, of the carrier frequency offset estimation in noise is detailed in Fig. 5.4. The scenario is the same as above with $N = 4$ users but transmitting over a set of 50 randomised channels with average power profile $|g_1[m]|$. The system is given 500 symbol periods to ensure convergence, and uses a window length of 200 symbols for the estimation of Ξ. Thereafter, the accuracy of Ξ is monitored over the next 500 symbol periods.

To demonstrate the achievable BER over blindly equalised dispersive channels with carrier offset, we consider two scenarios. The first scenario uses $N = 4$ users over 50 channels described above with average power profile $|g_1[m]|$. Here an equaliser of $L = 20$ coefficients has been used. The results for three different carrier offset frequencies, stated in Fig. 5.5, have been obtained by averaging over all 50 channel realisations, and are benchmarked against the performance of an MSE equaliser of same length. As seen in Fig. 5.4, the carrier offset estimation is difficult at low SNR values in agreement with [99], and hence leads to degraded performance compared to the MMSE. However, in all cases the carrier offset estimation makes a considerable difference to the convergence of the overall system when compared to a system without carrier offset estimation and subsequent compsensation.

A second scenario uses a set of 50 more dispersive channels, with average power profile $|g_2[m]|$, to transmit $N = 8$ users with the help of an $L = 64$ coefficient filter. The results for this case are given in Fig. 5.6, demonstrating good performance of the combined scheme.

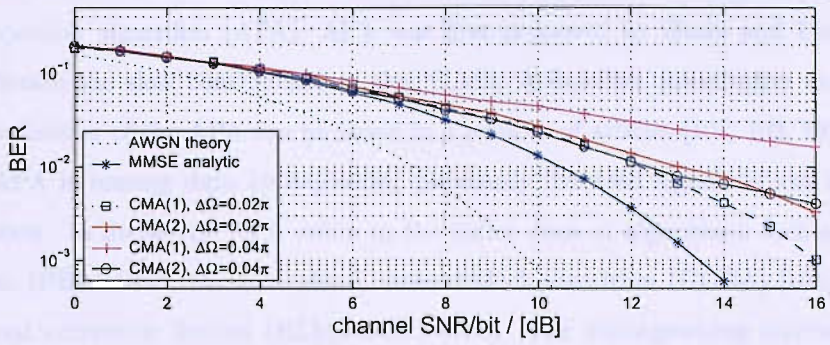

Figure 5.5: BER curves for transmission over $g_1[m]$; CMA(1) and (2) refer to operation with and without adjustment of Ξ.

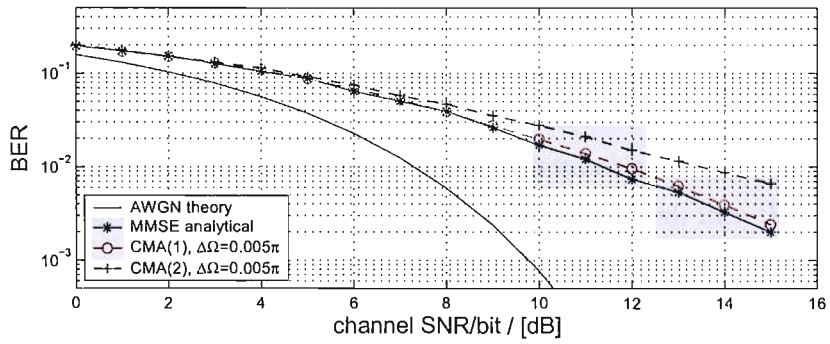

Figure 5.6: BER curves for transmission over $g_2[m]$; CMA(1) and(2) refer to operation with and without adjustment of Ξ.

5.2 Affine Projection FIRMER-CMA Scheme

In this section, we aim to speed up FIRMER-CMA's convergence by adopting the concept of the affine projection algorithm (APA). APA was first proposed by Ozeki and Umeda in 1984 [100] to ameliorate the slow convergence of the NLMS. A detailed quantitative analysis of the convergence behaviour of the APA can be found in a number of articles [101, 102, 103]. The main idea behind APA is reusing data by exploiting previously detected signal vectors to perform a faster adaptation. In literature, APA refers to the entire class of algorithms such as the partial rank algorithm (PRA) [104], the generalised optimal block algorithm (GOBA) [105], and NLMS with orthogonal correction factors (NLMS-OCF) [106]. The distinguishing attributes of these algorithms, which have been derived independently from different perspectives, is that they update the taps on the basis of multiple, delayed input signal vectors [101]. Furthermore, various versions of APA have been derived in [107, 108, 109, 110] whereby the latter has been termed the fast AP (FAP) algorithm.

All previously mentioned APA based algorithms are only suitable for trained systems. Consequently, Papadias in his work [111, 112, 76] has derived a blind APA based scheme, the so called Normalised Sliding Window Constant Modulus Algorithm (NSWCMA), by performing some insightful changes on the CM cost function [112, 76]. The latter algorithm has shown a faster convergence speed than the basic CMA and good ability to escape from local minima of its cost function [111, 76]. However, Papadias work has been initially designed for single user systems. Motivated by the performance achieved in [76], in the following we derive an affine projection blind multiuser equaliser similar in structure to the NSWCMA but suitable for downlink DS-CDMA systems. In Sec. 5.2.1, formulation of the proposed structure is presented, then the performance of the latter scheme is investigated in Sec. 5.2.2.

5.2.1 Formulation

In this section, we derive the affine projection FIRMER-CMA (AP-FIRMER-CMA) which updates the blind multiuser equaliser weight vector $\mathbf{w}$. In the Pth order AP-FIRMER-CMA, the P most recent data vectors are explicitly taken into account. For the sake of simplicity, multiple symbol-synchronous users are assumed to have the same rate and fully load the system. The multiple rate

and partial load cases are disscussed in Secs. 4.3 and 4.4 respectively and will not be considered next.

Similarly to [76, 112, 111], we use the modified CM cost function ξ_{CM} previously discussed in Sec. 4.5 which can be given by

$$\xi_{\mathrm{CM}} = \mathcal{E}\left\{\sum_{l=0}^{N-1} |d_l[n]-\hat{u}_l[n]|^2\right\} \quad , \tag{5.5}$$

$$\text{with} \qquad d_l[n] = \gamma\frac{\hat{u}_l[n]}{|\hat{u}_l[n]|} \quad . \tag{5.6}$$

The philosophy of the modified CM criterion suggests to force of every output value $\hat{u}_l[n]$ onto the nearest valid CM symbol $d_l[n]$ on a circle with radius γ around the origin. In fact, the modified form has a similar structure to the LMS algorithm which simplifies our task to utilise the affine projection concept for the FIRMER-CMA. In the following, the main steps of developing the AP-FIRMER-CMA are presented.

Firstly, we split (4.1) for the lth user's decoded symbol $\hat{u}_l[n]$ into a scalar product between the weight vector and an input vector,

$$\hat{u}_l[n] = \mathbf{w}^{\mathrm{H}}\mathbf{x}_l[n] \quad , \tag{5.7}$$

whereby $\mathbf{x}_l[n]$ represents a vector of filtered received signal samples,

$$\mathbf{x}_l[n] = \mathbf{H}_l\mathbf{r}_{nN} \quad . \tag{5.8}$$

Secondly, we retain a record of P past input vectors $\mathbf{x}_l[n-p]$, and the corresponding desired signals' values $d_l[n-p]$, $p = 0\cdots(P-1)$, which are collocated such that

$$\mathbf{X}_l[n] = [\mathbf{x}_l[n]\ \mathbf{x}_l[n-1]\ \cdots\ \mathbf{x}_l[n-P+1]] \quad , \tag{5.9}$$

$$\mathbf{d}_l[n] = [d_l[n]\ d_l[n-1]\ \cdots\ d_l[n-P+1]]^{\mathrm{T}} \quad . \tag{5.10}$$

Based on these records, we define an error vector $\mathbf{e}_l[n]$ at time instance n,

$$\mathbf{e}_l^*[n] = \mathbf{d}_l^*[n] - \mathbf{X}_l[n]^{\mathrm{H}}\mathbf{w}_n, \quad l = 0(1)N-1 \quad . \tag{5.11}$$

Based on this error vector, we want to perform a weight update such that

$$\mathbf{X}_l[n]^{\mathrm{H}}\mathbf{w}_{n+1} = \mathbf{d}_l^*[n], \quad l = 0(1)N-1 \quad , \tag{5.12}$$

Pth order AP-FIRMER-CMA Algorithm	
1:	update $\mathbf{X}_l[n] = \left[\mathbf{H}_l\mathbf{r}_{nN}\mathbf{H}_l\mathbf{r}_{(n-1)N}\cdots\mathbf{H}_l\mathbf{r}_{(n-P+1)N}\right]$, for $l = 0(1)N-1$
2:	update $\mathbf{d}_l[n] = [d_l[n]\ d_l[n-1]\ \cdots\ d_l[n-P+1]]^{\mathrm{T}}$, for $l = 0(1)N-1$
3:	$\mathbf{e}_l[n] = \mathbf{d}_l[n] - \mathbf{X}_l[n]^{\mathrm{T}}\mathbf{w}_n^*$ for $l = 0(1)N-1$
4:	$\mathbf{X}_l^\dagger[n] = \mathbf{X}_l[n](\mathbf{X}_l[n]^H\mathbf{X}_l[n] + \alpha\mathbf{I})^{-1}$
5:	$\mathbf{w}_{n+1} = \mathbf{w}_n + \mu\sum_{l=0}^{N-1}\mathbf{X}_l^\dagger[n]\mathbf{e}_l^*[n]$

Table 5.1: Affine projection algorithm for multiuser equalisation

is fulfilled. Combining (5.11) and (5.12), we obtain for the lth user

$$\mathbf{w}_{n+1} = \mathbf{w}_n + \mathbf{X}_l^\dagger[n]\mathbf{e}_l^*[n] \quad , \tag{5.13}$$

with $\mathbf{X}_l^\dagger[n]$ being the pseudo-inverse of the data matrix $\mathbf{X}_l[n]$,

$$\mathbf{X}_l^\dagger[n] = \mathbf{X}_l[n](\mathbf{X}_l[n]^H\mathbf{X}_l[n] + \alpha\mathbf{I})^{-1} \quad , \tag{5.14}$$

whereby it is assumed that $P < L$. The inversion is regularised by a small diagonal term α. Finally, by taking the contributions of all N users to the weight update in (5.13) into account, we arrive at the update rule

$$\mathbf{w}_{n+1} = \mathbf{w}_n + \mu\sum_{l=0}^{N-1}\mathbf{X}_l^\dagger[n]\mathbf{e}_l^*[n] \quad , \tag{5.15}$$

where μ is a relaxation factor. A numerically efficient implementation of the AP-FIRMER-CMA is listed in Tab. 5.1. This algorithm is virtually identical to the standard APA, but is application-specific in the way the data matrix and desired signal vectors are set up in step 1 according to (5.7) and (5.8).

It can be noted that for $P = 1$, we obtain the normalised FIRMER-CMA which updates the equaliser weights by exploiting only the actual filtered input vectors $\mathbf{x}_l[n]$. A similar derivation for the multiuser decision-directed (DD) mode can be readily deduced by replacing the desired data $d_l[n]$ described in (5.16) by $q(\hat{u}_l[n])$, where $q(\cdot)$ is the decision function which returns the symbol in the alphabet that is closest to $\hat{u}_l[n]$.

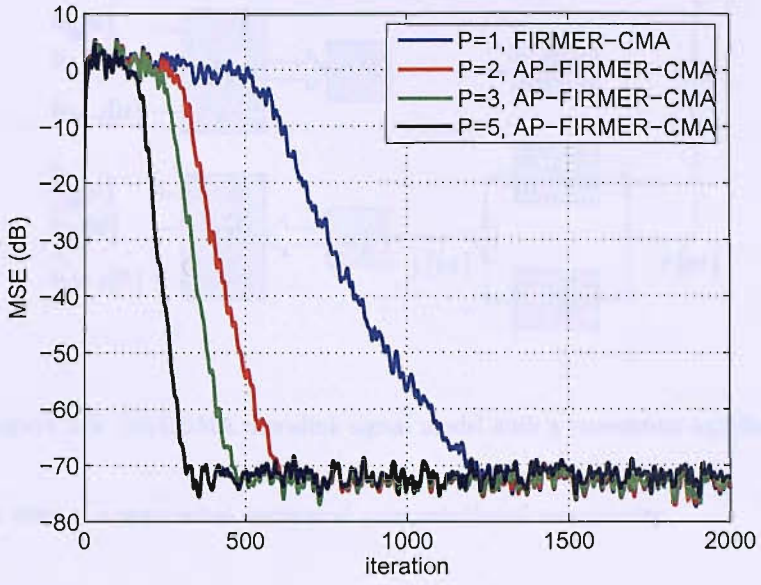

Figure 5.7: Convergence speed of AP-FIRMER for different projection order p values; the curves represent the ensemble MSE averaged across all 16 users.

5.2.2 AP-FIRMER-CMA Performance

In order to demonstrate the behaviour of the AP-FIRMER-CMA we transmit $N = 16$ QPSK user signals over a noise-free and dispersive channel $g_1[m]$, described previously in Sec. 4.2. We apply the proposed AP-FIRMER-CMA with a length $L = 10$ for different projection orders $P \in \{1, 2, 3, 5\}$. The adaptation is initialised with the second coefficient in the weight vector set to unity. The systems converge to various solutions such that the convolution of $g_1[m]$ and the adapted equaliser $\mathbf{w}$ is a complex rotation of the delayed Kronecker delta functions $e^{j\phi}\delta(m - \alpha)$. Both phase rotation ϕ and delay α are corrected prior to MSE measurements.

The relaxation is set to a fixed value $\mu = 0.03$ for the four systems of various order P. The MSE curves of the four AP-FIRMER-CMAs are shown in Fig. 5.7. By increasing the projection order P, a faster convergence than the normalised FIRMER-CMA algorithm ($P = 1$) is achieved. Note that the convergence rate improvement does not come at a detriment of the steady-state MSE in this noiseless simulation. Therefore, increasing the projection order P of AP-FIRMER-CMA appears to be a viable route to speed up the convergence rate without incurring a loss in MSE,

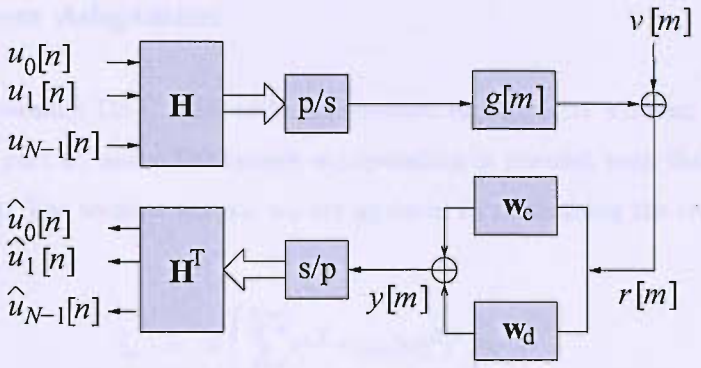

Figure 5.8: DS-CDMA downlink signal model with a concurrent equaliser.

although at the cost of a somewhat increased computational complexity.

5.3 Concurrent FIRMER-CMA and DD Mode

Since FIRMER-CMA is based on the CM criterion, it is prone to achieve only moderate levels of MSE after convergence, which may not be sufficiently low for the system to attain adequate BER performance. A possible solution to the latter problem is to switch to a decision-directed (DD) mode in order to further reduce the residual CMA steady state MSE [72]. In order to avoid error propagation due to incorrect decisions, the CMA's residual MSE should be sufficiently low. However in practice, such a low level of MSE may not always be achievable by the CMA [90, 49]. Consequently, a promising solution, suitable for single user transmission, has been proposed in [90], whereby a DD equaliser is concurrently operating with a CMA rather than switching to a DD adaptation after the CMA has converged. This concurrent CMA+DD equaliser is reported to achieve a significant enhancement in equalisation performance over the CMA [90].

In the following, a concurrent FIRMER-CMA+DD algorithm is derived, which is similar to [90] but suitable for synchronous DS-CDMA systems. Adaptation is performed by concurrently minimising two cost functions based on either a CM criterion or a DD scheme for all active users. In Sec. 5.3.1, we derive the proposed multiuser concurrent FIRMER-CMA+DD algorithm. Simulations of the proposed algorithm are presented in Sec. 5.3.2.

5.3.1 Concurrent Adaptation

We consider the downlink DS-CDMA system presented in Sec. 4.1.1 with an equaliser $\mathbf{w}$ which consists of a CMA part $\mathbf{w}_c$ and a DD branch $\mathbf{w}_d$ operating in parallel, such that $\mathbf{w} = \mathbf{w}_c + \mathbf{w}_d$, as depicted in Fig. 5.8. The weights $\mathbf{w}_c$ and $\mathbf{w}_d$ are updated by minimising the two cost functions ξ_c and ξ_d,

$$\xi_c = \mathcal{E}\left\{\sum_{l=0}^{N-1}(\gamma^2 - |\hat{u}_l[n]|^2)^2\right\}, \tag{5.16}$$

$$\xi_d = \mathcal{E}\left\{\sum_{l=0}^{N-1}|q(\hat{u}_l[n]) - \hat{u}_l[n]|^2\right\}, \tag{5.17}$$

whereby $q(\cdot)$ maps its input onto the nearest constellation point of the employed alphabet. The optimum vectors $w_{c,\text{opt}}$ and $w_{d,\text{opt}}$ are therefore obtained from

$$\mathbf{w}_{c,\text{opt}} = \arg\min_{\mathbf{w}_c} \xi_c, \tag{5.18}$$

$$\mathbf{w}_{d,\text{opt}} = \arg\min_{\mathbf{w}_d} \xi_d. \tag{5.19}$$

There is no unique solution to either (5.18) or (5.19), since minimising (5.16) or (5.17) is ambiguous due to an indeterminism in phase rotation in (5.16) and possible erroneous decisions in (5.17). However, by operating DD and CMA concurrently, the phase ambiguity found in FIRMER-CMA case, as discussed in Sec. 4.1.2, can be reduced by locking the solution onto the prescribed constellation pattern.

Example. In this example, the two cost functions ξ_c and ξ_d are plotted in Figs. 5.9 and 5.10 respectively, in dependency of an equaliser $\mathbf{w}$ with a single complex coefficient w_0. The system adopted here is a fully loaded DS-CDMA system with $N = 16$ users transmitting their signals over a distortionless and delayless channel with $SNR = 30dB$. The modulation scheme employed here is QPSK with $\gamma = 1$. Fig. 5.9 shows that ξ_c exhibits a manifold of optimum solutions satisfying $|w_0| = \gamma$. Yet, only four solutions can be seen in ξ_d due to the four possible QPSK constellation points.

In the following, we derive the concurrent FIRMER-CMA+DD algorithm which updates the multiuser equaliser vector $\mathbf{w}$, similarly to the single-user concurrent CMA+DD described in [90]. The

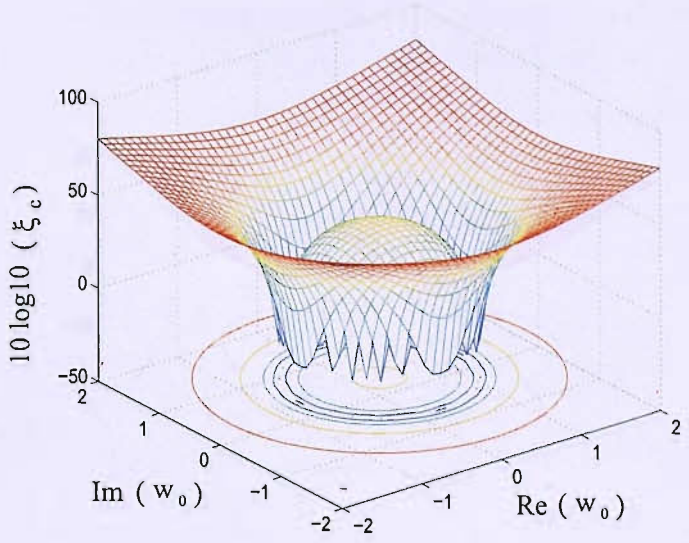

Figure 5.9: Cost function ξ_c in dependency of a single complex valued coefficient w_0.

main idea is to update the CMA part $\mathbf{w}_c$, which is followed by a DD adaptation only if the previous CMA adaptation is deemed successful. The proposed algorithm, which is updated at the symbol-rate with symbol time index n, can be described by the following steps:

1. The decoded signals $\hat{u}_l[n]$ are calculated for all users according to

$$\hat{u}_l[n] = \mathbf{w}_c^{\mathrm{H}}[n]\mathbf{x}_l[n] + \mathbf{w}_d^{\mathrm{H}}[n]\mathbf{x}_l[n], \text{ for } l = 0(1)N-1. \tag{5.20}$$

2. The CMA part $\mathbf{w}_c$ is updated according to the rule

$$\mathbf{w}_c[n+1] = \mathbf{w}_c[n] + \mu_c \sum_{l=0}^{N-1} e_{l,c}^{*}\mathbf{x}_l[n] \tag{5.21}$$

where $e_{l,c} = \hat{u}_l[n](\gamma^2 - |\hat{u}_l[n]|^2)$ and μ_c is the CMA step size. This stochastic gradient adaptation is identical to the FIRMER-CMA and is based on optimising an instantaneous cost function derived from (5.16) by dropping the expectation operator.

3. Intermediate signals $\tilde{u}_l[n]$, $l = 0(1)N-1$, are evaluated by exploiting the previously calculated $\mathbf{w}_c[n+1]$, such that

$$\tilde{u}_l[n] = \mathbf{w}_c^{\mathrm{H}}[n+1]\mathbf{x}_l[n] + \mathbf{w}_d^{\mathrm{H}}[n]\mathbf{x}_l[n]\,. \tag{5.22}$$

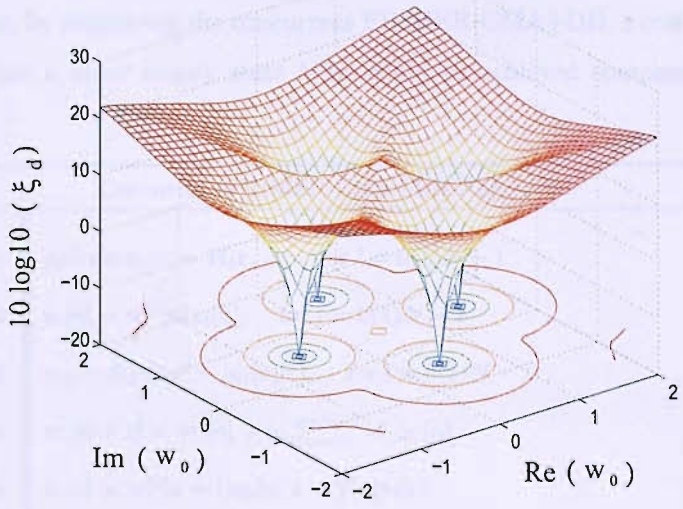

Figure 5.10: Cost function ξ_d in dependency of a single complex valued coefficient w_0.

4. Finally, the DD part of the algorithm adjusts $\mathbf{w}_d$ as

$$\mathbf{w}_d[n+1] = \mathbf{w}_d[n] + \mu_d \sum_{l=0}^{N-1} \delta(q(\tilde{u}_l[n]) - q(\hat{u}_l[n])) e_{l,d}^* \mathbf{x}_l[n], \tag{5.23}$$

where $e_{d,c} = q(\hat{u}_l[n]) - \hat{u}_l[n]$, and μ_d is the DD step size. The indicator $\delta(\cdot)$ is defined as

$$\delta(\alpha) = \begin{cases} 1 & \text{if } \alpha = 0 \\ 0 & \text{if } \alpha \neq 0 \end{cases}, \tag{5.24}$$

Therefore, the DD adaptation for a specific user is disabled if the CMA adaptation alters the decision.

The convergence of this concurrent scheme is governed by the step sizes in the algorithm. In practice, the DD step size μ_d can often be chosen much larger than the CMA step size μ_c. However, choosing too large values can cause serious error propagation due to incorrect decisions. Tab. 5.2 summarises the main equations of the proposed concurrent FIRMER-CMA+DD.

The potential drawback of DD adaptation is that if the hard decision is incorrect, error propagation occurs which subsequently degrades the equaliser performance. It has been shown that if the hard decisions before and after the CMA adaptation step are the same, then the DD decision is likely

to be correct [49]. For this reason, the DD weight vector $\mathbf{w}_d$ is only updated in the latter case similar to [90]. Hence, by employing the concurrent FIRMER-CMA+DD, a considerably enhanced convergence speed and a lower steady state MSE could be achieved compared to the standard FIRMER-CMA.

	Concurrent FIRMER-CMA+DD Algorithm
1:	update $\mathbf{x}_l[n] = \mathbf{H}_l \mathbf{r}_{nN}$, for $l = 0(1)N-1$
2:	$\hat{u}_l[n] = \mathbf{w}^{\mathrm{H}}[n]\mathbf{x}_l[n]$, for $l = 0(1)N-1$
3:	$e_{l,c} = \hat{u}_l[n](\gamma^2 - \lvert\hat{u}_l[n]\rvert^2)$, for $l = 0(1)N-1$
4:	$\mathbf{w}_c[n+1] = \mathbf{w}_c[n] + \mu_c \sum_{l=0}^{N-1} e_{l,c}^{*} \mathbf{x}_l[n]$
5:	$\tilde{u}_l[n] = \mathbf{w}_c^{\mathrm{H}}[n+1]\mathbf{x}_l[n] + \mathbf{w}_d^{\mathrm{H}}[n]\mathbf{x}_l[n]$
6:	$e_{l,d} = (q(\hat{u}_l[n]) - \hat{u}_l[n])$, for $l = 0(1)N-1$,
7:	$\mathbf{w}_d[n+1] = \mathbf{w}_d[n] + \mu_d \sum_{l=0}^{N-1} \delta(q(\tilde{u}_l[n]) - q(\hat{u}_l[n]))e_{l,d}^{*}\mathbf{x}_l[n]$
8:	$\mathbf{w}[n+1] = \mathbf{w}_c[n+1] + \mathbf{w}_d[n+1]$

Table 5.2: Concurrent FIRMER-CMA+DD multiuser equalisation algorithm.

5.3.2 Simulation Results

For the simulations below, we apply the proposed concurrent FIRMER-CMA+DD to two different stationary channel impulse responses, a short $g_1[m]$ and a more dispersive $g_2[m]$, characterised in Sec. 4.2. In the following, we first demonstrate the convergence behaviour and the steady-state MSE over noise-free channels, and thereafter characterise the evolution of the received constellation in a noisy environment.

Experiment 1. In order to demonstrate the convergence behaviour of the proposed algorithm, we transmit the QPSK signals of $N = 16$ users over $g_1[m]$ in the absence of channel noise. The length of the equaliser is $L = 10$, and the relaxation factors are chosen to be $\mu_c = 10^{-4}$ and $\mu_d = 10^{-2}$. The adaptation is initialised with both first coefficients in the weight vectors $\mathbf{w}_c$ and

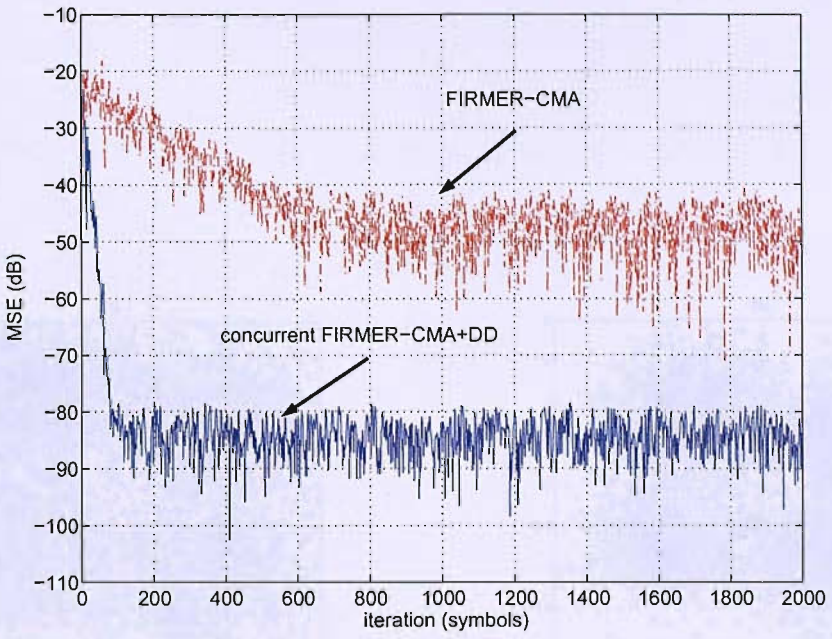

Figure 5.11: Comparison of convergence speed and steady-state MSE between the proposed concurrent FIRMER-CMA+DD algorithm and the standard FIRMER-CMA.

$\mathbf{w}_d$ set to 1/2 and zeroing all the remaining taps. The MSE performances of the proposed concurrent FIRMER-CMA+DD and the standard FIRMER-CMA algorithms are shown in Fig. 5.11. Evidently, a faster convergence and a lower steady-state can be achieved by the proposed concurrent algorithm compared to an adaptation based on FIRMER-CMA.

Experiment 2. For $N = 16$ QPSK users, we have adopted the concurrent FIRMER-CMA under SNR=10dB over the dispersive channel $g_2[m]$. The length of the equaliser is $L = 64$, and the relaxation factors are chosen to be $\mu_c = 10^{-6}$ and $\mu_d = 10^{-4}$. Fig. 5.12 depicts the decoded signal constellations of user $l = 0$ after adaptation of 5×10^3 symbols with (a) no equalisation performed, (b) a standard FIRMER-CMA equaliser, and (c) the concurrent FIRMER-CMA+DD. The results clearly show that the concurrent algorithm succeeded in opening the initially closed eye and overcoming the phase ambiguity encountered in the CMA scheme by locking onto the constellation pattern prescribed by $q(\cdot)$.

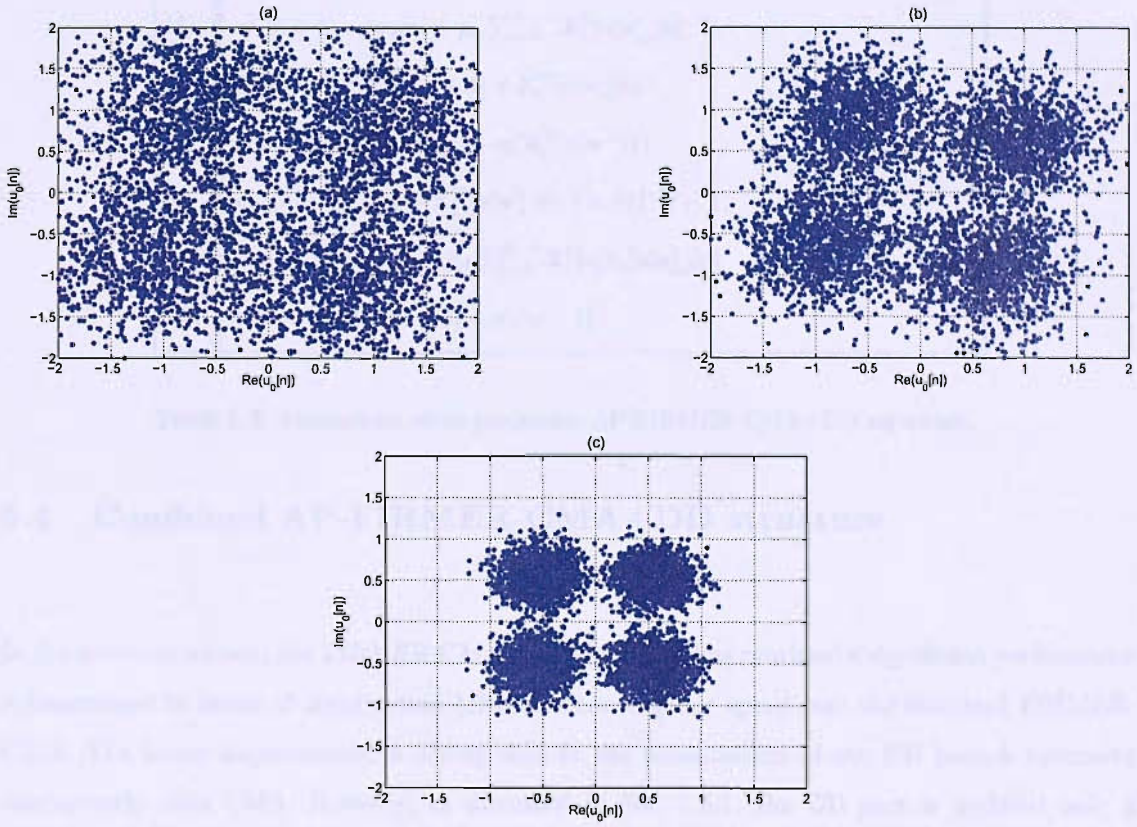

Figure 5.12: The decoded signal constellations of user $l = 0$ after adaptation of 5×10^3 symbols with (a) no equalisation (b) standard FIRMER-CMA equaliser and (c) concurrent FIRMER-CMA+DD.

	Pth order Concurrent AP-FIRMER-CMA+DD Algorithm
1:	update $\mathbf{X}_l[n] = \left[\mathbf{H}_l\mathbf{r}_{nN}\mathbf{H}_l\mathbf{r}_{(n-1)N}\cdots\mathbf{H}_l\mathbf{r}_{(n-P+1)N}\right]$, for $l = 0(1)N-1$
2:	update $\mathbf{d}_l[n] = [d_l[n]\ d_l[n-1]\ \cdots\ d_l[n-P+1]]^{\mathrm{T}}$, for $l = 0(1)N-1$
3:	$\mathbf{X}_l^{\dagger}[n] = \mathbf{X}_l[n](\mathbf{X}_l[n]^H\mathbf{X}_l[n] + \alpha\mathbf{I})^{-1}$
4:	$\mathbf{e}_{l,c}[n] = \mathbf{d}_{l,c}[n] - \mathbf{X}_l^{\mathrm{T}}[n]\mathbf{w}_n^*$ for $l = 0(1)N-1$
5:	$\mathbf{w}_c[n+1] = \mathbf{w}_c[n] + \mu_c\sum_{l=0}^{N-1}\mathbf{X}_l^{\dagger}[n]\mathbf{e}_{l,c}^*[n]$
6:	$\tilde{\mathbf{u}}_l[n] = \mathbf{X}_l^{\mathrm{T}}[n]\mathbf{w}_c^*[n+1] + \mathbf{X}_l^{\mathrm{T}}[n]\mathbf{w}_d^*[n]$
7:	$\Lambda_l[n]$=diag$(\Gamma\{\mathbf{q}(\tilde{\mathbf{u}}_l[n]) - \mathbf{q}(\mathbf{X}_l^{\mathrm{T}}[n]\mathbf{w}^*)\})$
8:	$\mathbf{e}_{l,d}[n] = \mathbf{d}_{l,d}[n] - \mathbf{X}_l^{T}[n]\mathbf{w}_n^*$ for $l = 0(1)N-1$,
9:	$\mathbf{w}_d[n+1] = \mathbf{w}_d[n] + \mu_d\sum_{l=0}^{N-1}\mathbf{X}_l^{\dagger}[n]\Lambda_l[n]\mathbf{e}_{l,d}^*[n]$
10:	$\mathbf{w}[n+1] = \mathbf{w}_c[n+1] + \mathbf{w}_d[n+1]$

Table 5.3: Concurrent affine projection AP-FIRMER-CMA+DD algorithm.

5.4 Combined AP-FIRMER-CMA+DD structure

In the previous section, the FIRMER-CMA+DD algorithm has provided a significant performance enhancement in terms of steady-state MSE and convergence speed over the standard FIRMER-CMA. The latter improvement is mainly due to the contribution of the DD branch operating concurrently with CMA. However, as discussed in Sec. 5.3.1, the DD part is updated only if the transition is considered secure. Therefore, the adaptation is generally reigned by the CMA rather than the DD algorithm especially in initially closed-eye systems. Thus, slow convergence may still persist in the proposed algorithm's performance. A possible solution to this problem is to accelerate FIRMER-CMA+DD by incorporating the APA in similar fashion to the AP-FIRMER-CMA scheme presented in Sec. 5.2.1. In this section, we derive a combined AP-FIRMER-CMA+DD structure in order to gain benefits of both previously proposed AP-FIRMER-CMA and FIRMER-CMA+DD algorithms. Based on formulations of these schemes in Secs. 5.2.1 and 5.3.1 respectively, the implementation of the Pth order AP-FIRMER-CMA+DD algorithm can be summarised in Tab. 5.3.

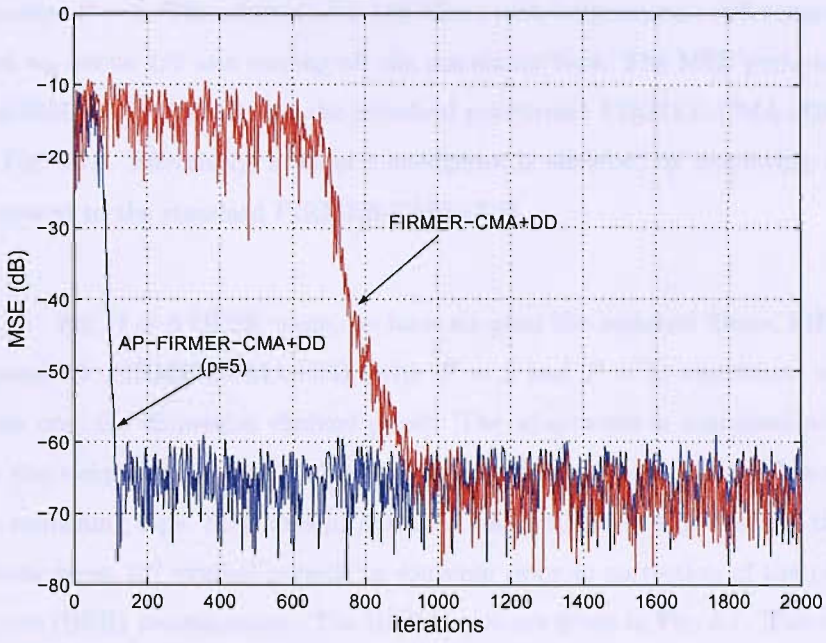

Figure 5.13: MSE convergence curves for the proposed AP-FIRMER-CMA+DD with projection order $P = 5$ and the FIRMER-CMA+DD.

The operators $\Gamma(\cdot)$ and $\mathbf{q}(\cdot)$ appear in Tab. 5.3, in step 7, are vectorial indicators and are defined, for an input vector $\mathbf{a} \in \mathbb{C}^{L_a}$, as:

$$\Gamma(\mathbf{a}) = [\delta(a_1)\ \delta(a_2)\ \cdots\ \delta(a_{L_a})] \quad , \tag{5.25}$$

$$\mathbf{q}\{\mathbf{a}\} = [q(a_1)\ q(a_2)\ \cdots\ q(a_{L_a})] \quad , \tag{5.26}$$

and $\mathrm{diag}(\mathbf{a}) \in \mathbb{C}^{L_a \times L_a}$ returns a square matrix with a diagonal $\mathbf{a}$ and zeros elements elsewhere. Next, we show by computer simulations that substantial performance improvement can be gained over either techniques separately. We first demonstrate the convergence behaviour and the steady-state MSE over noise-free channels , and thereafter characterise the bit error rate performance of the proposed algorithm.

Experiment 1. In order to demonstrate the convergence behaviour of the proposed algorithm, we transmit $N = 16$ QPSK user signals over a noise-free and dispersive channel $g_1[m]$. The length of the equaliser is $L = 10$, the relaxation factors are chosen to be $\mu_c = 5 \times 10^{-3}$, $\mu_d = 2 \times 10^{-2}$ and

the projection order $P = 5$. The adaptation is initialised with both second coefficients in the weight vectors $\mathbf{w}_c$ and $\mathbf{w}_d$ set to 1/2 and zeroing all the remaining taps. The MSE performances of the proposed AP-FIRMER-CMA+DD and the standard concurrent FIRMER-CMA+DD algorithms are shown in Fig. 5.13. Effectively, a faster convergence is achieved by employing the proposed algorithm compared to the standard FIRMER-CMA+DD.

Experiment 2. For $N = 4$ QPSK users, we have adopted the matched filters, FIRMER-CMA, and the proposed AP-FIRMER-CMA+DD (with $P = 3$ and $P = 5$) algorithms under various SNR conditions over the dispersive channel $g_1[m]$. The adaptation is initialised with both first coefficients in the weight vectors $\mathbf{w}_c$ and $\mathbf{w}_d$, of an equaliser of length $L = 10$, set to 1/2 and zeroing all the remaining taps. Step sizes μ_c and μ_d are appropriately adjusted and the algorithms have always been given 10^3 symbol periods to converge prior to correction of the phase rotation and bit error rate (BER) measurement. The BER curves are given in Fig. 6.7. The results clearly show that the proposed algorithm exhibits a similar BER performance for various values of P and outperforms both the standard FIRMER-CMA and matched filter receiver with a considerable gain, as can be seen in Fig. 6.7.

5.5 Concluding Remarks

Carrier frequency offset. The influence of a carrier frequency offset on the FIRMER-CMA and its compensation have been considered. While standard CM algorithms are invariant to carrier frequency offset [113, 114], it has been shown that the filtered-error filtered regressor-structure destroys this useful property. Instead, the algorithm has to be supplied with a carrier offset estimate to work accurately, for which a solution is proposed. The combined scheme of FIRMER-CMA and the blind estimation of the carrier frequency offset has shown good results in terms of convergence speed and BER performance, and in some cases very closely approaches the MMSE solution.

AP-FIRMER-CMA. An affine projection algorithm has been incorporated into the FIRMER-CMA. This algorithm, named AP-FIRMER-CMA, is very similar to other APA schemes, but differs in its specific application through the code filtering of the data matrix and the multiple error structure. Properties of the proposed algorithm have been investigated in simulations, and

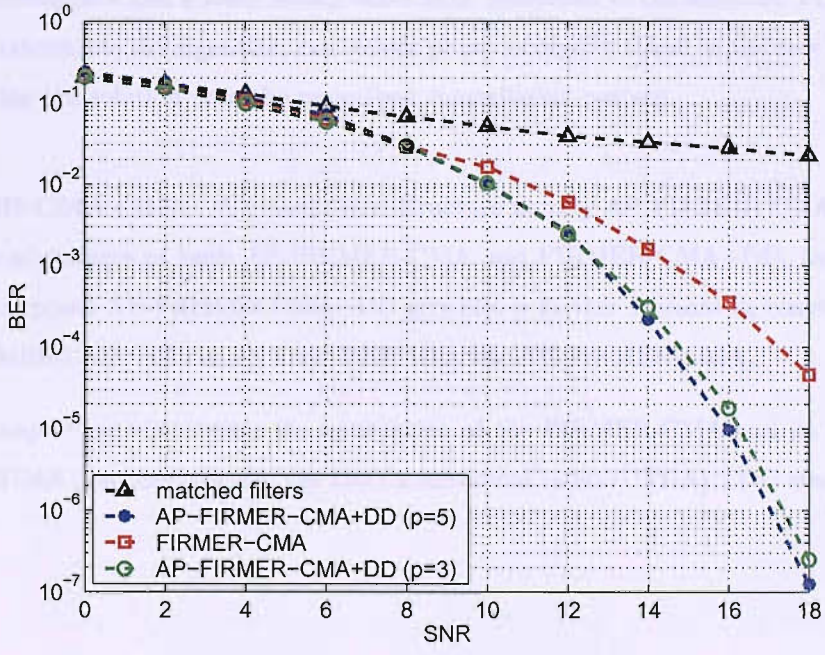

Figure 5.14: BER performance of a system transmitting over $g_1[m]$ using matched code filters (i.e. no equalisation), FIRMER-CMA and AP-FIRMER-CMA+DD algorithms.

a faster convergence over the normalised FIRMER-CMA approach with no BER loss has been noted when using higher projection orders. At the expense of a somewhat increased complexity, this blind scheme offers considerably enhanced convergence speed over previous work which makes it an attractive candidate for the DS-CDMA downlink.

FIRMER-CMA+DD. A concurrent FIRMER-CMA+DD algorithm has been derived. The proposed algorithm is based on performing both CMA and DD adaptation concurrently and enables faster convergence and a lower steady-state MSE compared to the standard FIRMER-CMA approach. Furthermore, the algorithm can reduce phase ambiguity found in the case of FIRMER-CMA by locking the solution onto the prescribed constellation pattern.

AP-FIRMER-CMA+DD. A consolidated structure namely AP-FIRMER-CMA+DD, which combines the advantages of both AP-FIRMER-CMA and FIRMER-CMA+DD, has been introduced. The proposed AP-FIRMER-CMA+DD provides a further increase in convergence speed over the FIRMER-CMA+DD and a lower BER than the AP-FIRMER-CMA.

In the next chapter we will explore the application of the FIRMER-CMA and its variants to a specific DS-CDMA downlink system, the UMTS terrestrial radio (UTRA) TDD standard.

Chapter 6

Case Study: FIRMER-CMA for UMTS-TDD System

In this chapter, we propose a semi-blind channel equalisation scheme for the downlink time-division duplex (TDD) component of the Universal Mobile Telecommunication System (UMTS) Terrestrial Radio Access (UTRA). In addition to the basic MSE chip rate equalisation performed over the training field of each UMTS-TDD time burst, a semi-blind adaptation, similar in structure to the FIRMER-CMA/LMS algorithm presented in Sec. 4.3, is adopted over data fields. In partially loaded scenarios, a number of inactive users are exploited to load pilot signals in order to enhance the system tracking performance and eliminate the typical CMA phase ambiguity problem. In Sec. 6.1, a description of the UMTS-TDD physical channel is given. Based on the definition of a signal model in Sec. 6.2, a hybrid CM/MSE cost function with its stochastic gradient algorithm are derived in Sec. 6.3. The performance of the proposed scheme in terms of MSE and BER in both fully and partially loaded systems and the effect of various loading conditions on the proposed algorithm behaviour are illustrated in Sec. 6.4 through various simulations. Finally, a new UMTS-TDD burst structure, which is more suitable for the proposed pilot-assisted scheme and provides better spectrum efficiency than the standard bursts, is introduced in Sec. 6.5.

6.1 UMTS-TDD Physical Channel

The TDD component of the UMTS provides a high transmission rate, an efficient use of the spectrum and a flexible capacity allocation. It has previously become the basis for the third generation (3G) standard, and most likely will be selected as the main duplex mode operation for fourth generation (4G) systems [115].

The UMTS-TDD mode provides uplink and downlink services within the same frequency band separated in time through the use of different time slots. Each slot can support parallel spreading codes with a maximum spreading factor of 16 [3]. Fifteen of these time slots are gathered in one frame, whereby each frame has a duration of 10 ms [3] as shown in Fig. 6.1(a). Within every time slot, users can transmit their signals simultaneously by means of different spreading codes. The time slot contribution from a single user is referred to as a burst. Each burst is a combination of two data fields, a midamble and a guard period. There are two burst types proposed in [3], namely burst type 1 and type 2. As illustrated in Fig. 6.1(b), both types have the same length of 2560 chips and are terminated by a guard period of 96 chips in order to avoid overlapping with consecutive time slots. Burst type 1 has a longer midamble suitable for cases where long training periods are required for adaptation and tracking.

The modulation technique used in UMTS-TDD is mainly QPSK [3]. Therefore, every two bits are mapped into one of four possible complex symbols. The spreading process takes place prior to transmission and consists of two operations: channelisation and scrambling. First, symbols are spread by means of real valued channelisation codes in order to separate users' signals. Spreading codes used in TDD mode are OVSF codes introduced previously in Sec. 2.4, with spreading gain $N \in \{1, 2, 4, 8, 16\}$ [3]. Note that the spreading factor used in the following analysis is $N = 16$. After channelisation, the resulting sequence is scrambled in order to separate transmitters. Scrambling occurs through chip-by-chip multiplication of the aggregate sequence by a complex code $\mathbf{c}$ [3].

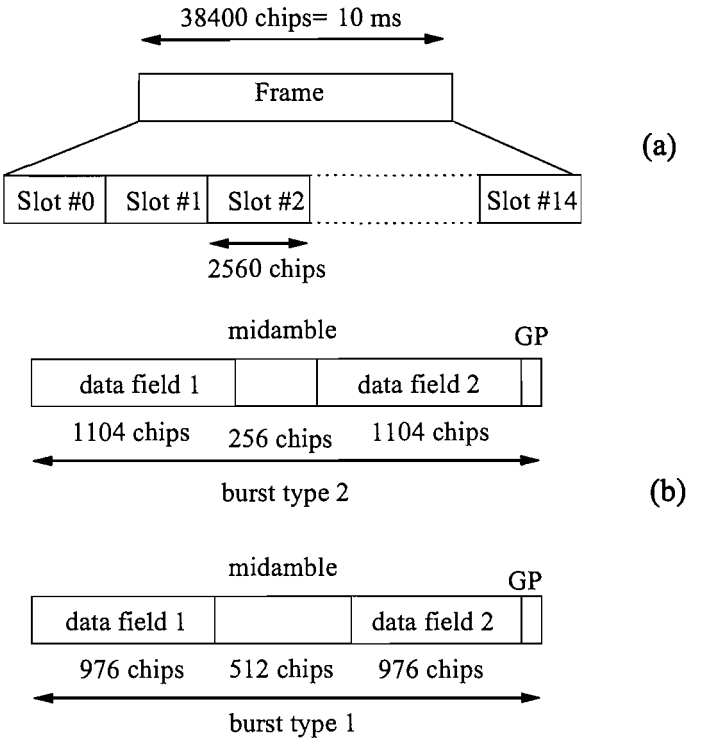

Figure 6.1: Time structure in UMTS-TDD: (a) basic frame structure, and (b) burst structure.

6.2 Signal Model

We consider the UMTS-TDD downlink model in Fig. 6.2 with a maximum of N symbol-synchronous active users. In the following, we assume that $N = 16$ and that users have the same rate for simplicity. In the case of a partially loaded system with $K \leq N$, we assume the first K users with signals $u_l[n]$, $l = 0(1)K-1$, to be active, the following $N_p \leq N-K$ to be pilots with signals $p_l[n]$, $l = 0(1)N_p - 1$, while the remaining $N - K - N_p$ signals are assumed to be zero. The signals $u_l[n]$ are code multiplexed using Walsh sequences of length N extracted from a Hadamard matrix $\mathbf{H}$. The resulting chip-rate signal, running at N times the symbol rate, is transmitted over a channel with a dispersive impulse response $g[m]$ and corruption by additive white Gaussian noise $v[m]$, which is assumed to be independent of the transmitted signal $s[m]$.

The dispersive channel $g[m]$ destroys the orthogonality of the Walsh codes, such that direct decoding of the received signal $r[m]$ with code-matched filtering by $\mathbf{H}^{\mathrm{T}}$ will lead to MAI and ISI

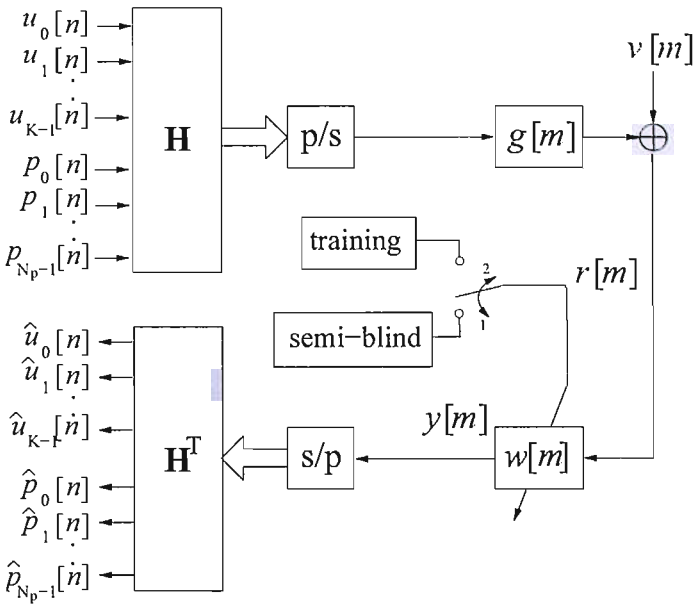

Figure 6.2: Signal model.

corruption of the decoded user signals $\hat{u}_l[n]$, $l = 0(1)K-1$. In order to re-establish orthogonality of the codes, a chip level equaliser $w[m]$ with L taps has been utilised. The equalisation is performed in both midamble period and data fields — in the former by means of the training sequence at the chip rate based on the NLMS algorithm, in the latter by using a semi-blind FIRMER-CMA/LMS scheme. In the following, we propose a semi-blind updating scheme for the equaliser coefficients $w[m]$.

6.3 Semi-Blind Equalisation Criteria

We first derive detected user signals $\hat{u}_l[n]$, $l = 0(1)K-1$ and pilot signals $\hat{p}_j[n]$, $j = K(1)K+N_p-1$ as a function of the equaliser $w[m]$. Based on this, we state a suitable cost function to be minimised in order that the equaliser's weights can be adapted. By following a derivation similar to the steps performed in Sec. 4.1, the lth decoded user signal $\hat{u}_l[n]$ and the jth decoded pilot $\hat{p}_j[n]$ can be readily written in analogous forms,

$$\hat{u}_l[n] = \mathbf{w}^{\mathrm{H}}\,\mathbf{H}_l\,\mathbf{r}_{nN}, \tag{6.1}$$

$$\hat{p}_j[n] = \mathbf{w}^{\mathrm{H}}\,\mathbf{H}_j\,\mathbf{r}_{nN}, \ , \tag{6.2}$$

with $\mathbf{H}_l \in \mathbb{C}^{L\times(N+L-1)}$ and $\mathbf{H}_j \in \mathbb{C}^{L\times(N+L-1)}$ being convolutional matrices comprising of the lth user's and the jth pilot's flipped code vectors and $\mathbf{r}_{nN} \in \mathbb{C}^{N+L-1}$ being a vector containing received data sampled at the chip rate.

6.3.1 Cost Function

Since the modulation scheme used for UMTS-TDD is mainly QPSK, or in some cases PSK [3], the K active users' signals $u_l[n]$ consist of symbols with a constant modulus γ. Therefore, by forcing the received symbols $\hat{u}_l[n]$ of all users onto the constant modulus γ, as previously for FIRMER-CMA, and by minimising the mean square error between the received values $\hat{p}_j[n]$ and the known transmitted symbols $p_j[n]$, a semi-blind cost function ξ is proposed. This cost function is introduced to adapt the equaliser weights and potentially track any channel variations. Note that the remaining $N-K-N_p$ inactive users should be taken into consideration, since otherwise the equalisation criterion is under-determined and the correct signals would not necessarily be extracted in the despreading operation. As explained in Sec. 4.3, it was found to be best in terms of convergence speed, steady-state error and transmit power to force the inactive users to zeros in the MSE sense, thus ensuring that the overall system is fully determined.

Therefore, the proposed cost function consists of three terms and is formulated as ξ,

$$\xi = \mathcal{E}\left\{\sum_{l=0}^{K-1}(\gamma^2-|\hat{u}_l[n]|^2)^2\right\}+\mathcal{E}\left\{\sum_{j=K}^{K+N_p-1}|p_j[n]-\hat{p}_j[n]|^2\right\}+ \\ +\mathcal{E}\left\{\sum_{i=K+N_p}^{N-1}|\hat{u}_i[n]|^2\right\} \ . \tag{6.3}$$

The equaliser's coefficients in $\mathbf{w}$ can be determined such that the above cost function is minimised,

$$\mathbf{w}_{\mathrm{opt}} = \arg\min_{\mathbf{w}}\xi \ . \tag{6.4}$$

Note that in the absence of any pilot signals, a manifold of solutions exists for (6.4) due to the indeterminism of the CM criterion to rotations in phase.

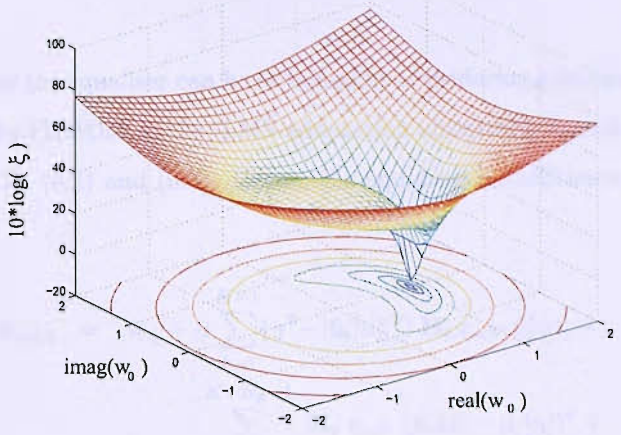

Figure 6.3: Cost function ξ in dependency of a single complex valued coefficient w_0, for a partially loaded system with 10 active users and 6 pilots.

6.3.2 Phase Ambiguity Elimination

Since an ambiguity with respect to a complex rotation $e^{j\varphi}$ ($\varphi \in [0; 2\pi]$) cannot be resolved by CM criteria, the rotation invariance can be overcome by exploiting the presence of a pilot, or in its absence by loading at least one inactive user with a pilot signal. However, this solution is valid only for partially loaded scenarios and issues such as the use of differential encoding or the transmission of a synchronisation word may still persist.

Example. In order to give an idea of the cost function and to show how pilots remove the phase ambiguity, the following example is presented. Firstly, we assume a fully loaded system with $N = 16$ users employing QPSK with $\gamma = 1$ over a distortion-less and delay-less channel $g[m] = \delta[m]$ with a signal to noise ratio (SNR) of 20 dB. Previously, Fig. 4.2 in Chapter 4 showed the cost function ξ in dependency of an equaliser $\mathbf{w}$ with a single complex coefficient w_0. The cost function indicates that there is a manifold of in the CM-sense optimal solutions satisfying $|w_{0,\text{opt}}| = 1$. Secondly, we assume that the system is partially loaded by $K = 10$ active users and 6 pilots. Thus, as shown in Fig. 6.3, the cost function ξ reduces to a single global optimum $w_{0,\text{opt}} = 1$ and the phase ambiguity is removed.

6.3.3 Pilot-Assisted Adaptation

Simple adaption rules for the equaliser can be obtained by considering a stochastic gradient descent technique. Similar to the FIRMER-CMA/LMS adaptation algorithm, an iterative update rule can be derived by using (6.1), (6.2) and (6.3). Hence, the equaliser's coefficients vector $\mathbf{w}_n$ at time n can be updated as

$$\begin{aligned}\mathbf{w}_{n+1} &= \mathbf{w}_n + \mu \sum_{l=0}^{K-1} (\gamma^2 - |\hat{u}_l[n]|^2)\, \mathbf{H}_l\, \mathbf{r}_{nN}\, \hat{u}_l^*[n] - \\ &\quad - \sum_{j=K}^{K+N_p-1} \mathbf{H}_j\, \mathbf{r}_{nN}\, (p_j[n] - \hat{p}_j[n])^* + \\ &\quad \sum_{i=K+N_p}^{N-1} \mathbf{H}_i\, \mathbf{r}_{nN}\, \hat{u}_i^*[n]. \end{aligned} \tag{6.5}$$

where μ is the algorithm step size. The first term in (6.5) is equivalent to a fully loaded blind FIRMER-CMA which differs from the standard CM algorithm [15] or its extension in [17] by the inclusion of a code-filtered term $\mathbf{H}_l\, \mathbf{r}_{nN}$ rather than just the equaliser input $r[n]$. The additional two terms in (6.5) are due to pilot signals and signals of inactive users.

6.4 Simulation Results

The stochastic gradient algorithm derived in Sec. 6.3.3 is experimentally tested and evaluated below for the UMTS-TDD physical channel with $N = 16$, presented in Sec. 6.1, by using both burst types 1 and 2. Simulations are performed over the dispersive channel $g_1[m]$ given in Sec. 4.2. The length of the equaliser is $L = 10$, and the step size is experimentally chosen to be about an order of magnitude below the onset of divergence. In Sec. 6.4.1, we assume a fully loaded scenario and compare the proposed semi-blind scheme with a strategy of chip-rate equalisation performed in the training period. Then, in Sec. 6.4.2 we evaluate the performance enhancement achieved by the introduction of pilots in the partially loaded system. Finally, the effects of various pilot loading conditions and the training sequence length on the BER performance are illustrated in Sec. 6.4.3.

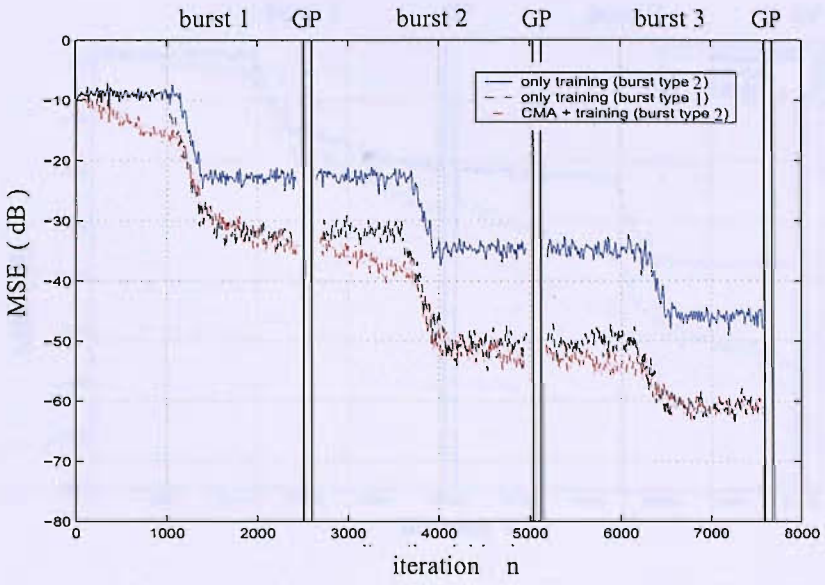

Figure 6.4: MSE curves of the proposed algorithm for a $N = 16$ users UMTS-TDD system over a duration of three bursts for the shorter burst type 2, compared to an LMS-type training based method for both burst types.

6.4.1 Fully loaded Scenario

For the fully loaded UMTS-TDD system, all possible 16 QPSK user signals are transmitted, while no pilots are used. In order to achieve an optimum response, the adaptation is initialised with the first coefficient in the weight vector set to unity. The proposed adaptation scheme is implemented in a noise-free channel by using bursts of type 2, which have the shortest training period of 256 chips only. As shown in Fig. 6.4, the proposed algorithm outperforms the two other schemes when the equalisation is performed in both burst types but only over the training period. The remaining error floor is due to model truncation. Therefore, by using blind adaptation in combination with training in type 2, the same MSE is reached when only training in type 1 mode where a longer midamble is used. The shortening of the midamble at no performance gain loss instead of gain through the inclusion of the CMA is equivalent to an increase in data throughput of 13%. This means that by using the proposed scheme, the spectral efficiency could be raised by approximately 13% by using burst type 2 instead of burst type 1 at a similar MSE performance albeit at a somewhat higher computational cost.

Figure 6.5: MSE curves of the proposed algorithm in 10 users UMTS-TDD environment with or without pilots over two bursts of type 2.

6.4.2 Partially Loaded Scenario

For a partially loaded system with $K = 10$ user signals, either 4 or 6 pilots are transmitted under similar channel conditions presented in Sec. 6.4.1. Note that with the introduction of pilots, no phase correction is needed and the choice of the initial weight vector is not crucial. Here, the first coefficient is set to unity. The MSE curves represented in Fig. 6.5 are obtained over a noise-free channel. It can be seen that the introduction of six pilots exhibits a faster convergence than schemes where either four pilots or none are used.

6.4.3 Effect of Pilot Loading on BER

To show the effect of various loading conditions on the BER performance of the proposed algorithm, we perform two experiments. In the first experiment, we consider a UMTS-TDD system with $K = 10$ active users and p pilots with $0 \leq p \leq 6$, whereby we calculate the BER for different number of loaded pilots and various SNRs. As shown in Fig. 6.6, loading more pilots enhances the BER performance of the system for relatively medium to high SNRs, while nearly no improvement in BER performance can be noted for low SNRs.

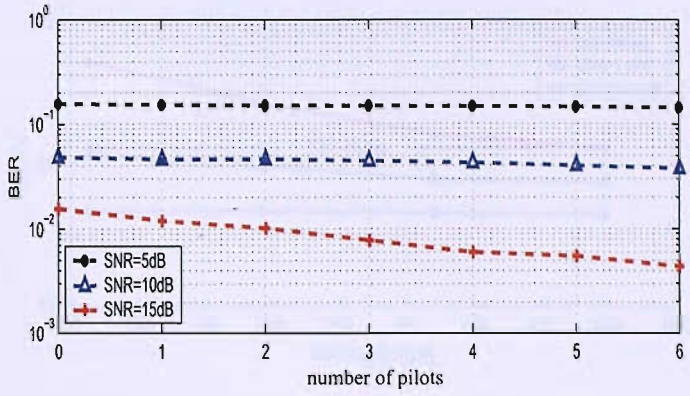

Figure 6.6: effect of the number of pilots on the BER performance corresponding to the case of 10 active users.

In the second experiment, the BER is calculated for different midamble sizes, which we aim to shorten with respect to the values proposed in [3]. The length of the equaliser is $L = 10$, and the propagation environment used is a three paths quasi time-varying channel, whereby it is assumed to be invariant over each time slot with $SNR = 20dB$. The BER is averaged over 1000 time slots for the various loading conditions. As is depicted in Fig. 6.7, the performance of the pilot-assisted algorithm is dramatically better than the classical training equalisation. A considerable reduction in BER and significant increase in data rate are achieved by loading the pilots. For example, by loading only one pilot over a small midamble of size 64 chips, we obtain a BER performance almost similar to the classical scheme where the adaptation is performed over a seven times longer midamble, as shown in Fig. 6.7. Hence, 384 chips could be saved and used for data transmission instead. This means a gain of about 16% in data throughput at no loss in BER. Moreover, by loading more pilots the BER could be reduced. For example, a reduction of at least 63% is obtained by loading three pilots for the previous short midamble, as presented in Fig. 6.7. However, we have noticed no further improvement in BER as further pilots are added to the scheme.

6.5 New Burst Structure

Based on the observations in Sec. 6.4 of the performance comparison between trained adaptation based on the LMS and semi-blind adaptation using FIRMER-CMA/LMS, a new burst structure is

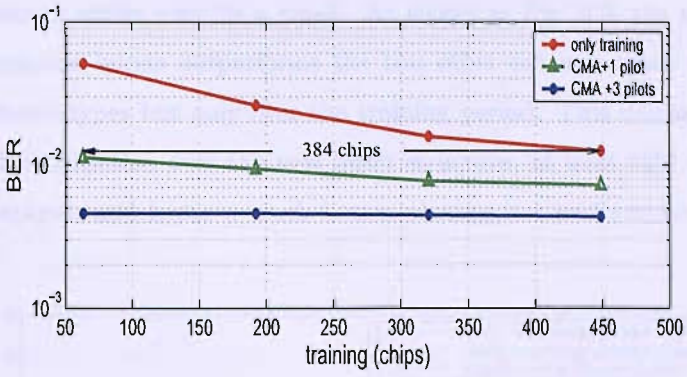

Figure 6.7: Effect of the training sequence length and pilot loading on the BER performance over a quasi-time varying channel with $SNR = 20dB$.

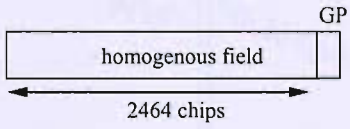

Figure 6.8: New burst structure.

proposed in this section. Similar to existing busts, the new burst had a total length of 2560 chips with a guard period of 96 chips. The main difference is that the new burst does not contain any training period and comprises of one long homogeneous field of 2464 chips, as shown in Fig. 6.8. In terms of spectrum efficiency, a considerable gain in data rate can be achieved by using such a homogeneous burst.

For example, if we consider a partially loaded system with K active users, where $16-K$ spreading codes of maximum length are currently unused, a pilot signal can be loaded by using one of these unused codes. Therefore, by using the homogeneous burst instead of burst type 1, a gain of around 26% in data rate can be obtained. Furthermore, the maximum number of symbols which can be loaded into one time slot, using the above proposed strategy, is 15×2464 symbols, rather than 16×1952 symbols when burst type 1 is adopted. In other terms, the time slot's capacity is increased by approximately 18%. Another advantage of the new burst is that, unlike existing bursts, no switching [116] is required during data transmission. However, the proposed structure may not be efficient in cases of fully loaded systems, where no burst is available for pilot loading

and when the number of active users is a small. As shown in Fig. 6.9, the proposed algorithm utilising the homogeneous bursts outperforms the two other schemes when the equalisation is performed in both burst types but only over the training period. This means that by using the proposed semi-blind equalisation over the new burst structure, at least 26% could be gained in terms of data throughput, and hence a much better convergence performance in terms of MSE can be achieved.

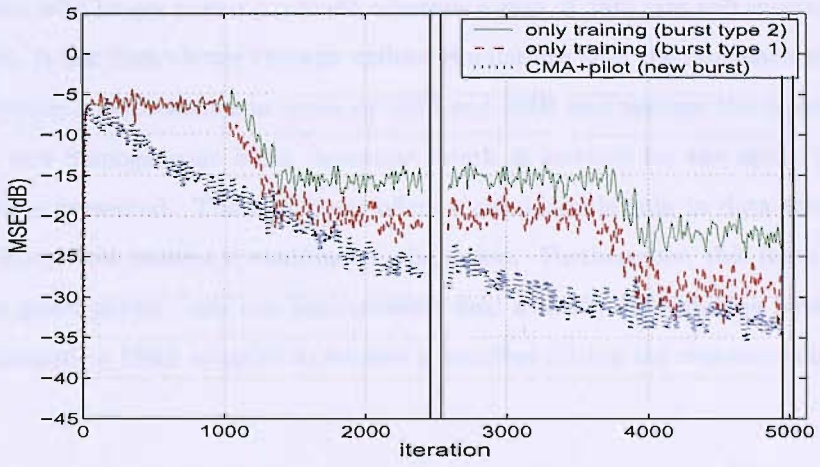

Figure 6.9: MSE learning curves for equalisation algorithms for a UMTS-TDD system with 15 active users, comparing the proposed algorithm over two homogeneous bursts, and equalisation over only midambles of both type 2 (256 chips) and type 1 (512 chips).

6.6 Concluding Remarks

A semi-blind FIRMER-CMA/LMS equalisation approach for a UMTS-TDD downlink scenario has been presented, with the aim of enforcing CM conditions on the various active users' signals and MSE criteria on either introduced pilots or the remaining inactive users. The algorithm provides a continuous channel tracking and presents a better convergence behaviour over the basic training equalisation even with longer training periods, whereby a gain of data rate and spectrum efficiency can be achieved. It has been shown through various simulations that the implementation of pilots enhances the system's performance in terms of MSE and BER and resolves the typical CM phase ambiguity. A new homogeneous burst structure, which is suitable for the above pilot-assisted strategy, has been presented. The new burst offers a considerable gain in data throughput and spectrum efficiency, and ensures a continuous adaptation. Furthermore, this burst includes, in addition to the guard period, only one homogeneous field whereby no switching between training and decision-directed or blind adaptation scheme is required during the transmission of a burst.

Chapter 7

Conclusions and Future Work

7.1 Conclusions

Motivated by the significant system capacity improvement provided by multiuser detection, the low-complexity and the robustness of CMA, and the potential of unleashing the power of complex signal processing algorithms in future software defined radio system, we have investigated and proposed a robust multiuser adaptive equaliser for a downlink DS-CDMA system, which operates at the chip level and has low computational complexity.

A brief background of a DS-CDMA system has been presented, whereby a simple mathematical framework for a synchronous baseband model has been derived. By analysing this model, it has been shown that MAI and ISI affect and limit the performance and the capacity of the system. The weak performance of the conventional receiver in the presence of dispersiveness of the channel has been identified and hence more powerful detectors are indispensable. Various alternative detection techniques have been presented; specifically, it has been found that multiuser detection enables a significant improvement in capacity and spectrum efficiency. However, its complexity and prior knowledge requirement of the interferer users' timings and signatures render it unsuitable for downlink applications. Alternatively, it has been shown that adaptive blind multiuser equalisation strategies could make multiuser detection practical for such applications. The adaptive equalisation concept used to combat the channel distortions has been reviewed and discussed. Special attention has been dedicated to the performance and the robustness of the

popular blind CMA algorithm.

In response to the above scenario, a new blind multiuser equalisation approach, the so-called filtered-R multiple error CM algorithm (FIRMER-CMA), has been proposed. This new approach has been first derived for fully loaded and single rate systems, where it aims to enforce CM conditions on the various detected user signals in the receiver. A stochastic gradient algorithm, the FIRMER-CMA, has been developed, which differs from previous CM algorithms by a code-prefiltering of its input. This algorithm has been extensively tested and has shown good convergence behaviour and stable operation.

In partially loaded systems, it has been shown that for the inactive users the injection of even low power signals in combination with a CM criterion is inferior to the introduction of an MSE cost function that compares decoded symbols of inactive users with zero. The inclusion of an MSE criterion has led to the so-called FIRMER-CMA/LMS, which has the additional advantage of a lower implementational cost without increasing the power of the transmitted signal. For multi-rate transmission, two modified FIRMER-CMA/LMS equalisation approaches using either variable spreading length (VSL) or multi-code (MCD) access modes have been presented. It has been shown that the FIRMER-CMA variant for the VSL scheme presents faster convergence and outperforms the MCD-based equaliser in both fully and partially loaded systems.

Both computational complexity and implementational flexibility of FIRMER-CMA have been addressed. The algorithm has been modified to be implemented in different modes such as blind or semi-blind, fully or partially loaded and single rate or multi-rate settings. Furthermore, it has been interpreted in a form that easily permits to incorporate decision directed (DD), least mean squares (LMS), or minimum output energy (MOE) adaptation schemes into the FIRMER-CMA update. The algorithm has been shown to exhibit a moderate complexity.

While standard CM algorithms are invariant to carrier frequency offset, we have shown that the filtered-error filtered regressor-structure destroys this property. As a result, FIRMER-CMA is sensitive to carrier frequency offset, whereby a modified update algorithm has been proposed that requires to be fed with an accurate estimate of the offset. Therefore, the algorithm has been supplied with a carrier offset estimate to work accurately in the presence of a carrier frequency offset. The combined scheme of FIRMER-CMA and blind estimation of the carrier frequency offset has demonstrated good results in terms of convergence speed and BER performance, and in

some cases very closely approaches the MMSE solution.

In order to speed up convergence, an affine projection algorithm, the AP-FIRMER-CMA, has been derived. This algorithm is very similar to other APA schemes, but differs in its specific application through the code filtering of the data matrix. Properties of the proposed algorithm have been investigated in simulations, and a faster convergence over the normalised FIRMER-CMA approach with no BER loss has been noticed when using higher projection orders. At the expense of a somewhat increased complexity, this blind scheme offers considerably enhanced convergence speed over standard FIRMER-CMA which makes it an attractive candidate for the DS-CDMA downlink.

In a further effort to increase the FIRMER-CMA's convergence speed, a concurrent FIRMER-CMA+DD algorithm has been proposed. This algorithm is based on performing both CMA and DD adaptation concurrently and enables faster convergence and lower steady state mean square error compared to the standard FIRMER-CMA approach. Furthermore, the algorithm can reduce the phase ambiguity of the FIRMER-CMA by locking the detected user symbols onto a prescribed constellation pattern rather than a constant modulus only. A consolidated AP-FIRMER-CMA+DD structure, which combines advantages of both the AP-FIRMER-CMA and FIRMER-CMA+DD, has been introduced. The proposed AP-FIRMER-CMA+DD provides a further increase in convergence speed over the FIRMER-CMA+DD and a lower BER than the AP-FIRMER-CMA.

Finally, a semi-blind equalisation approach based on the FIRMER-CMA/LMS algorithm for a UMTS-TDD downlink scenario has been investigated. Some unused codes have been exploited to load pilot signals. This pilot-assisted scheme has provided a continuous channel tracking and presented better convergence behaviour over equalisation based on a training sequence, even if training periods are lengthened. This results in a significant gain data throughput and spectrum efficiency. It has been shown through various simulations that the implementation of pilots enhances the system performance in terms of MSE and BER and resolves the typical CM phase ambiguity. Furthermore, a new homogeneous burst structure, which is suitable for the above pilot-assisted strategy, has been presented. The new burst structure offers a considerable gain in data rate and spectrum efficiency and ensures a continuous adaptation. Another advantage of using the proposed burst structure is that no switching is required during data transmissions,

since it includes only one homogeneous field in addition to the existing guard period.

7.2 Future Work

Based on the research outlined in this thesis, the following areas are of interest for potential further investigation:

The equaliser type used in this thesis is a baud-spaced equaliser (BSE). It is well known that a pure delay of the combined channel-BSE is not achievable unless an infinite-length BSE is considered [15]. Furthermore, channels which have zeros near the unit circle could pose conditioning problems to BSE design [63]. Possible solution to these limitations is to use a fractionally spaced equaliser (FSE) instead of BSE. Indeed, in addition to the insensitivity to sampling phase and reduced noise enhancement [117] provided by FSE, one feature of FSEs virtually unnoticed until 1990's was the possibility that under ideal conditions a fractionally spaced equaliser of finite time-span could perfectly equalise an FIR channel [15]. Furthermore, as mentioned in Sec. 4.5, the FIRMER-CMA's computational complexity can further be reduced by implementing a fractionally spaced equaliser due to its simple length constraint.

The approach proposed in Sec. 4.5, which is based on a decreased population of virtual users with higher level constellation maps, seems to be a promising strategy in terms of providing lower-complexity and higher adaptation rate compared to the standard FIRMER-CMA. However, more investigations are required to test and assess the performance and the behaviour of this scheme. For example, we should notice that the resulting input signals of virtual users are no longer uncorrelated. Fig. 7.1 shows the probability density function of virtual users' transmitted signals in case of $N = 16$. As it can be seen, the source is shaped and no longer equally distributed. The new shape tends to have a Gaussian distribution (Kurtosis factor close to 3 [15]).

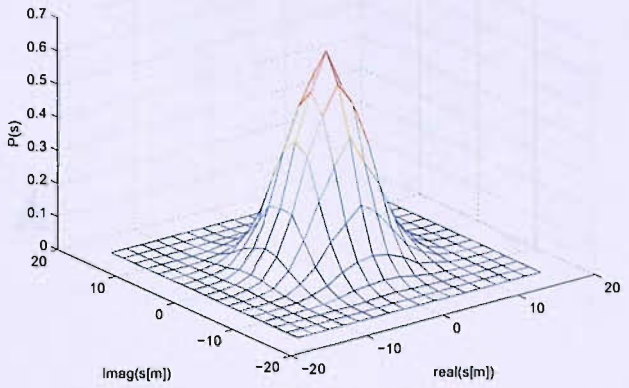

Figure 7.1: probability density function of the transmitted chips $s[m]$ for a 16 DS-CDMA downlink system

There is currently significant interest in the study of multiple input multiple output (MIMO) wireless systems, regarding their user capacity enhancement in a variety of environments. However, our proposed equaliser is originally intended for single input single output (SISO) systems and some modifications on the structure of FIRMER-CMA algorithm are required to fit MIMO systems [118, 119].

Finally, the pilot-assisted equalisation scheme, proposed for the UMTS TDD in Chapter 6, achieves improvements in terms of data throughput, spectrum efficiency, MSE, and BER performances. In fact, this scheme is only based on the standard FIRMER-CMA and neither the affine projection concept or the concurrent strategy are considered. Hence, including the combined AP-FIRMER-CMA+DD algorithm into the new burst structure can be expected to further improve system performance.

Appendix A

Derivation of the Minimum Mean Square Error Solution

This appendix presents a comprehensive derivation of the optimum equaliser's weights (3.13) and the corresponding minimum mean square error solution (3.14). By considering the expression of $e[n]$ obtained in (3.8), we first derive the squared magnitude of the recovery error as follow

$$\begin{aligned} |e[n]|^2 &= \left[\left(\mathbf{w}^{\mathrm{H}}\mathbf{G} - \mathbf{f}_{\alpha}^{\mathrm{H}}\right)\mathbf{s}_n + \mathbf{w}^{\mathrm{H}}\mathbf{v}_n\right]\left[\left(\mathbf{w}^{\mathrm{H}}\mathbf{G} - \mathbf{f}_{\alpha}^{\mathrm{H}}\right)\mathbf{s}_n + \mathbf{w}^{\mathrm{H}}\mathbf{v}_n\right]^{\mathrm{H}} \\ &= \left[\left(\mathbf{w}^{\mathrm{H}}\mathbf{G} - \mathbf{f}_{\alpha}^{\mathrm{H}}\right)\mathbf{s}_n + \mathbf{w}^{\mathrm{H}}\mathbf{v}_n\right]\left[\mathbf{s}_n^{\mathrm{H}}\left(\mathbf{G}^{\mathrm{H}}\mathbf{w} - \mathbf{f}_{\alpha}\right) + \mathbf{v}_n^{\mathrm{H}}\mathbf{w}\right] \\ &= \left(\mathbf{w}^{\mathrm{H}}\mathbf{G} - \mathbf{f}_{\alpha}^{\mathrm{H}}\right)\mathbf{s}_n\mathbf{s}_n^{\mathrm{H}}\left(\mathbf{G}^{\mathrm{H}}\mathbf{w} - \mathbf{f}_{\alpha}\right) + \left(\mathbf{w}^{\mathrm{H}}\mathbf{G} - \mathbf{f}_{\alpha}^{\mathrm{H}}\right)\mathbf{s}_n\mathbf{v}_n^{\mathrm{H}}\mathbf{w} + \\ &\quad \mathbf{w}^{\mathrm{H}}\mathbf{v}_n\mathbf{s}_n^{\mathrm{H}}\left(\mathbf{G}^{\mathrm{H}}\mathbf{w} - \mathbf{f}_{\alpha}\right) + \mathbf{w}^{\mathrm{H}}\mathbf{v}_n\mathbf{v}_n^{\mathrm{H}}\mathbf{w}. \end{aligned} \tag{A.1}$$

Then, we define the covariance matrix $\mathbf{R}_{ss} \in \mathbb{C}^{(L_c+L-1)\times(L_c+L-1)}$ of the source sequence $s[n]$, the covariance matrix $\mathbf{R}_{vv} \in \mathbb{C}^{L\times L}$ of the noise $v[n]$, and the cross-correlation matrix $\mathbf{R}_{sv} \in \mathbb{C}^{(L_c+L-1)\times L}$ between $s[n]$ and $v[n]$ such as

$$\mathbf{R}_{ss} = \mathcal{E}\{\mathbf{s}_n\mathbf{s}_n^{\mathrm{H}}\}, \quad \mathbf{R}_{vv} = \mathcal{E}\{\mathbf{v}_n\mathbf{v}_n^{\mathrm{H}}\}, \quad \text{and} \quad \mathbf{R}_{sv} = \mathcal{E}\{\mathbf{s}_n\mathbf{v}_n^{\mathrm{H}}\}. \tag{A.2}$$

where $\mathcal{E}\{.\}$ is the expectation operator. Therefore, the expectation of (A.1) can be given by

$$\begin{aligned}
\mathcal{E}\{|e[n]|^2\} &= \mathcal{E}\{(\mathbf{w}^{\mathrm{H}}\mathbf{G} - \mathbf{f}_\alpha^{\mathrm{H}})\,\mathbf{s}_n\mathbf{s}_n^{\mathrm{H}}\,(\mathbf{G}^{\mathrm{H}}\mathbf{w} - \mathbf{f}_\alpha)\} + \mathcal{E}\{(\mathbf{w}^{\mathrm{H}}\mathbf{G} - \mathbf{f}_\alpha^{\mathrm{H}})\,\mathbf{s}_n\mathbf{v}_n^{\mathrm{H}}\mathbf{w}\} + \\
&\quad \mathcal{E}\{\mathbf{w}^{\mathrm{H}}\mathbf{v}_n\mathbf{s}_n^{\mathrm{H}}\,(\mathbf{G}^{\mathrm{H}}\mathbf{w} - \mathbf{f}_\alpha)\} + \mathcal{E}\{\mathbf{w}^{\mathrm{H}}\mathbf{v}_n\mathbf{v}_n^{\mathrm{H}}\mathbf{w}\} \\
&= (\mathbf{w}^{\mathrm{H}}\mathbf{G} - \mathbf{f}_\alpha^{\mathrm{H}})\,\mathcal{E}\{\mathbf{s}_n\mathbf{s}_n^{\mathrm{H}}\}\,(\mathbf{G}^{\mathrm{H}}\mathbf{w} - \mathbf{f}_\alpha) + (\mathbf{w}^{\mathrm{H}}\mathbf{G} - \mathbf{f}_\alpha^{\mathrm{H}})\,\mathcal{E}\{\mathbf{s}_n\mathbf{v}_n^{\mathrm{H}}\}\,\mathbf{w} + \\
&\quad \mathbf{w}^{\mathrm{H}}\mathcal{E}\{\mathbf{v}_n\mathbf{s}_n^{\mathrm{H}}\}\,(\mathbf{G}^{\mathrm{H}}\mathbf{w} - \mathbf{f}_\alpha) + \mathbf{w}^{\mathrm{H}}\mathcal{E}\{\mathbf{v}_n\mathbf{v}_n^{\mathrm{H}}\}\,\mathbf{w} \\
&= (\mathbf{w}^{\mathrm{H}}\mathbf{G} - \mathbf{f}_\alpha^{\mathrm{H}})\,\mathbf{R}_{ss}\,(\mathbf{G}^{\mathrm{H}}\mathbf{w} - \mathbf{f}_\alpha) + (\mathbf{w}^{\mathrm{H}}\mathbf{G} - \mathbf{f}_\alpha^{\mathrm{H}})\,\mathbf{R}_{sv}\mathbf{w} + \\
&\quad \mathbf{w}^{\mathrm{H}}\mathbf{R}_{sv}^{\mathrm{H}}\,(\mathbf{G}^{\mathrm{H}}\mathbf{w} - \mathbf{f}_\alpha) + \mathbf{w}^{\mathrm{H}}\mathbf{R}_{vv}\mathbf{w} \quad . \qquad \text{(A.3)}
\end{aligned}$$

Here, we assume both $v[n]$ and $s[n]$ are statistically independent and identically distributed (i.i.d.) processes, with zero means ($\mathcal{E}\{s[n]\} = \mathcal{E}\{v[n]\} = 0$). Therefore, we can rewrite the covariance matrix of the source such that $\mathbf{R}_{ss} = \sigma_s^2\mathbf{I}_{Lc+L-1}$ and the covariance matrix of $v[n]$ becomes $\mathbf{R}_{vv} = \sigma_v^2\mathbf{I}_L$, where $\mathbf{I}_{Lc+L-1}$and $\mathbf{I}_L$ are identity matrices, σ_s^2 is the variance of $s[n]$, and σ_v^2 is the variance of the noise. Furthermore, we consider $s[n]$ and $v[n]$ are jointly uncorrelated sequences which yields to zeroing all elements of $\mathbf{R}_{sv}$. Hence, by adopting the above assumptions the expression (A.3) can be further simplified as follow

$$\begin{aligned}
\mathcal{E}\{|e[n]|^2\} &= (\mathbf{w}^{\mathrm{H}}\mathbf{G} - \mathbf{f}_\alpha^{\mathrm{H}})\,\sigma_s^2\,(\mathbf{G}^{\mathrm{H}}\mathbf{w} - \mathbf{f}_\alpha) + \mathbf{w}^{\mathrm{H}}\sigma_v^2\mathbf{w} \\
&= \sigma_s^2\left[(\mathbf{w}^{\mathrm{H}}\mathbf{G} - \mathbf{f}_\alpha^{\mathrm{H}})\,(\mathbf{G}^{\mathrm{H}}\mathbf{w} - \mathbf{f}_\alpha) + \frac{\sigma_v^2}{\sigma_s^2}\mathbf{w}^{\mathrm{H}}\mathbf{w}\right] \\
&= \sigma_s^2\left[(\mathbf{w}^{\mathrm{H}}\mathbf{G} - \mathbf{f}_\alpha^{\mathrm{H}})\,(\mathbf{G}^{\mathrm{H}}\mathbf{w} - \mathbf{f}_\alpha) + \lambda\mathbf{w}^{\mathrm{H}}\mathbf{w}\right] \\
&= \sigma_s^2\left[\mathbf{w}^{\mathrm{H}}\mathbf{G}\mathbf{G}^{\mathrm{H}}\mathbf{w} - \mathbf{w}^{\mathrm{H}}\mathbf{G}\mathbf{f}_\alpha - \mathbf{f}_\alpha^{\mathrm{H}}\mathbf{G}^{\mathrm{H}}\mathbf{w} + \mathbf{f}_\alpha^{\mathrm{H}}\mathbf{f}_\alpha + \mathbf{w}^{\mathrm{H}}\lambda\mathbf{I}_L\mathbf{w}\right] \\
&= \sigma_s^2\left[\mathbf{w}^{\mathrm{H}}\left(\mathbf{G}\mathbf{G}^{\mathrm{H}} + \lambda\mathbf{I}_L\right)\mathbf{w} - \mathbf{w}^{\mathrm{H}}\mathbf{G}\mathbf{f}_\alpha - \mathbf{f}_\alpha^{\mathrm{H}}\mathbf{G}^{\mathrm{H}}\mathbf{w} + \mathbf{f}_\alpha^{\mathrm{H}}\mathbf{f}_\alpha\right] \qquad \text{(A.4)}
\end{aligned}$$

with $\lambda = \frac{\sigma_v^2}{\sigma_s^2} = \frac{1}{\mathrm{SNR}}$ is the inverse of the signal to noise ration SNR. The expression in (A.4) is a quadratic function in terms of the equaliser vector $\mathbf{w}$ and should have a unique solution for a fixed value of the delay α. In order to obtain this solution a complex derivative of (A.4) could be calculated by using Wirtinger calculus [64, 120] and equated to zero. This calculus is not considered here and simpler derivation is adopted next. The latter derivation is mainly based on a technique called "completing the square" [15]. In this technique we first put $\mathbf{A} = \mathbf{G}\mathbf{G}^{\mathrm{H}} + \lambda\mathbf{I}_L$

and $\mathbf{AB} = \mathbf{Gf}_\alpha$. Hence, the following formulation arises

$$\begin{aligned}
\mathcal{E}\{|e[n]|^2\} &= \sigma_s^2 \left[\mathbf{w}^{\mathrm{H}}\mathbf{A}\mathbf{w} - \mathbf{w}^{\mathrm{H}}\mathbf{AB} - \mathbf{B}^{\mathrm{H}}\mathbf{A}^{\mathrm{H}}\mathbf{w} + \mathbf{f}_\alpha^{\mathrm{H}}\mathbf{f}_\alpha\right] \\
&= \sigma_s^2 \left[\mathbf{w}^{\mathrm{H}}\mathbf{A}\mathbf{w} - \mathbf{w}^{\mathrm{H}}\mathbf{AB} - \mathbf{B}^{\mathrm{H}}\mathbf{A}\mathbf{w} + \mathbf{f}_\alpha^{\mathrm{H}}\mathbf{f}_\alpha\right] \\
&= \sigma_s^2 \left[\left(\mathbf{w}^{\mathrm{H}} - \mathbf{B}^{\mathrm{H}}\right)\mathbf{A}\left(\mathbf{w} - \mathbf{B}\right) - \mathbf{B}^{\mathrm{H}}\mathbf{AB} + \mathbf{f}_\alpha^{\mathrm{H}}\mathbf{f}_\alpha\right] \\
&= \sigma_s^2 \left[\left(\mathbf{w}^{\mathrm{H}} - \mathbf{B}^{\mathrm{H}}\right)\mathbf{A}\left(\mathbf{w} - \mathbf{B}\right) - \mathbf{f}_\alpha^{\mathrm{H}}\mathbf{G}^{\mathrm{H}}\mathbf{A}^{-1}\mathbf{G}\mathbf{f}_\alpha + \mathbf{f}_\alpha^{\mathrm{H}}\mathbf{f}_\alpha\right] \\
&= \sigma_s^2 \left[\left(\mathbf{w} - \mathbf{B}\right)^{\mathrm{H}}\mathbf{A}\left(\mathbf{w} - \mathbf{B}\right) + \mathbf{f}_\alpha^{\mathrm{H}}\left(\mathbf{I}_{L_p} - \mathbf{G}^{\mathrm{H}}\mathbf{A}^{-1}\mathbf{G}\right)\mathbf{f}_\alpha\right]. \qquad \text{(A.5)}
\end{aligned}$$

Note that $\mathbf{A} = \mathbf{A}^{\mathrm{H}}$ and $\mathbf{A}$ is a positive finite matrix since $\lambda > 0$. The expression (A.5) shows a typical form of a quadratic function where the optimum solution can be readily deduced from expression (A.5) such that

$$\begin{aligned}
\mathbf{w}_{\mathrm{opt}} &= \mathbf{B} \\
&= \mathbf{A}^{-1}\mathbf{G}\mathbf{f}_\alpha \\
&= \left(\mathbf{G}\mathbf{G}^{\mathrm{H}} + \lambda\mathbf{I}_L\right)^{-1}\mathbf{G}\mathbf{f}_\alpha \quad . \qquad \text{(A.6)}
\end{aligned}$$

and the corresponding minimum mean square error solution is simply given by

$$\begin{aligned}
\min_{\mathbf{w}} \mathcal{E}\{|e[n]|^2\} &= \sigma_{ss}^2 \left[\mathbf{f}_\alpha^{\mathrm{H}}\left(\mathbf{I}_{L_p} - \mathbf{G}^{\mathrm{H}}\mathbf{A}^{-1}\mathbf{G}\right)\mathbf{f}_\alpha\right] \\
&= \sigma_{ss}^2 \left[\mathbf{f}_\alpha^{\mathrm{H}}\left(\mathbf{I}_{L_p} - \mathbf{G}^{\mathrm{H}}\left(\mathbf{G}\mathbf{G}^{\mathrm{H}} + \lambda\mathbf{I}_L\right)^{-1}\mathbf{G}\right)\mathbf{f}_\alpha\right] \quad . \qquad \text{(A.7)}
\end{aligned}$$

In other terms the MMSE solution for a specific α is the diagonal element with index α of the matrix $\sigma_{ss}^2\left[\mathbf{I}_{L_p} - \mathbf{G}^{\mathrm{H}}\left(\mathbf{G}\mathbf{G}^{\mathrm{H}} + \lambda\mathbf{I}_L\right)^{-1}\mathbf{G}\right]$.

Mathematical Notations

General Notations

h	scalar quantity
$\mathbf{h}$	vector quantity
$\mathbf{H}$	matrix quantity
$h(t)$	function of a continuous variable t
$h[n]$	function of a discrete variable n
h_n	short hand form for $h[n]$ for dense notation
$H(z)$	z-transform of a discrete function $h[n]$

Relations and Operators

$\circ\!\!-\!\!\bullet$	transform pair, e.g. $h[n] \circ\!\!-\!\!\bullet H(e^{j\Omega})$ or $h[n] \circ\!\!-\!\!\bullet H(z)$
$(\cdot)^*$	complex conjugate
$(\cdot)^H$	Hermitian (conjugate transpose)
$(\cdot)^T$	transpose
$\mathcal{E}\{\cdot\}$	expectation operator
$(\cdot)^{-1}$	inverse operator
$(\cdot)^\dagger$	pseudo-inverse operator
∇	gradient operator (vector valued)
$\mathrm{q}(\cdot)$	decision function
$\mathbf{q}(\cdot)$	vectorial decision operator

$\delta(\cdot)$	Kronecker delta function
$\Gamma(\cdot)$	vectorial Kronecker delta operator
$\text{sgn}(\cdot)$	signum function
$\text{diag}(\cdot)$	diagonal matrix with elements $(\cdot)$
$\text{argmin}(\cdot)$	argument of the function $(\cdot)$ minimum
$\angle(\cdot)$	angle of $\cdot$
$\lceil\cdot\rceil$	ceiling operator (round up)
$\lfloor\cdot\rfloor$	floor operator (round off)
$\lvert\cdot\rvert$	magnitude operator

Sets and Spaces

$\mathbb{C}$	set of complex numbers
$\mathbb{C}^{M\times N}$	set of $M \times N$ matrices with complex entries
$\mathbb{R}$	set of real numbers
$\mathbb{R}^{M\times N}$	set of $M \times N$ matrices with real entries
$\mathbb{Z}$	set of integer numbers

Symbols and Variables

α	delay index
γ	constant modulus
γ_l	lth user's constant modulus
μ	adaptive algorithm step size
ϕ	phase rotation
ξ_c	CM branch of the concurrent cost function
ξ_d	DD branch of the concurrent cost function
ξ	cost function
ξ_{CM}	constant modulus cost function
$\xi_{\text{CM},l}$	lth user's CM cost function

$\xi_{\mathrm{MSE},l}$	lth inactive user's MSE cost function
$\xi_{\mathrm{CM/MSE}}$	hybrid cost function
Ξ	estimated carrier frequency offset
$\Delta\Omega$	carrier frequency offset
$\mathbf{0}_{N\times f}$	$N \times f$ zero matrix
$\mathbf{b}$	combined channel-equaliser impulse response
$c[m]$	scrambling sequence
$\mathbf{c}$	scrambling code vector
d	number of previous symbols
d_l	lth user's sub-stream's number
$e[n]$	error signal of LMS equaliser
f	number of remaining chips
$g[m]$	channel chip rate impulse response
$\mathbf{g}$	channel impulse response vector
$\mathbf{G}$	CIR Toplitz matrix
$\tilde{\mathbf{G}}$	modified $\mathbf{G}$
$G(z)$	channel transfer function
$\mathbf{h}_l$	lth user's spreading code vector
$\hat{\mathbf{h}}_l$	lth flipped user's spreading code vector
$\mathbf{h}_l^{N_l}$	lth user's spreading code vector of length N_l
$\tilde{\mathbf{h}}_l[nN]$	lth user's modified and time-varying code vector
$\mathbf{H}$	matrix of active users' spreading sequences
$\mathbf{H}_{nN}$	modified time varying spreading matrix
$\mathbf{H}_l[nN]$	convolutional time varying matrix
$\mathbf{H}_\mathrm{N}$	Hadamard matrix of order N
$\mathbf{I}_\mathbf{K}$	$K \times K$ identity matrix
$\mathbf{J}_N$	$N \times N$ reverse identity matrix
l	user index
L	equaliser length
L_c	channel length
K	number of active users

M	maximum number of synchronous users
n	symbol index
m	chip index
N	spreading factor
N_l	lth user's spreading factor
$\mathcal{O}$	complexity order
$\mathbf{p}$	cross-correlation vector
P	algorithm's order
p	Godard algorithm's order
$p_l[n]$	lth pilot signal
$\mathbf{P}$	system matrix
$\mathbf{q}_l$	lth user's correlator vector
$\mathbf{q}_{l,i}$	lth user's correlator sub-vector
$r[m]$	chip rate received signal
$\mathbf{r}_{nN}$	received signal vector
R_p	dispersion constant
$\mathbf{R}$	auto-correlation matrix
$s[m]$	chip rate transmitted signal
$\mathbf{s}_{nN}$	transmitted signal vector
T	symbol period
$u[n]$	single user transmitted signal
$\hat{u}[n]$	single user decoded signal
$u_l[n]$	lth user's signal
$\tilde{u}_l[n]$	lth user's hard decoded signal
$\hat{u}_l[n]$	lth user's soft decoded signal
$\mathbf{u}_n$	users' transmitted symbols vector
$\hat{\mathbf{u}}_n$	decoded symbols vector
$\mathbf{u}_n^{(d)}$	actual and d previous symbols of all users
$v[m]$	noise chip rate sequence
$\mathbf{v}_{nN}$	noise vector
$\mathbf{w}$	coefficient vector of an equaliser

$\mathbf{w}_c$	CM branch of $\mathbf{w}$
$\mathbf{w}_d$	DD branch of $\mathbf{w}$
$\mathbf{w}_{\text{opt}}$	optimum coefficient vector
$\mathbf{w}_{\text{VSL}}$	optimum coefficient vector
$\mathbf{w}_{\text{MCD}}$	optimum coefficient vector
$\mathbf{x}[n]$	input sequence to single user equaliser
$\mathbf{x}_n$	input vector to single user equaliser
$y[m]$	equaliser's chip rate output signal
z	z-transform variable

Acronyms

3G	third generation
4G	fourth generation
3GPP	third generation partnership project
8-PAM	eight phase amplitude modulation
8-PSK	eight phase shift keying
ALBER	approximate least bit error rate
AM	amplitude modulation
APA	affine projection algorithm
AWGN	additive white Gaussian noise
BER	bit error rate
BS	base station
BSE	baud spaced equaliser
CCL	cross correlation
CIR	channel impulse response
CM	constant modulus
CMA	constant modulus algorithm
CDMA	code division multiple access
DD	decision directed
DL	downlink
DS	direct sequence
DS-CDMA	direct sequence-code division multiple access
DEF	decision equaliser feedback
ETSI-SMG	European telecommunications standards institute-special mobile group

FAP	fast affine projection
FDD	frequency division duplex
FDMA	frequency division multiple access
FEC	forward error correction
FH	frequency hopping
FIR	finite impulse response
FIRMER	filtered-R multiple error
FM	frequency modulation
FSE	fractionally spaced equaliser
GOBA	generalised optimal block algorithm
GSM	global system for mobile communications
IEEE	institute of electrical and electronics engineers
IS-95	Interim Standard 95
LBER	least bit error rate
LCMA	lattice constant modulus algorithm
LE	linear equaliser
LMS	least mean square
MAI	multiple access interference
MAP	maximum a posteriori
MBER	minimum bit error rate
MCD	multi-code
MF	matched filter
MIMO	multiple input multiple output
MLSE	maximum likelihood sequence estimation
MMSE	minimum mean square error
MPG	multiple processing gait
MOE	minimum output energy
MS	mobile station
MSE	mean square error
NLMS	normalised least mean square
NSWCMA	normalised sliding window constant modulus algorithm

PE	Perfect Equalisation
PIC	parallel interference cancellation
PN	pseudo nóise
PRA	partial rank algorithm
OCF	orthogonal correction factors
OVSF	orthogonal variable spreading factor
8PSK	eight phase shift keying
QAM	quadrature amplitude modulation
QPSK	quadrature phase shift keying
RLS	recursive least squares
SDD	soft decision directed
SDMA	space division multiple access
SDR	software defined radio
SIC	serial interference cancellation
SOS	second order statistics
SS	spread spectrum
TDD	time-division duplex
TDMA	time division multiple access
UL	uplink
UMTS	universal mobile telecommunications system
UTRA	UMTS terrestrial radio access
VPG	variable processing gain
VSL	variable spreading length
WCDMA	wide-band code division multiple access

List of Figures

List of Tables

Bibliography

[1] M. Haardt, A. Klein, R. Koehn, S. Oestreich, M. Purat, V. Sommer, and T. Ulrich, "The TD-CDMA Based UTRA TDD Mode," *Selected Areas in Communications, IEEE Journal on*, vol. 18, no. 8, pp. 1375 -1385, August 2000.

[2] T. Ojanpera and R. Prasad, "An Overview of Air Interface Multiple Access for IMT-2000/UMTS," *IEEE Communications Magazine*, vol. 36, no. 9, pp. 82–86, September 1998.

[3] 3GPP TS 25.213, "Spreading and Modulation (FDD)," *Third Generation Partnership Project V5.1.0*, Jun 2001.

[4] 3GPP TS 25.223, "Spreading and Modulation(TDD)," *Third Generation Partnership Project V5.3.0*, April 2003.

[5] L. Hanzo, E. L. Yang, L. L.and Kuan, and K. Yen, *Single- and Multi-Carrier DS-CDMA: Multi-User Detection, Space-Time Spreading, Synchronisation, Networking and Standards* , John Wiley and Sons, January 2003.

[6] S. Verdu, *Multiuser Detection*, Cambridge University Press, Cambridge,UK, 1998.

[7] G. Woodward and B.S. Vucetic, "Adaptive Detection for DS-CDMA," *IEEE Communications Magazine*, vol. 86, no. 7, pp. 1413 -1434, July 1998.

[8] M. Honig, U. Madhow, and S. Verdu, "Blind Adaptive Multiuser Detection," *IEEE Transactions on Information Theory*, vol. 41, no. 4, pp. 944–960, July 1995.

[9] S. Moshavi, "Multi-User Detection for DS-CDMA Communications," *IEEE Communications Magazine*, vol. 34, no. 10, pp. 124–136, 1996.

[10] M. Honig and M.K. Tsatsanis, " Adaptive Techniques for Multiuser CDMA Receivers," *Signal Processing Magazine, IEEE*, vol. 17, no. 3, pp. 49–61, May 2000.

[11] A. Klein, ""Data Detection Algorithms Specially designed for the Downlink of CDMA mobile radio systems"," *in Proc. VTC97, Phoenix, AZ*, pp. 203–207, May 1997.

[12] I. Ghauri and D. T. M. Slock, "Linear Receiver for the DS-CDMA Downlink Exploiting Orthogonality of Spreading Sequences," *32nd Asilomar Conf. on Signals, Systems, and Computers,*, 1998.

[13] D. Godard, "Self-Recovering Equalization and Carrier Tracking in Two-Dimensional Data Communication Systems ," *Communications, IEEE Transactions on [legacy, pre - 1988]*, vol. 28, no. 11, pp. 1867 –1875, November 1980.

[14] J. R. Treichler and B. G. Agee, ""A New Approach to Multipath Correction of Constant Modulus Signals"," *IEEE Transactions on Acoustics, Speech, and Signal Processing*, vol. Vol.31, no. No.2, pp. pp.459–472, February 1983.

[15] C. R. Johnson, P. Schniter, T. J. Endres, J. D. Behm, D. R. Brown, and R. A. Casas, "Blind Equalization Using the Constant Modulus Criterion: A Review," *Proceedings of the IEEE*, vol. 86, no. 10, pp. 1927–1950, October 1998.

[16] K. Fukawa and H. Suzuki, "Orthogonalizing Matched Filter (OMF) Detection for DS-CDMA Mobile Radio Systems," *IEEE GlobeCom conference*, vol. 1, pp. 385–389, 1994.

[17] C. Papadias and A. Paulraj, "A Constant Modulus Algorithm for Multiuser Signal Separation in Presence of Delay Spread Using Antenna Arrays," *IEEE signal processing letters*, vol. 4, no. 6, pp. 178–181, 1997.

[18] Y. Huang and P. M. Djuri, "Multiuser Detection of Synchronous Code-Division Multiple-Access Signals by Perfect Sampling," *IEEE Transactions on Signal Processing*, vol. 50, pp. 1724–1734, 2002.

[19] S. Weiss and Hadef, "Blind Chip-Rate Multiuser Equalisation," in *IEE Colloquium on DSP Enabled Radios*, Livingston, Scotland, Sep. 2003.

[20] S. Weiss, M. Hadef, M.and Konard, and M. Rupp, "Adaptive Chip-Rate Equalisation for TD-CDMA Downlink Receiver," in *37th Asilomar Conference on Signals, Systems, and Computers*, Pacific Grove, USA, November 2003.

[21] M. Hadef and S. Weiss, "A Blind Synchronous Multi-User DS-CDMA Equaliser with Partial Loading," in *International Symposium on Control, Communications, and Signal Processing*, Hammamet, Tunisia, March 2004.

[22] M. Hadef and S. Weiss, "Adaptive Blind Chip-Level Multiuser Detection in Multi-Rate Synchronous DS-CDMA System with Partial Loading," in *Proceedings of 2nd International Workshop on Signal Processing for Wireless Communications*, Kings' College London, UK, June 2004.

[23] M. Hadef, S. Weiss, and M. Rupp, "Adaptive Blind Multiuser DS-CDMA Downlink Equaliser," *IEE Electronics Letters*, 2005.

[24] S. Weiss and M. Hadef, M.and Rupp, "Blind Multi-User Equalisation for a Dispersive DS-CDMA Downlink under Carrier Frequency Offset Conditions," in *Proceedings of 12th European Signal Processing Conference* , Vienna, Austria, September 2004.

[25] M. Hadef and S. Weiss, "Affine Projection Algorithm for Blind Multiuser Equalisation of Downlink DS-CDMA system," *39th Asilomar Conference on Signals, Systems, and Computers*, October/November 2005.

[26] M. Hadef and S. Weiss, "Concurrent Constant Modulus Algorithm and Decision Directed Scheme for Synchronous DS-CDMA Equalisation," *IEEE Workshop on Statistical Signal Processing (SSP)*, July 2005.

[27] M. Hadef and S. Weiss, "A Fast Converging Concurrent Affine Projection Algorithm for Blind Multiuser Equalisation," *2nd IEE/EURASIP Conference on DSP Enabled Radio*, September 2005.

[28] M. Hadef and S. Weiss, "A Semi-Blind Channel Equalisation Strategy for the UMTS-TDD Downlink," in *Proceedings of the 3rd Workshop on the Internet, Telecommunications, and Signal Processing*, Adelaide, Australia, December 2004.

[29] M. Hadef and S. Weiss, "A Pilot-Assisted Equalisation Scheme for the UMTS-TDD Downlink with Partial Loading," in *IEEE 61st Semiannual Vehicular Technology Conference (VTC)*, Stockholm, Sweden, May 2005.

[30] M. Hadef and S. Weiss, "A New UMTS-TDD burst structure with a semi-blind Equalisation scheme," *39th Asilomar Conference on Signals, Systems, and Computers*, October/November 2005.

[31] B. Walke, P. Seidenberg, and M. P. Althoff, *UMTS The Fundamentals*, Wiley, Chichester, UK, 2003.

[32] G. R. J. Povey, "Effects of Synchronisation and Asymmetry in UTRA-TDD 3G Mobile Communication Technologies," *3G Mobile Communication Technologies, 2000. First International Conference on (IEE Conf. Publ. No. 471)*, vol. 1, pp. 86–88, March 2000.

[33] S. M. Heikkinen, H. Haas, and G. J. R. Povey, "Investigation of Adjacent Channel Interference in UTRA-TDD System," *UMTS Terminals and Software Radio (Ref. No. 1999/055), IEE Colloquium on*, vol. 13, pp. 1–6, April 1999.

[34] J. C. Yu, X. Wang, A. H. Madsen, and G. Messier, "Group Blind Multiuser Detection for UTRA-TDD," *Vehicular Technology Conference, 2001. VTC 2001 Spring. IEEE VTS 53rd*, vol. 1, pp. 492–496, May 2001.

[35] A. J Viterbi, *CDMA Principles of Spread Spectrum Communication*, Addison Wesley Wireless Communications Series, Massachusetts, USA, 1995.

[36] K. Feher, *Wireless Digital Communications:Modulation and Spread Spectrum Applications*, Prentice Hall, New Jersey, USA, 1995.

[37] J. G. Proakis, *Digital Communications*, McGraw-Hill Series, New York, USA, third edition, 1995.

[38] B. Sklar, *Digital Communications: Fundamentals and Applications*, Prentice Hall, Englewood Cliffs, 1988.

[39] R. Kohno, R. Meidan, and L.B. Milstein, "Spread Spectrum Access Methodes for Wireless Communications," *IEEE Communications Magazine*, vol. 33, no. 1, pp. 58–67, Jannuary 1995.

[40] E.H. Dinan and B. Jabbari, "Spreading Codes for Direct Sequence CDMA and Wideband CDMA Cellular Networks," *IEEE Communications Magazine*, vol. 36, no. 9, pp. 48–54, September 1998.

[41] D. Garcia-Alis, *On Adaptive MMSE Receiver Strategies for TD-CDMA*, Ph.D. thesis, University of Strathclyde, 2001.

[42] H.K. Sim and D.G.M. Cruickshank, "An Iterative Multiuser Receiver for FEC Coded CDMA," *Spread Spectrum Techniques and Applications, 2000 IEEE Sixth International Symposium on*, vol. 2, pp. 728–732, September 2000.

[43] A. Kapur and M. K. Varanasi, "Multiuser Detection for Overloaded CDMA Systems," *IEEE Transactions on Information Theory*, vol. 49, no. 7, pp. 1728–1742, July 2003.

[44] Theodore S Rappaport, *Wireless Communications, Principles and Practice*, Prentice Hall PTR, New Jersey, 1st edition, 1996.

[45] Z. Xie, C. K. Rushforth, and R.T Short, "Multiuser Signal Detection Using Sequential Decoding," *IEEE Transactions on Communications*, vol. 38, pp. 578–583, May 1990.

[46] S. Chen, A. K. W. Samingan, M. Mulgrew, and L. Hanzo, "Adaptive minimum-BER linear multiuser detection for DS-CDMA signals in multtipath channels," *sp*, vol. 49, pp. 1240–1247, 2001.

[47] I. N. Psaromiligkos, S. N. Batalama, and D. A. Pados, "On Adaptive minimum probability of error linear filter receivers for DS-CDMA channels," *IEEE Transactions on Signal Processing*, vol. 47, pp. pp.1092–1102, 1999.

[48] Sheng Chen, *Least Bit Error Rate Adaptive Multiuser Detection*, Soft Computing in Communications,. Springer Verlag, 2003.

[49] S Chen, "Adaptive linear filtering design with minimum symbol error probability criterion," *Int. J. Automation and Computing*, to appear 2005.

[50] J. Patel, P.and Holtzman, "Analysis of a Simple Successive Interference Cancellation Scheme in a DS-CDMA System," *Selected Areas in Communications, IEEE Journal on*, vol. 12, pp. 796–806, June 1994.

[51] Y. Li and R. Steel, "Serial Interference Cancellation Method for CDMA ," *Electronics Letters*, vol. 30, pp. 1581–1583, September 1994.

[52] T. B. Oon, R. Steel, and Y. Li, "Cancellation Frame Size for a Quazi-Single-Bit Detector in aSynchronous CDMA Channel," *Electronics Letters*, vol. 33, pp. 258–259, February 1997.

[53] T. B. Oon, R. Steel, and Y. Li, "Performance of an Adaptive Successive Serial-Parallel CDMA Cancellation Scheme in a Flat Fading Channels ," *IEEE Vehiculaire Technology Conference*, vol. 1, pp. 193–197, May 1997.

[54] M. Sawahashi, Y. Miki, H Andoh, and K Higuchi, "Pilot Symbol-Assisted Coherent Multistage Interference Canceller Using Recursive Channel Estimation for DS-CDMA Mobile Radio ," *IEICE Transactions on Communications*, vol. E79-B, pp. 1262–1270, September 1996.

[55] P. Alexender, L. Rasmussen, and C. Schlegel, "A linear Receiver for Coded Multiuser CDMA," *IEEE Transactions on Communications*, vol. 45, no. 5, pp. 605–610, May 1997.

[56] R Lupas and S. Vedru, "Linear Multiuser Detectors for Synchronous Code-Division Multiple-Access Channels," *IEEE Transactions on Information Theory*, vol. 35, pp. 123–136, January 1989.

[57] U. Madhow and M Honig, "MMSE Interference Suppression for Direct Sequence Spread Spectrum CDMA," *IEEE Communications Magazine*, vol. 42, pp. 3178–3188, December 1994.

[58] R. Schober, W. H. W. H. Gerstacker, , and L.H. J. Lampe, "Comparison of MOE and Blind LMS," *IEE communications letters*, vol. 7, pp. 204–206, 2003.

[59] O. L. Frost, III, "An Algorithm for Linearly Constrained Adaptive Array Processing," *Proceedings of the IEEE*, vol. 60, no. 8, pp. 926–935, August 1972.

[60] John G. Proakis, ""Channel Equalization"," in *The Mobile Communications Handbook*, Jerry D. Gibson, Ed., chapter 6, pp. 56–80. CRC Press / IEEE Press, 1996.

[61] J. R. Treichler, I. Fijalkow, and C. R. Johnson, "Fractionally Spaced Equalizers: How Long Should They Really Be?," *IEEE Signal Processing Magazine*, vol. 13, no. 3, pp. 65–81, May 1996.

[62] John J. Shynk, "Adaptive IIR Filtering," *IEEE Acoustics, Speech, and Signal Processing Magazine*, vol. 6, no. 2, pp. 4–21, April 1989.

[63] T.J Endres, *Equalizing with Fractionally-Spaced Constant Modulus and Second-Order-Statistics Blind Receivers*, Ph.D. thesis, University of Cornell, USA, May 1997.

[64] R. F. Fischer, *Precoding and Signal shaping for Digital Transmission*, John Wiley & sons, New York, USA, 2002.

[65] B. Widrow and S. D. Stearns, *Adaptive Signal Processing*, Prentice Hall, Englewood Cliffs, New York, 1985.

[66] S. Haykin, *Adaptive Filter Theory*, Prentice Hall, Englewood Cliffs, 3rd edition, 1996.

[67] B. Widrow and Hoff., "Adaptive Switching Circuits," *IRE Western Electric Show and Convention Record*, vol. 4, pp. 96–104, August 1960.

[68] B. Widrow, J. McCool, and M. Ball, "The Complex LMS Algorithm," *Proceedings of the IEEE*, vol. 63, pp. 719–720, August 1975.

[69] W. A. Gardner, ""A New Method of Channel Identification"," *IEEE transactions in communications*, vol. 39, no. 6, pp. pp.813–817, June 1991.

[70] Lang Tong, Guanghan Xu, and Thomas Kailath, ""Blind Identification and Equalization Based on Second-Order Statistics: A Time Domain Approach"," *IEEE Transactions on Information Theory*, vol. Vol.40, no. No.2, pp. pp.340–349, March 1994.

[71] R. W. Lucky, ""Techniques for Adaptive Equalization of Digital Communication Systems"," *Bell Syst. Tech.*, vol. Vol.45, pp. pp.255–286, February 1966.

[72] O. Macchi and E. Eweda, "Convergence Analysis of Self-Adaptive Equalizer," *Information Theory, IEEE Transactions*, vol. 30, no. 2, pp. 161–176, March 1984.

[73] Y. Sato, ""A Method of Self-Recovering Equalization for Multilevel Amplitude-Modulation Systems"," *Communications, IEEE Transactions*, vol. 23, no. 6, pp. 679–682, June 1975.

[74] J. K. Byoung-Jo, *Blind Equalization for Short Burst Wireless Communications*, Ph.D. thesis, Stanford University, USA, January 1998.

[75] R. Gooch, M. Ready, and J. Svoboda, "A Lattice-Based Constant Modulus adaptive filter," in *Asilomar Conference*, Pacific Grove, 1987.

[76] C. Papadias and D.T.M. Slock, "Normalized Sliding Window Constant Modulus and Decision-Directed Algorithms: a Link Between Blind Equalization and Classical Adaptive Filtering," *IEEE signal processing transactions*, vol. 45, no. 1, pp. 231–235, 1997.

[77] S. Haykin, *Blind Deconvolution*, Prentice Hall, Englewood Cliffs, 1994.

[78] S. Weiss and R. W. Stewart, *On Adaptive Filtering in Oversampled Subbands*, Shaker Verlag, Aachen, Germany, 1998.

[79] E.M. Wang, Z.and Dowling, "Stochastic conjugate gradient constant modulus blind equalizer for wireless communications," in *ICC, IEEE International Conference*, Jun 1996, vol. 2, pp. 832–836.

[80] K et al Hilal, "A convergence study of the constant modulus algorithm leading to a normalised-cma and a block normalised-cma," in *EUSIPCO-92*, August 1992, vol. 1, pp. 135–138.

[81] J.P. LeBlanc, I. Fijalkow, and C.R.Jr. Johnson, "CMA Fractionally Spaced Equalizers: Stationary Points and Stability under IID and temporally correlated sources ," *International Journal of Adaptive Contr. Sign. processing*, 1998.

[82] I. Stirling, D. Garcia-Alis, S. Weiss, G. Rice, and R.W. Stewart, "A Joint Adaptive MMSE Downlink Receiver," in *Asilomar Conference on Signals, Systems, and Computers*, Monterey, CA, November 2000.

[83] P. Schniter and A. R. Margetts, "Adaptive Chip-Rate Equalization of Downlink Multirate Wideband CDMA," in *Asilomar Conference on Signals, Systems, and Computers*, Monterey, CA, November 2002, pp. 1228–1232.

[84] S. Lambotharan, J.A. Chambers, and A.G. Constantinides, "Adaptive blind retrieval techniques for multi-user ds-cdma signals," *IEE Electronics Letters*, vol. Vol.35, no. No.9, pp. pp.693–695, 1999.

[85] Z. Xu and P. Liu, "Code-Constrained Blind Detection of CDMA Signals in Multipath Channels," *IEEE Transactions on Signal Processing*, vol. 9, pp. 389–392, 2002.

[86] T. K. Moon and W. C. Stirling, *Mathematical Methods and Algorithms*, Prentice Hall, Upper Saddle River, NJ, 1999.

[87] S.J. Elliott, I.M. Stothers, and P.A. Nelson, "A Multiple Error LMS Algorithm and its Application to the Active Control of Sound and Vibration," *IEEE Transactions on Acoustics, Speech and Signal Processing*, vol. Vol.35, no. No.10, pp. pp.1423–1434, 1987.

[88] W. H. Press, S. A. Teukolsky, W. T. Vetterling, and B. P. Flannery, *Numerical Recipes in C*, Cambridge University Press, Cambridge, 2nd edition, 1992.

[89] C. Toker, G. Lambotharan, J.A. Chambers, and B. Baykal, "Channel shortening filter design based on polynomial methods," *Vehicular Technology Conference, (VTC) Spring*, vol. 1, pp. 565–569, 2004.

[90] F.C.C. De Castro and D.S. De Castro, M.C.F.and Arantes, "Concurrent blind deconvolution for channel equalization," *ICC, IEEE International Conference*, vol. 2, pp. 366–371, June 2001.

[91] S. Chen, "Low complexity concurrent constant modulus algorithm and soft decision directed scheme for blind equalisation," *Image and Signal Processing, IEE Proceedings*, vol. 150, no. 5, pp. 312–320, October 2003.

[92] F. Petre, M. Moonen, M. Engels, B. Gyselinckx, and H.D. Man, "Pilot-Aided Adaptive CHip Rate Equalizer Receiver for Interference Suppression in DS-CDMA Forward Link," in *IEEE Vehicular Technology Conference*, Sept. 2000, vol. 1, pp. 303–308.

[93] I. Chih-Lin and R.D. Gitlin, "Multi-code CDMA Wireless Personal Communications Networks," *ICC IEEE International Conference*, vol. 2, pp. 1060–1064, June 1995.

[94] M. Jinghong and J.K. Tugnait, "Blind Detection of Multirate Asynchronous CDMA Signals in Multipath Channels," *IEEE Transactions on Acoustics, and Signal Processing,*, vol. 1, pp. 36–40, September 2002.

[95] S Braithwaite, *Personal Communications*, UN, London, 1st edition, 2005.

[96] N. Jablon, "Joint Blind Equalization, Carrier Recovery, and Timing Recovery for High-Order QAM Signal Constellations," *IEEE Trans. Signal Processing*, vol. 40, pp. 1383–1397, June 1992.

[97] A. Belouchrani and W. Ren, "Blind Carrier Phase Tracking with Garanteed Global Convergence," *IEEE Transactions on Signal Processing*, vol. 45, pp. pp.1889–1894, July 1997.

[98] C. Tibenderana, *A High-Performance, Efficient, and Reliable Receiver for Bluetooth Signals*, Ph.D. thesis, University of Southampton, 2005.

[99] L. Rustako, A. Jr.and Greenstein, R. Roman, and A. Saleh, "Using Times-Four Carrier Recovery in M-QAM Digital Radio Receivers," *Selected Areas in Communications, IEEE Journal*, vol. 5, no. 3, pp. 524–533, 1987.

[100] K. Ozeki and T. Umeda, "An Adaptive Filtering Algorithm Using an Orthogonal Projection to an Affine Subspace and Its Properties," *Electronics and Communications in Japan*, vol. Vol.67-A, no. No.5, pp. pp.19–27, February 1984.

[101] S. G. Sankaran and A. A. Beex, "Convergence behavior of affine projection algorithms," *Signal Processing, IEEE Transactions on [see also Acoustics, Speech, and Signal Processing, IEEE*, vol. Vol.48, no. No.4, pp. 1086 – 1096, April 2000.

[102] N. J. Bershad, D. Linebarger, and S. McLaughlin, "A Stocahstic Analysis of the Affine Projection Algorithm for Gaussian Autoregressive Inputs," *in Proc. IEEE Conf. Acoustics, Speech, Signal Processing*, vol. 6, pp. 3837–3840, May 2001.

[103] S. J. M. De almeida, J. C. M. Bermudez, N.J. Bershad, and M.H. Costa, "A Statistical Analysis of the Affine Projection Algorithm for Unity Step Size and Autoregressive Inputs," *Circuits and Systems I: IEEE Transactions on Fundamental Theory and Applications*, vol. 52, no. 7, pp. 1394 – 1405, July 2005.

[104] S. G. Kratzer and D. R. Morgan, "The Partial-Rank Algorithm for Adaptive Beamforming," *SPIE Int. Soc. Optic. Eng.*, vol. Vol.564, pp. pp.9–14, 1985.

[105] D. R. Morgan and S. G. Kratzer, "On a Class of Computationally Efficient, Rapidly Converging, Generalized NLMS Algorithms," *Signal Processing Letters, IEEE*, vol. 3, no. 8, pp. 245–247, August 1996.

[106] S. G. Sankaran and A. A. Beex, "Normalized LMS Algorithm with Orthogonal Correction Factors," *Thirty-First Asilomar Conference on Signals, Systems and Computers*, vol. Vol.2, pp. 1670–1673, November 1997.

[107] D. T. M. Slock, "The Block Underdetermined Covariance (BUC) Fast Transversal Filter (FTF) algorithm for adaptive filtering ," *Asilomar Conference on Signals, Systems and computers*, pp. 26–28, October 1992.

[108] M. Montazeri and P. Duhamel, "A Set of Algorithms Linking NLMS and Block RLS Algorithms," *IEEE Transactions on Signal Processing*, vol. Vol.43, no. No.2, pp. pp.444–453, Feb. 1995.

[109] M. Tanaka, Y. Kaneda, and J. Kojima, "Fast Projection Algorithm and its Step Size Control," *Acoustics, Speech, and Signal Processing,ICASSP*, vol. 2, pp. 945–948, May 1995.

[110] S. L. Gay, "A Fast Affine Projection Algorithm," in *Proc. IEEE International Conference on Acoustics, Speech, and Signal Processing*, 1995, vol. V, pp. 3023–3026.

[111] C. Papadias and D.T.M. Slock, "New Adaptive Blind Algorithms for Constant Modulus Constellations," *in Proc. ICASSP-94*, vol. III, pp. 507–510, 1994.

[112] C. Papadias and D.T.M. Slock, "Normalized Sliding Window Constant Modulus Algorithm for Blind Equalization," *in Proc. 14th GRETSI Symp. Signal Image Processing*, pp. 13–16, September 1993.

[113] J.R. Treichler, M.G. Larimore, and J.C. Harp, "Practical blind demodulators for high-order QAM signals," *Proceedings of the IEEE*, vol. 86, no. 10, pp. 1907–1926, October 1998.

[114] M. Rupp, "On the Learning Behaviour of Decision Feedback Equalizers," in *Asilomar Conference on Signals, Systems, and Computers*, Monterey, CA, October 1999.

[115] R. Esmailzadeh, M. Nakagawa, and A Jones, "TDD-CDMA for the 4th generation of wireless communication," *Wireless Communications, IEEE*, vol. 10, no. 4, pp. 8–15, August 2003.

[116] S. Weiss, H. Mohamad, and M Hadef, "Switching Between Two Different Fractionally Spaced Adaptive Equalisation Structures," in *IMA Conference on Mathematics in Communications*, Lancaster, England, December 2002.

[117] R. D. Gitlin, J. F. Hayes, and S. B. Weinstein, *Data Communications Principles*, Plenum Press, 1992.

[118] Chunguang. Liu, "CMA on Multiuser MIMO System Chip-Rate Equalisation," M.S. thesis, School of Electronics and Computer Science, University of Southampton, October 2004.

[119] S. Bendoukha, H. Hadef, and S. Weiss, "Adaptive Receivers for Space-Time Spreading over Dispersive Channels," *40th Asilomar Conference on Signals, Systems, and Computers*, p. accepted for publication, November 2006.

[120] W. Fischer and I. Lieb, *Funktionentheorie*, Vieweg Verlag, Braunschweig, Germany, 1983.